Technische Universität München
Fakultät für Medizin
Institut für Virologie

Investigation of Environmental and Epigenetic Etiologies Driving Cholangiolar and Hepatocellular Neoplasias

DETIAN YUAN

Vollständiger Abdruck der von der Fakultät für Medizin der Technischen Universität München zur Erlangung des akademischen Grades eines Doktors der Naturwissenschaften genehmigten Dissertation.

Vorsitzenderr: Prof. Dr. Roland M. Schmid

Prüfer der Dissertation:

1. Prof. Dr. Mathias Heikenwälder
2. Prof. Dr. Dirk Haller
3. Prof. Dr. Martin Zenke (RWTH Aachen)

Die Dissertation wurde am 24.07.2015 bei der Fakultät für Medizin der Technischen Universität München eingereicht und durch die Fakultät für Medizin am 25.02.2016 angenommen.

Table of content

SUMMARY

Adult tissue renewal and homeostasis are governed by the balance between elimination of damaged cells and supplement of new cells, dysregulation of which is a critical hallmark of many human diseases including cancer. Proper cell fate decisions and cellular identity maintenance are essential for this balance, whereas deregulated cell fate decision and loss of cellular identity are critical steps at the origin of tumorigenesis. Nowadays, while much remains to be learned about fundamental cellular and molecular controls of these processes, it is generally accepted that the cell fate decision and cellular identity maintenance are regulated by the combination of extrinsic signals (e.g. environmental clues and signaling pathways) and intrinsic signals (e.g. transcription factors and epigenetic modifications).

Liver cells are inherently susceptible to a wide variety of damage imposed by toxins or chemicals due to their central role of metabolism and detoxification. Thus, normal turnover and regeneration of liver parenchyma cells are pivotal for liver homeostasis and function. Due to the unique cell plasticity of hepatocytes and cholangiocytes, mechanisms underlying liver homeostasis have been a long-standing debate. Liver cell turnover and regeneration could be accomplished by (a) self-duplication of terminal differentiated hepatocytes or cholangiocytes, (b) de-differentiation and/or trans-differentiation of hepatocytes or cholangiocytes, and (c) activation and lineage specification of liver progenitor cells. These processes are tightly coordinated by both extrinsic and intrinsic clues. Elucidating the underlying regulatory mechanism not only provides insight into the physiological maintenance of the liver, but also has clinical significance for liver pathogenesis, including alcoholic liver disease, nonalcoholic fatty liver disease, fibrosis, cirrhosis and cancer.

Therefore my PhD thesis investigated these issues in several model systems and focus on: (a) role of oxidative microenvironment in lineage commitment of liver progenitor cells, (b) role of epigenetic status of hepatocytes in hepatocyte homeostasis, and (c) role of inflammatory microenvironment in hepatocellular carcinoma (HCC) development.

In the first study, termed “Mitochondrial defects in hepatocytes cause cholangiolar hyper-proliferation via Kupffer cell-mediated paracrine TNFα signaling”, I established a mouse model of chronic mitochondrial defect by genetically deleting the main mitochondria chaperone, HSP60, specifically from hepatocytes. I found that hepatocytic mitochondrial

dysfunction and oxidative stress trigger a carcinogenic niche for LPCs in favor of cholangiolar differentiation and neoplastic growth. Mitochondrial dysfunction stimulates Kupffer cells, which produce tumor necrosis factor α and activate JNK signaling to establish cholangiocellular fate. Overwhelming cholangiolar differentiation leads to regeneration defects and neoplastic lesions. Pharmacological depletion of Kupffer cell or genetic ablation of TNFR1 reverses the mis-differentiation of LPCs and rescues the regeneration defects, implying a role of typical inflammatory signaling in lineage commitment of adult stem cells. Taken together, our findings identify a novel non-cell-autonomous network, established by mitochondrial dysfunction and oxidative stress triggered TNFα signaling, as a pivotal regulator of LPC commitment to the cholangiolar lineage. Targeting this network provides novel opportunities for liver injury and therapy of intrahepatic cholangiocellular carcinoma.

In the second study termed “HDAC2 deficiency in hepatocytes leads to HCC development”, we investigated the effects of the knockout of an individual HDAC, HDAC2, on hepatocyte homeostasis. The HDAC2 hepatocyte-specific knockout mice showed no abnormalities compared to control littermates, suggesting the functional redundancy of HDAC family members. We further aged a large cohort of knockout mice and surprisingly found a low HCC incidence. HCC development in HDAC2 deficient mice were not caused by cell death or compensatory proliferation because no obvious cell death or hepatocyte proliferation was observed in livers from unaffected mice. Histological characterization of the HDAC2 deficient tumors confirmed their malignancy features. Most strikingly, the majority of the tumors were steatohepatitic HCC, a special morphologic variant of HCC associated with metabolic risk factors. Further studies of the link between alterations of lipogenesis and HDAC2 deficiency are urgently needed due to the currently ongoing clinical trials of HDAC inhibitors in cancer patients.

The last study included in my thesis termed “Inflammatory micro-niche promotes HCC development with crucial survival and growth factors” focused on the oncogenic role of liver inflammatory microenvironment. Here, my colleagues, Dr. Finkin and Prof. Pikarsky, generated a new mouse model of HCC with ectopic lymphoid-like structures prior to HCC development. The lymphoid-like structures formed inflammatory micro-niche wherein progenitor malignant hepatocytes first appear and thrive. My colleagues and I showed that these progenitors eventually egress their micro-niches and form HCCs. We further proved that the inflammatory micro-niche promoted malignant transformation of

hepatocytes through LTβR signaling and its downstream cytokines like CCL20 and CCL17. Our findings indicate that aberrant immune activation in the liver can promote early stages of carcinogenesis by creating a micro-niche within which cancer progenitors can evolve. Hence, compromising micro-niche formation by specific immune cell ablation or targeting its nursing function by cytokine blockade may provide new means for HCC prevention and early treatment.

Abbreviations

8-OHdG	8-hydroxy-2-deoxyguanosine
AP-1	Activator protein 1
aCGH	array-based copy number analysis
AFP	α-fetoprotein
ALT	Alanine aminotransferase
AP	Alkaline phosphatase
AST	Aspartate aminotransferase
ATP	Adenosine triphosphate
BDL	Bile duct ligation
BEC	Bile duct epithelial cell
BHA	Butylated hydroxyanisole
CCl4	Carbon tetrachloride
ChIP	Chromatin immunoprecipitation
CK19	Cytokeratin 19
Col-IV	Collagen IV
CoxIV	Complex IV
CytC	Cytochrome c
DDC	3,5-diethoxycarbonyl-1,4-dihydro-collidine
DEN	Diethylnitrosamine
DNMT	DNA methyltransferase

DSS	Dextran sodium sulfate
erUPR	Endoplasmic reticulum upfolded protein response
ER	Estrogen receptor
Erk1/2	Extracellular signal-regulated kinase 1/2
FADD	Fas-Associated protein with Death Domain
Gpx	Glutathione peroxidase
GS	Glutamine synthetase
HAT	Histone acetyltransferase
HBV	Hepatitis B virus
HCC	Hepatocellular carcinoma
HCC-CC	Hepatocellular carcinoma and cholangiocarcinoma
HCV	Hepatitis C virus
HDAC	Histone deacetylase
HE	Hematoxylin eosin
HGF	Hepatocyte growth factor
Hnf4α	Hepatocyte nuclear factor 4 alpha
HSP	Heat shock protein
ICC	Intrahepatic cholangiocarcinoma
Ig	Immunoglobulin
IKK	IκB kinase
IL	Interleukin
JAK1	Janus kinase 1

JNK	c-Jun N-terminal kinase
LPC	Liver progenitor cell
LTα	lymphotoxin α
LTβ	Lymphotoxin β
LTβR	Lymphotoxin β receptor
MAPK	Mitogen activated protein kinase
mt	Mitochondrial
NASH	Non-alcoholic steatohepatitis
NF-κB	Nuclear factor-κB
NIK	NF-κB-inducing kinase
Nqo1	NAD(P)H dehydrogenase 1
NuRD	Nucleosome-remodeling HDAC
OSM	Oncostatin M
p-	Phosphorylated
PCR	Polymerase chain reaction
PDAC	Pancreatic ductal adenocarcinoma
PERK	PKR-like endoplasmic reticulum kinase
PKR	Protein kinase RNA
SIRT	Sirtuin
SOD	Superoxide dismutase
Srxn1	Sulfiredoxin 1
STAT	Signal transducer and activator of transcription

TdT	Terminal deoxynucleotidel transferase
TFAM	Mitochondrial transcription factor A
TGFβ	Transforming Growth Factor β
TLR2	Toll-like receptor-2
TNF	Tumor necrosis factor
TUNEL	TdT-mediated dUTP nick end labelling
UPR	Upfolded protein response
WT	Wild-type

1. INTRODUCTION

1.1 The Liver

1.1.1 Liver functions and architecture

The liver is the largest glandular organ in the body and plays indispensable roles in many processes, including metabolism (e.g. protein synthesis, storage metabolites and detoxification), digestion (e.g. bile secretion), and immune-regulatory function [1, 2]. Accounting for 2 to 5% of body weight, it receives ~1.5 liters of blood every minute via the hepatic artery and portal vein. Nutrients absorbed in the digestive tract are processed in the liver and stored for use by all somatic cells. The liver is also characterized by a unique capacity for regeneration, recovering complete mass and function even under the circumstance that less than one-third of the cells remain uninjured [2-4]. Common liver diseases include hepatitis infection, fatty liver disease, cholestasis, cirrhosis, cancer as well as acute or chronic liver damage from alcohol, aflatoxins, and some drugs [5, 6]. Loss of normal liver architecture is considered to be an important index of certain liver diseases like cirrhosis [7]. Structurally and histologically, the liver architecture is composed of five tissue systems: vascular system, hepatocytes and hepatic lobule, hepatic sinusoidal cells, biliary system, and stroma [7, 8]. Liver cells can be divided into parenchymal cells (hepatocytes), which account for approximately 78% of the liver tissue volume, and non-parenchymal cells, which constitute around 6.3% [9, 10]. Among the non-parenchymal cells, 2.8% are endothelial cells, 2.1% Kupffer cells, and 1.4% hepatic stellate cells [11, 12]. The extracellular space represents approximately 16% of the liver tissue volume [12, 13].

1.1.2 The hepatocyte

Hepatocytes fulfill numerous central metabolic functions of the liver [14]. Hepatocytes are usually considered to be homogeneous. The hepatic lobule, structural and functional unit of the liver, consists of 15–25 hepatocytes forming liver cell plates (Figure 1). Hepatocytes radiate outward from central vein in the center [8, 15]. Portal triads, composed of bile ducts and terminal branch of the hepatic artery and portal vein, distribute regularly at the vertices of the lobules [16]. Between the two cell plates, blood flows from the portal tract to the terminal hepatic venule, forming sinusoid [17]. Sinusoid facilitates the exchange of substances between blood and hepatocytes, which plays essential roles for liver’s metabolism functions [17, 18].

1.1.3 The biliary system and cholangiocytes

The biliary system of the liver functions to deliver hepatocyte-secreted bile to into the gall bladder and small intestine [19]. Biliary epithelial cells, also known as cholangiocytes, accounting for 3.5% of the liver nuclear population, form a continuous surface from the smallest biliary units to the large intrahepatic and extrahepatic bile ducts [20]. Cholangiocytes respond to exposure to microbes though several immunological pathways, leading to cholangiocyte proliferation or loss [21]. In aminal models, cholangiocyte proliferation has been observed following bile duct ligation (BDL) and chronic feeding of bile acids [21, 22]. Malignant transformation of the hyperproliferative cholangiocytes leads to a specialized subtype of liver cancer - cholangiocarcinoma [23].

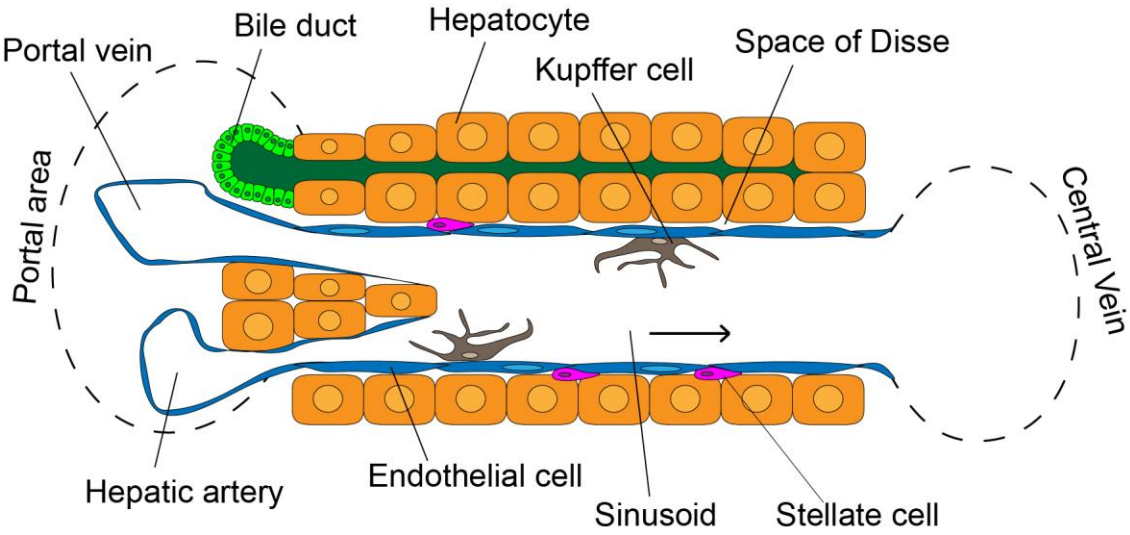

Figure 1. The structure of a hepatic lobule. The hepatic lobule is considered to be the structural and functional unit of the liver. The hepatic lobule is comprised of row of hepatocytes radiating out from central vein. Hepatic artery, portal vein and bile duct are situated around the perimeter of the hepatic lobule, composing the portal area. Blood from hepatic artery and portal vein enters the central vein through sinusoids.

1.1.4 Kupffer cells and TNFα

As the largest population of innate immune cells in the liver, Kupffer cells, or liver-resident macrophages, are crucial cellular components of the intrahepatic innate immune system [24]. Besides the well-studied scavenger and phagocytic functions, macrophages

are activated and secret pro-inflammatory cytokines and growth factors in the setting of tissue damage, virus infection and exposure to toxic agents [25-27]. In adult livers, the majority of inflammatory cytokines such as tumor necrosis factor α (TNFα), IL-1 and IL-6 are secreted by Kupffer cells [27].

TNFα is a powerful pro-inflammatory cytokine which influences host defense and lymphoid tissue organogenesis [28]. TNFα functions through two specific cell surface receptors, a 55 kDa receptor (TNFR1), which is expressed in most cell types, and a 75 kDa receptor (TNFR2), which is restricted to immune and endothelial cells [29]. Engagement of one of the receptors further activates various downstream effectors including Nuclear factor-κB (NF-κB), c-Jun N-terminal kinase (JNK), p38 mitogen activated protein kinase (MAPK) and signal transducer and activator of transcription 3 (STAT3) in a context-dependent manner [30-32]. Most recently, the developmental and homeostatic functions of TNFα in various tissues were identified, which include altering adipocyte differentiation and adipocyte lipid metabolism, establishing hematopoietic stem cell fate in embryonic hematopoiesis and programming postnatal hippocampal development and memory [29, 33, 34]. TNFα and its receptors are also highly expressed in the murine fetal liver, suggesting a possible role of TNFα signaling in fetal liver development [35]. Production of TNFα by Kupffer cells increases upon various pathological conditions including liver injury, virus infection and exposure to toxic agents such as alcohol and aflatoxin [25, 27, 36, 37]. TNFα has also been implicated in the progression of liver cancer by sensitizing hepatocytes to TNF-related cell death [36-38] and promoting clonal expansion of neoplastic cells [27, 39, 40]. Attenuation of Kupffer cell activation or its downstream TNFα signaling leads to reduced hepatocyte cell death and less compensatory proliferation, thereby limiting liver cancer progression [26, 40-42]. As an important aspect of tissue homeostasis, liver progenitor cell (LPC) proliferation and differentiation are also accompanied by Kupffer cell activation and inflammatory reaction [43-45]. Thereby, how Kuppfer cells and TNFα are involved in these processes is worth investigating.

1.2 Liver Cancer

1.2.1 Classification and epidemiology

Liver cancer is the sixth most common cancer worldwide, with more than 782,000 new cases diagnosed in 2012 (6% of the total) (http://www.cancerresearchuk.org). With

around 700,000 deaths per year, liver cancer is the second leading cancer-related death in the world, following lung cancer (18.2%) [46]. According to morphological and phenotypical criteria, liver cancer may be epithelial, mesenchymal, or mixed. The three types of liver cancer are hepatocellular carcinoma (HCC), intrahepatic cholangiocarcinoma (ICC), and combined hepatocellular carcinoma and cholangiocarcinoma (HCC-CC) [47]. HCC originates from the hepatocytes while ICC originates from the cholangiocytes. HCC-CC possesses the histopathological features of both HCC and ICC coexisting within the same tumor (Figure 2). These three types of liver cancers show distinct clinical features, survival outcome and prognostic factors [48]. Comprehensive genomic profiling of human HCC and ICC samples by next generation sequencing also reveals distinct genomic traits of these two different pathological entities and implies different therapeutic targets [49, 50].

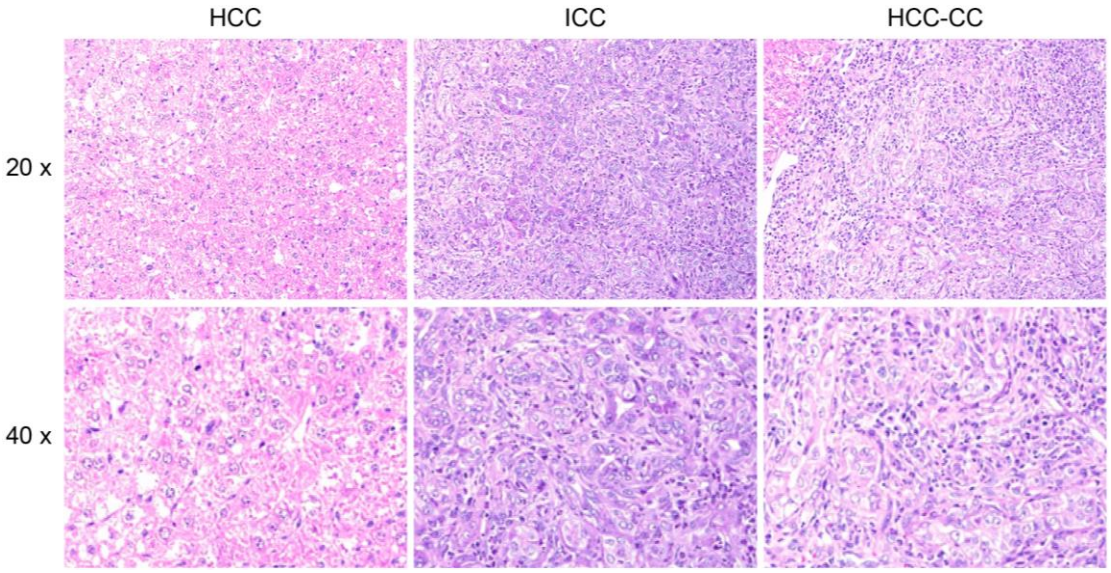

Figure 2. Classification of liver cancers. Liver cancers are highly heterogeneous diseases. Histologically, primary liver cancers are divided into three classes: HCC, ICC and the intermediate type HCC-CC. HCC is featured by a trabecular pattern, while ICC is characterized by a tubular pattern and usually exhibits abundant fibrous stroma. The combined HCC-CC shows both elements, in which the tubular pattern and fibrous stroma is contiguous with a trabecular or solid pattern.

The incidence rate of liver cancer keeps increasing worldwide. A statistical analysis of patients diagnosed with liver cancer in England revealed that the incidence of ICC during

1999~2001 increased by 16-fold compared to that during 1971~1973, while HCC incidence rates increased by 3-fold over the same time period (http://www.ncin.org.uk/). Similar increases in the incidence of HCC and ICC have also been observed in the American and Oceanian populations [51, 52]. Interestingly, the international trends between 1973 and 2007 showed that liver cancer incidence was declining in several Asian populations [52], The differences of trends of liver cancer worldwide are probably due to changes in exposure to risk factors (e.g., HCV transmission in European) and the implementation of preventive measures. Additionally, other possible risk factors such as alcohol consumption, obesity, and nonalcoholic fatty liver disease may also contribute to the burden of liver cancer [53].

1.2.2 Hepatocellular carcinoma

Hepatocellular carcinoma (HCC) is a major health problem, being the second leading cause of cancer-related deaths worldwide. In most cases, human HCC development is driven by chronic liver inflammation. The most prominent inflammatory etiologies linked to HCC include chronic viral hepatitis due to infection with hepatitis B virus (HBV) or hepatitis C virus (HCV) and non-alcoholic steatohepatitis (NASH) [54]. Both hepatitis viruses cause liver injury, inflammation, and cirrhosis and are currently responsible for approximately 80% of HCC cases [55]. Additionally, the epidemic of overweight and metabolic syndrome has emerged as a relevant risk factor, and body-mass index is also significantly associated with higher rates of death due to liver cancer [53]. Still, more than 50% of all HCC cases worldwide arise on the background of a chronic HBV infection.

The link between pro-inflammatory signaling pathways (e.g. NF-κB) in driving chronic inflammation induced HCC development has already be corroborated in several mouse models [26, 56]. Chronic inflammation is one of the most prevalent underlying conditions for tumour development, accounting for approximately 20% of human cancer [57]. Formation of hepatic lymphatic follicles is a prominent pathological hallmark of chronic viral infection, in particular HCV, yet a role for these immune follicles in HCC pathogenesis has not been suggested or explored. Human liver parenchyma infected with HBV or HCV also displays signs of NF-κB activation and it was shown that the HCV RNA polymerase can generate small cellular RNAs that lead to IκB kinase (IKK) activation [58], directly linking viral hepatitis with persistent IKK-NF-κB signaling.

1.2.3 Intrahepatic cholangiocarcinoma

ICC is a highly malignant liver cancer typically diagnosed at therapy-resistant advanced stages, with poor prognosis and increasing incidence worldwide [59-61]. Advanced ICC has limited therapeutic options available at present. The cellular origins and the molecular mechanisms underlying the ICC progression are still poorly delineated [62, 63]. Besides a biliary origin of ICC [64], clinicopathological study has suggested that LPCs are also one of the orgin of ICC [65]. Komuta and colleagues examined the clinicalpathological features of human ICC specimens: over 90% of the ICC showed ductular reaction-like structures, featured by small monotonous and/or anastomosing glands, and were strongly positive for cytokeratin 19 (CK19), a marker for LPCs [66].

Clinical observations also show that ICC can be caused not only by disease affecting bile duct epithelial cells (BECs), such as primary sclerotizing cholangitis, bile duct cysts, and hepatolithiasis, but also by diseases that cause hepatocyte injury, such as hepatitis C or B infection, alcohol abuse, and non-alcoholic steatohepatitis (NASH) [67-69]. Since one of the common features of hepatitis C or B infection, alcohol abuse and NASH is the induction of mitochondrial dysfunction, hepatocytic mitochondrial defect might play a role in liver injury and ICC progression.

1.3 Liver Regeneration, Inflammation and Cancer

1.3.1 Liver regeneration and mouse models

As mentioned above, liver has unique capacity to regenerate even with only one third of the hepatocytes uninjured. The most studied liver regeneration model in rodents is the two-thirds partial hepatectomy model, which was first described by Higgins and Anderson in 1931 [4]. This model remains one of the most widely used models for the study of liver regeneration. In this model, the two largest lobes of the liver, which account for approximates 70% liver mass, are surgically removed. The remaining lobes enlarge and restore the original liver mass over 1~2 weeks after surgery. Notably, the LPCs are not involved in the regeneration process in partial hepatectomy model [70, 71]. Thus it is not suitable to study LPC-mediated liver repair.

Chemical injury models represent another experimental system to study liver injury and regeneration. One commonly used agent is carbon tetrachloride (CCl4), which generates hepatocyte-toxic free radicals followed by centrilobular necrosis and hepatic fibrosis [72].

Compared with partial hepatectomy model, CCl4 injection model induces severe necrosis and acute cholestasis, similar to a subset of clinical liver injury cases [73]. Another agent 3,5-diethoxycarbonyl-1,4-dihydro-collidine (DDC) is also an effective inducer of liver regeneration by causing extensive and prolonged liver damage [74]. In contrast to the other two models mentioned before, liver regeneration in DDC model is considered to be accomplished by both hepatocytes and LPCs [74], thus this model are also used to investigate the roles of LPCs in HCC development, for example by feeding HBx transgenic mice with DDC diet [75].

1.3.2 Molecular pathways underlying liver regeneration

During the last decades, molecular studies of gene expression in regenerating livers have gained insights into various signaling pathways which are activated in different phase of liver regeneration post-surgery. Comparing the gene expression profiles of the liver in priming phase with those in later phase revealed that a series of transcription factors are elevated transiently, while many of others keep highly expressed throughout the regeneration process. Transcription factors that are activated rapidly after operation include NF-κB, STAT3, JNK, extracellular signal-regulated kinase 1/2 (Erk1/2) and receptor tyrosine kinases [76].

IL6/STAT3 pathway during liver regeneration

STAT3 are rapidly activated in the remaining liver within minutes to hours after hepatectomy [77]. IL6 is one of the most important cytokines capable of stimulating STAT3 activation [78]. Once bound to IL6, IL6R activates Janus kinase 1 (JAK1), which then phosphorylates STAT3 [79, 80]. Phosphorylated STAT3 translocates into the nucleus and initiates the transcription program. Impaired liver regeneration was observed in IL6-/- mice, featured by liver necrosis and liver failure, which could be rescued by a single preoperative dose of IL6 administration [77, 81, 82]. Mechanistically, blunted DNA synthesis with depressed activator protein 1 (AP-1), Myc, and cyclin D1 was found only in hepatocytes but not in other non-parenchymal cells, indicating that IL6 is critical for liver regeneration though initiating DNA synthesis response [82].

TNFα signaling during liver regeneration

Studies using type I tumor necrosis factor receptor (TNFR1) knockout mice revealed the role of TNFα signaling in regulating IL6/STAT3 pathway in regenerating hepatocytes [83, 84]. TNFR1 knockout mice displayed severe defects of DNA synthesis and hepatocyte replication during the first 4 days after hepatectomy, leading to >50% lethality. The

remaining animals showed delayed restoration of the liver mass. STAT3 and AP-1 activity were depressed by the lack of TNFR1, which could be reversed by injection of IL6 before operation. Similar phenotype was observed in rats that were given TNFα neutralizing antibody [85]. Pretreatment with anti-TNFα antibodies inhibited c-Jun upregulation and decreased AP-1 DNA binding activity, leading to a delayed regeneration [85]. These studies suggest that TNFα acts in a paracrine way to promote initiation of regeneration by activating cytokine pathways like IL6/STAT3 axis, or by inducing growth-related genes, such as c-Jun.

HGF/Met pathway during liver regeneration

As a well-characterized mitogen for hepatocytes, hepatocyte growth factor (HGF) can induce DNA synthesis and cell replication in cultured hepatocytes. The HGF precursor is rapidly activated by proteases after partial hepatectomy, reaching the peak at 1 hour post-surgery [86]. Mature HGF binds to and activates the receptor tyrosine kinase Met. Liver-specific knockout of Met or pharmacological blockade of HGF by antibodies impaired recovery after liver injury [87].

Conclusion

In addition to the above mentioned pathways, a broad array of developmental signals has also been added into the whole picture, including transforming growth factor β (TGFβ) signal, Wnt/β-catenin pathway, Hedgehog signal and so on. Many of these pathways function redundantly, making the signaling network highly complex. Studying the mechanism underlying liver regeneration not only helps to inform clinical knowledge for patients with severe liver injury, but also provides insight into liver cancer resulted from dysregulation of regeneration pathways.

1.3.3 Pro-inflammatory signaling and LPCs

Inflammatory signaling in the liver is closely linked to tissue repair and regeneration [88, 89]. In livers, Kupffer cells, are the major contributor of pro-inflammatory cytokines and growth factors in the setting of tissue damage, virus infection and exposure to toxic agents [25-27, 90]. Recent studies indicate that various pro-inflammatory pathways can exert their function via directly regulating the adult stem cell proliferation and/or their subsequent lineage commitment [91]. For example, Ferenc and colleagues described a cell-intrinsic role of toll-like receptor-2 (TLR2) signaling in normal intestinal and mammary

epithelial cells and oncogenesis [89]. In a dextran sodium sulfate (DSS) induced mouse colitis model that mimics human inflammatory bowel diseases, TLR2 knockout in the intestinal epithelium significantly impairs regeneration. Consistently, deletion of TLR2 in breast epithelial cells markedly reduces mammary repopulation. Similar phenotype is obtained by ablation of TLR2 downstream targets like MYD88. Notably, inhibition of TLR2 signaling decreases the growth of intestinal tract tumors and breast cancer. These observations suggest that dysregulated inflammation may lead to excessive expansion of stem cell pool for tissue healing, resulting into uncontrolled regeneration and tumorogenesis, and inhibition of inflammatory signaling might have therapeutic value for cancer treatment. In the context of liver homeostasis, previous studies have observed close links between inflammatory response and LPC accumulation during chronic liver injury [44, 45]. However, the underlying signaling mechanisms that link pro-inflammatory signaling and LPC lineage commitment have not been elucidated.

1.4 Mitochondrial Function and Oxidative Stress

1.4.1 Mitochondria and human disease

With the primary function of generating adenosine triphosphate (ATP) through oxidative phosphorylation, mitochondria are essential cellular organelles of eukaryotic cells [92]. Mitochondria are double-membrane organelles which are highly specialized: the outer mitochondrial membrane fully surrounds the inner membrane, separated by the intermembrane in between [93-95]. The outer membrane contains many pore proteins which allow the passage of ions and small molecules, while the inner membrane is impermeable and loaded with proteins involved in electron transport and ATP synthesis. The inner membrane forms cristae to increase the surface area for the transport of electrons, which is considered to be significant for mitochondrial functionality. It also contains various carrier proteins, mediating the transport of metabolites in and out of the matrix space. Mitochondrial matrix is the site of the citric acid cycle, or the Krebs cycle [96]. The citric acid cycle produces the electrons, which enter the electron transport chain by the oxidative phosphorylation system in the inner membrane and produce ATP by ATP synthesis [97, 98]. Additionally, the mitochondrial matrix also contains enzymes involved in synthesis or metabolism of amino acids, ketones, urea, pyrimidines and nucleotides, playing pivotal roles in many key aspects of cellular metabolism, such as iron metabolism and the urea cycle [99].

In particular, mitochondria retain their own genome, named as mtDNA. mtDNA mainly encodes rRNA and tRNA, RNA species required for mitochondrial protein biosynthesis, and a small number of oxidative phosphorylation proteins [100, 101]. The replication of mitochondria is independent of cell cycle but stimulated by energy demand. However, the majority of mitochondrial proteins are encoded by nuclear genes and synthesized in cytoplasm [102, 103]. These newly synthesized proteins are transported into mitochondria with their unfolded conformation. The proper folding of these nuclear encoded mitochondrial proteins takes place in the matrix by mitochondrial chaperones, such as heat shock protein 60 kD (HSP60), HSP70, HSP100 [104].

Genetic defects of mitochondrial functions, especially the oxidative phosphorylation system, affect the efficient production of cellular energy [105]. Mitochondrial disorders not only damage organs with high-energy requirement like brain, muscle, heart and the renal system, but also participate in a variety of age-associated degenerative diseases. In 1959, Ernster described a patient whose skeletal muscle biopsy contained a large excess of mitochondria with abnormal morphology, which is considered to be one of the earliest hints that mitochondrial defects are linked to human disease. The next milestone in understanding the role of mitochondrial disorders was the identification of the first pathogenic mutations in mtDNA associated with human neurological disorders [106]. Notable, the concept of mitochondrial disorders extended into the field of cancer by Otto Warburg who reported that cancer cells exhibited "aerobic-glycolysis" in 1930. Growing evidences indicate that mutations in genes encoding mitochondrial protein contribute to the development of cancer. For example, specific mutations in fumarate hydratase (FH) are associated with hereditary leiomyomatosis and renal cell carcinoma [107, 108].

1.4.2 Mitochondrial unfolded protein response

Protein-folding homeostasis is essential for normal cell functions. Maintenance of protein-folding homeostasis in eukaryotic cells is governed by different signaling pathways related to different cellular compartments [109]. Due to the structural and functional features of mitochondria mentioned above, protein-folding homeostasis in mitochondria is challenged by: 1) complex architecture, 2) reactive oxygen species (ROS) generated from oxidative phosphorylation process and 3) high susceptibility of mtDNA due to the lack of higher-order structure [110-112]. HSP60 and HSP70 are two main components of mitochondrial protein-folding machinery [104, 113]. HSP60, by forming a barrel-shaped complex with HSP10, primarily facilitates the folding of small, soluble

monomeric proteins [114], while HSP70 promotes translocation of the importing polypeptides and prevents their aggregation [115].

Perturbations of mitochondrial protein-folding homeostasis, such as elevated mitochondrial biogenesis and accumulation of oxidized protein by ROS, threaten the mitochondrial environment and function [116-118]. Unfolded or mis-folded proteins are monitored and sensed by a specialized signaling pathway – mitochondrial upfolded protein responses (mtUPR) [119, 120]. mtUPR transduces stress response from mitochondria into nucleus and initiated transcriptional program to balance the protein load and protein-folding machinery [111, 121, 122].

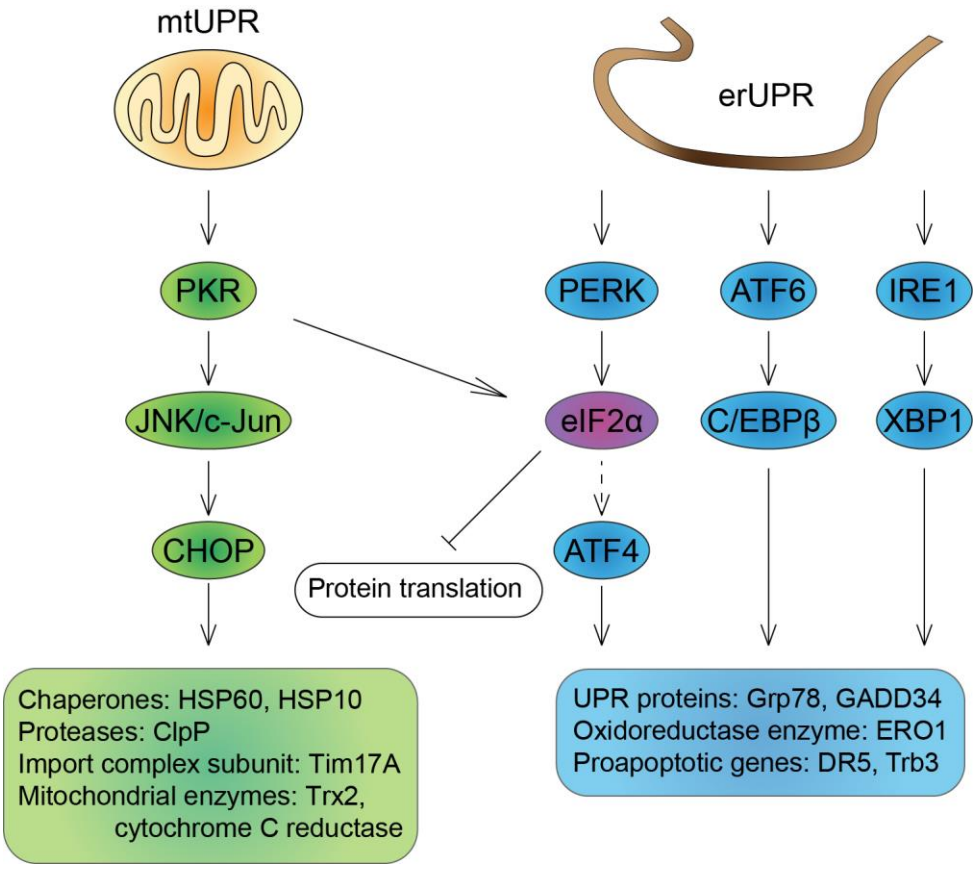

Figure 3. A simplified diagram of the mtUPR and erUPR signaling network. Perturbations of mitochondrial proteostasis activate PKR, which further phosphorylate JNK, leading to increased AP-1 transcriptional activity. CHOP and C/EBPβ are directly upregulated by AP-1. Dimers of CHOP and C/EBPβ induce nucleus events of mtUPR by upregulating mitochondrial chaperones and enzymes. Likewise, accumulation of unfolded proteins in ER triggers three pathways, which sensor the proteostasis state and finally transduce the signal into the nucleus, upregulating ER

chaperones and enzymes. Both mtUPR and erUPR can phosphorylate eIF2α by PKR and PERK irrespectively, resulting into translational attenuation to reduce the protein load of organelles.

In the mammals, upregulation of CHOP and C/EBPβ is suggested to be an early event in the mtUPR, which is transcriptional regulated by c-Jun binding to AP-1 elements in their promoter regions in a JNK2 dependent way [123]. Heterodimer of CHOP and C/EBPβ transcription factors binds to specific mtUPR promoter element and activates the target genes, including HSP60, HSP10, proteases ClpP, the import complex subunit Tim17A, and mitochondrial enzymes Trx2 and cytochrome C reductase [124]. Additionally, accumulation of unfolded proteins in mitochondria activates PKR, which induces global translational attenuation by phosphorylating eIF2α. Tim17A is selectively decreased in response to eIF2α phosphorylation, thereby adapting mitochondrial protein import [125].

mtUPR and endoplasmic reticulum upfolded protein response (erUPR) are closely linked due to the physical interactions between ER and mitochondria [126-128]. It is widely accepted that the protein kinase RNA (PKR)-like endoplasmic reticulum kinase (PERK) signaling pathway within the erUPR can also regulate mitochondria protein-folding homeostasis under the circumstance of ER stress via eIF2α [129]. Particularly, erUPR processes another two signaling pathways - Bip/IRE1/XBP1 pathway and ATP6 pathway - which are rather unique in response to ER stress [130, 131]. These pathways eventually upregulate genes encoding ER chaperones and UPR proteins, such as Grp78, GADD34, ERO1 and Trb3 [128, 131]. A graphic depiction of mtUPR, erUPR and their crosstalk is shown in Figure 3.

1.5 Epigenetic Regulation and Cancer

1.5.1 Epigenetic regulation

The last decades have witnessed a tremendous advance in our knowledge concerning roles of epigenetic regulation in both physiological situations (e.g. development and organogenesis) and pathological situations (e.g. inflammation and cancer). Besides genetic alterations, a broad array of abnormalities in cancer cells (e.g. oncogene activation, silencing of tumor suppressor genes, impairment of DNA repair system and genomic instability) are caused by epigenetic dysregulation [132-135]. Compared to DNA mutations and chromosomal aberrations, epigenetic alterations are reversible, which enable them to be attractive drug targets [136-138].

Epigenetics is defined as “heritable changes in gene activity and expression that occur without alteration in DNA sequence” [139]. Two major aspects of epigenetic modification are: chemical modifications to DNA (e.g. DNA methylation phosphorylation, ubiquitination and sumoylation) and modifications to DNA-associated histone proteins (e.g. histone acetylation and deacetylation).

DNA methylation

DNA methylation, predominantly found in cytosines within CpG dinucleothides, is one of the best characterized epigenetic modifications [140]. CpG sites are not equally distributed in the genome, tending to cluster at the 5’ ends of genes or in the regions of highly repetitive sequences [141]. Methylated CpGs are linked to transcriptional silencing, which is essential for normal development [142, 143]. DNA methylation in heterochromatic regions, in cooperation with histone modification, contributes to condensation of chromatin into heterochromatin [144]. This structure is important for the maintenance of genomic stability [145]. Aberrant patterns of DNA methylation are seen in various human diseases, including developmental abnormality and cancer [146-149]. Particularly, the genome of cancer cells is featured by global hypomethylation [150]. Hypomethylation of CpGs on the promoter of oncogenes and transposons leads to elevated transcription, contributing to genomic instability and tumorigensis [151, 152]. Conversely, hypermethylation of CpGs of tumor suppressor genes leads to the transcriptional silencing of these genes, which is also considered as a hallmark of many human cancers [153].

DNA methylation in mammalians is catalyzed by DNA methyltransferase (DNMT) family, including DNMT1, DNMT3a, and DNMT3b [154, 155]. DNMT1 is responsible for copying DNA methylation patterns to the daughter strands of DNA during DNA replication by recognizing hemimethylated CpGs [156], while DNMT3a and 3b preferentially target unmethylated CpGs, thereby classified as de novo methyltransferases [157]. Genetic deletion of DNMTs in mouse models results in embryonic lethality, emphasizing the importance of DNA methylation for normal embryonic development [157, 158].

Histone modifications

Eukaryotic DNA is organized into nucleosome arrays for proper genome compaction [159]. As the fundamental unit of chromatin, nucleosome comprise approximately 147 bp of DNA wrapped about 1.7 times around the core histone octamer, H2A, H2B, H3 and H4 [159]. Posttranslational modification of these histones regulates the structure of

chromatin as well as its accessibility to other remodeling machinery, fine-tuning many nucleus processes, including DNA replication, transcription, recombination and DNA repair [160, 161].

Compared to DNA methylation, histone modifications are more dynamic. There are several types of modifications on the amino terminals of the core histones, including acetylation, methylation, phosphorylation, ubiquitination, etc [161]. The chromatin immunoprecipitation (ChIP) assay is widely used to study the distribution of specific histone modification on DNA [162]. Combined with the next-generation sequencing technique, ChIP assay can be utilized to investigate the occupancy of the interested histone modification throughout the genome, contributing to a vastly growing knowledge about how histone modification(s) regulate gene expression in a more comprehensive and less-biased way [163].

1.5.2 Histone acetylation and deacetylation

Reversible changes in chromatin structure are essential for transcription, replication and repair in eukaryotes. One of the best-characterized chromatin modifications is histone acetylation and deacetylation, which influence the accessibility of DNA for transcription factors and the general DNA replication machinery [164, 165]. This highly dynamic process, controlled by two types of enzymes - histone acetyltransferases (HATs) and histone deacetylases (HDACs) - is a pivotal part of normal physiology during embryonic development and tissue homeostasis [166]. Deregulation of HATs and HDACs has been extensively investigated in many disorders, including cancer, inflammation and degenerative diseases during the last decades [167, 168]. Several broad-spectrum HDAC inhibitors are currently in various stages of clinical trials for tumor therapy [169-172]. However, considering the pleiotropic cellular effects of different HDACs, it is essential to understand the specific function of individual HDACs in order to design targeted therapeutics with increased potency and minimal side effects [173].

In mammalian, there are 18 members of HDAC family. Based on their sequence similarity to yeast counterparts, these 18 members can be divided into four groups (class I, II, III and IV) [166]. HDACs of class I, II and IV are dependent on Zn^{2+} for deacetylase activity, which are also called classical HDACs [174, 175]; whereas the other 7 NAD^{+}-dependent HDACs, belonging to class III HDACs, are more often referred to as sirtuins (SIRTs) [176]. As shown in Figure 4, class I HDACs, most closely related to yeast

(Saccharomyces cerevisiae) RPD3, comprise HDAC1, 2, 3 and 8; class II HDACs, divided into subclass IIa (HDAC4, 5, 7 and 9) and subclass IIb (HDAC6 and 10), share protein domains with similarity to HDA1. Due to a low sequence similarity to either RPD3 or HDA1, HDAC11 is grouped into class IV [177]. Although closely linked, these 11 classical HDACs differ in structure, subcellular localization and expression patterns. Class I HDACs are expressed in most cell types and localized predominantly to the nucleus [178]. Especially, HDAC1 and HDAC2 show the most degree of homology (approximately 85% similarity) [179]. HDAC1 and HDAC2 generally form homo- and heterodimers between each other in corepressor complexes Sin3, nucleosome-remodeling HDAC (NuRD), CoREST, and PRC2 complexes [180, 181]. Class II HDACs shuttle between nucleus and cytoplasm and exhibit more tissue restricted expression patterns, suggesting roles in the establishment of cell identity [182].

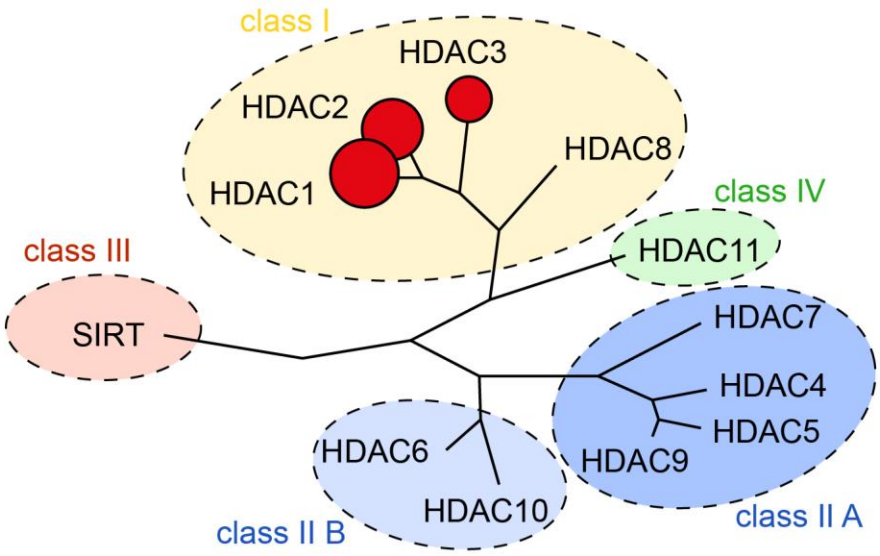

Figure 4. Unrooted phylogenetic tree of mammalian HDACs. Mammalian genome encodes 18 HDACs, which can be divided into 4 classes based on the sequence similary to their yeast counterparts. HDACs in different classes display different expression pattern, enzymatic function and cellular localization. Class I HDACs are expressed ubiquitously and localized in nucleus predominantly, while class II HDACs shuttle between nucleus and cytoplasm and show tissue specific expression. Differing with class I, II, IV HDACs, whose activity depend on Zn^{2+}, class III HDACs, also referred to as SIRTs, require NAD^{+} for their enzymatic function.

1.5.3 HDACs and cancer

Histone hypoacetylation is found in many human cancers [183-185]. In a mouse model of multistage skin carcinogenesis, Fraga M.F. and colleagues showed that loss of monoacetylation of histone H4 is an early event of tumor development, and the extent of hypoactylation accumulates throughout the genome with the cancer progression [186]. In addition, histone hypoacetylation is also linked to tumor invasion and metastasis. For example, a pathological study with human gastrointestinal tumors revealed that reduced histone acetylation correlates with depth of tumor invasion and nodal metastasis [187]. Another study of prostate cancer indicated that histone H3 acetylation is associated with lower recurrence risk [188]. These observations provide a basis for the clinical value of monitoring histone acetylation levels in cancer patients.

Elevated expression of HDACs is one of the explanations for histone hypoacetylation in cancers. Tremendous efforts have been geared toward figuring out the pattern of HDACs expression in human cancers. The levels of individual HDACs vary in different cancer types. Overexpression of HDAC1 has been found in gastric, lung, esophageal, colon and breast cancers [189-191]. HDAC2 is overexpressed in colorectal, cervical, gastric and liver cancers [192-196]. Increased HDAC3 is reported in colon cancer [190]. In addition, HDAC3 expression, coupled with HDAC1, correlates with estrogen and progesterone receptor expression in breast cancer [191]. Other studies have reported high level of HDAC6 in breast cancers and HDAC8 in neuroblastoma [197, 198]. These findings support the idea that HDACs are promising anti-cancer targets.

Overexpression of HDACs contributes to transcriptional repression of tumor suppressor genes by histone hypoacetylation on their promoters, such as cyclin-dependent kinase inhibitor p21, whose expression is lost in many human cancers [199-202]. Another example is E-cadherin, whose expression is repressed by the corepressor complex Sin3A composed of HDAC1, 2 and the transcription factor Snail [203]. HDACs can also exert their function by deacetylating non-histone proteins like p53 [204]. Deacetylation of p53 on lysine 373/382 decreases its stability, thus leading to checkpoint failure and uncontrolled cell proliferation [205, 206].

1.5.4 HDAC2 and HCC

HDAC2, a class I HDAC, represses gene expression by associating with nuclear receptor and ligand-dependent co-repressors, such as NuRD and mSin3 [207-209]. Expression of HDAC2 was reported to be elevated and linked to clinicopathological indicators and patient survival in several cancer types [210-213]. A number of clinical

observations also indicated that the roles of HDAC2 do not completely overlap with the other HDACs. For example, high expression of HDAC1 was associated with improved overall survival in estrogen receptor (ER) -positive breast cancers, while high expression of HDAC2 was correlated with improved overall survival in ER-negative tumors [214]; in pancreatic ductal adenocarcinoma (PDAC), HDAC2, but not HDAC1, confers resistance towards the topoisomerase II inhibitor etoposide [215].

Altered expression of HDAC2 has been frequently observed in HCC and predicts poor prognosis [195, 196]. Particularly, in a study of HDAC1/2/3 and 7 in HCC, HDAC2 is the only independent predictor of patient survival, although the expression of individual HDAC1, 2, and 3 correlates with the clinicopathological factors, such as differentiation status and proliferation index [216]. Moreover, several HCC risk factors like HBV and HCV strongly induce expression of HDAC1/2 [217, 218]. Nowadays, several HDAC inhibitors in clinical trials show highly encouraging and promising benefits in advanced HCC patients [219, 220], thus more studies are required to clarify the specific role of HDAC2 in HCC development to ascertain drug specificity and minimize side effects.

1.6 NF-κB signaling and HCC

1.6.1 NF-κB signaling

NF-κB transcription factors are central regulators and coordinators of cell survival, immunity and inflammation [221, 222]. Generally, in unstimulated cells NF-κB dimers are retained in the cytoplasm in an inactive state through interaction with the IκB inhibitory proteins [223]. A plethora of pro-inflammatory stimuli triggers IKK dependent phosphorylation, ubiquitilation and proteasomal degradation of IκB proteins [224]. Free NF-κB dimers translocate to the nucleus, where they activate target gene transcription [225]. IKK consists of two catalytic subunits, IKKα and IKKβ, and a regulatory subunit, IKKγ/NEMO [226, 227]. While IKKα is not required for activation of NF-κB by most pro-inflammatory stimuli, IKKβ is instrumental for NF-κB activation in most cell types [221, 228]. An alternative, non-canonical NF-κB pathway is known to play an important role in lymphocyte development [229]. In this IKKβ independent pathway, signals from TNF receptor family members, such as Lymphotoxin β receptor (LTβR) and CD40, are integrated by NF-κB-inducing kinase (NIK) [230, 231], which activates IKKα leading to processing of NF-κB2/p100 to the active p52 protein and to nuclear accumulation of p52:RelB dimers [232-234].

1.6.2 NF-κB signaling and HCC

In recent years it has become clear that NF-κB provides a major link between inflammation and carcinogenesis [57, 235, 236]. Activated NF-κB is frequently observed in human HCC in malignant hepatocytes [237-240]. Many NF-κB target genes are implicated in HCC pathogenesis [241], and diminished activity of the NF-κB pathway or its downstream effectors is associated with accelerated apoptosis of malignant cells and improved HCC prognosis [242, 243]. Moreover, activation of NF-κB in HCC adjacent non-tumor tissues correlates with poor prognosis and a high recurrence rate, suggesting that NF-κB activation may play a role in early disease progression [244]. While most of the data points to the role of the canonical NF-κB pathway in HCC, in which p50:RelA (p65) is the predominant heterodimer involved in gene regulation in hepatocytes, some evidence suggests involvement of the non-canonical pathway as well [245].

Oncogenic role of NF-κB signaling in mouse HCC model

Studies aimed at assessing the functional role of the NF-κB pathway in mouse models of HCC, yielded conflicting results, in some cases showing a pro-tumorigenic role, in others an anti-tumorigenic role and still others showing no effect of NF-κB manipulation on HCC formation [236, 246]. A pro-tumorigenic role, linking chronic inflammation and hepatocarcinogenesis, was shown in Mdr2-/- mice, which spontaneously developed hepatitis followed by HCC at a later age, through activation of NF-κB by TNFα secreted from adjacent inflammatory cells [56, 247]. In a different mouse model, transgenic mice over-expressing the cytokines lymphotoxin α (LTα) and lymphotoxin β (LTβ) in a hepatocyte-specific manner developed chronic progressive hepatitis which culminated in HCC [90]. Development of chronic hepatitis as well as HCC in these mice was dramatically dependent on hepatocyte NF-κB, as inhibition of NF-κB by hepatocyte-specific IKKβ ablation completely abolished hepatocarcinogenesis [248, 249]. IKKβ ablation also prevented hepatocarcinogenesis in transgenic mice that express the HCV genome [250]. Notably, the HCV RNA polymerase can generate small cellular RNAs that lead to IKK activation and LTβ induction [58].

Tumor-suppressor role of NF-κB signaling in mouse HCC model

In contrast, in some other models of HCC, in particular those that depend on liver damage and death-driven compensatory proliferation, NF-κB was found to suppress tumor development [246]. Hepatocyte-specific IKKβ ablation markedly enhances HCC

induction in the chemical carcinogenesis model induced by diethylnitrosamine (DEN) which depends on liver injury [26]. The anti-tumorigenic activity of hepatocyte IKKβ was attributed to its protective effect in non-neoplastic hepatocytes via induction of NF-κB-dependent pro-survival and antioxidant genes, thereby suppressing compensatory proliferation of pre-malignant hepatocytes [26]. Similar findings were obtained upon hepatocyte-specific deletion of NEMO/IKKγ. In this case, mice spontaneously developed steatohepatitis followed by HCC, due to the hypersensitivity of NEMO-deficient hepatocytes to Fas-Associated protein with Death Domain (FADD)-mediated and oxidative-stress-dependent death [251]. Finally and of note, expressing a constitutively active IKKβ transgene in hepatocytes had no measurable effect on HCC formation in mice [252]. Thus, the ability of hepatitis viruses to activate NF-κB and the common association of chronic hepatitis with hepatocyte NF-κB activation in human livers, stands in contrast to the current findings in many mouse models of HCC. Furthermore, the contradictory results described above underscore the complex role of NF-κB in hepatocarcinogenesis and the difficulties associated with targeting this pathway in the clinical setting.

2. MATERIALS AND METHODS

2.1 Materials

2.1.1 Reagents

Product	Supplier
Agarose	Peqlab
Alexa Fluor® 594	Life Technologies
Bovine Serum Albumin, BSA	Sigma-Aldrich
DMSO	Sigma-Aldrich
EDTA	Roch
Ethanol	Roth
Fetal Calf Serum	Life Technologies
Fluoromount-G® Mounting Media (+/-Dapi)	Sourthernbiotech
Glucose	Roth
Glutamin 200mm	Gibco
Goat Serum	Life Technologies
Insulin	Sanofi Aventis
Isopropanol	Roth
Methanol	Roth
Non-Essential Amino Acids 100x	Gibco
PBS	Life Technologies
Penicillin/Streptomycin	Biochrom AG
HRP-Substrate	Thermo Scientific
Protein ladder	Thermo Scientific
Sucrose	Roth
Tissue-Tek O.C.T.	Sakura
Triton X-100	Roth

Trizol Reagent	Life Technologies
β-Mercaptoethanol 50mM	Gibco

2.1.2 Cell culture mediums

DMEM complete medium	
DMEM	500 ml
FCS	50 ml
Pen/Strep (5000 I.U. / ml)	5 ml
L-Glutamine (200 mM)	5 ml
NEAA (100x)	5 ml

RPMI complete medium	
RPMI 1640 medium	500 ml
FCS	50 ml
Pen/Strep (5000 I.U. / ml)	5 ml
NEAA (100x)	5 ml

Hepatoblasts culture medium/Basal medium	
William's E Medium	500 ml
FCS	50 ml
Pen/Strep (5000 I.U. / ml)	5 ml
Insulin (40 IU / ml)	320 µl
EGF (20 ng/µl)	500 µl
NEAA (100x)	5 ml

Hepatocytic differentiation medium	
William's E Medium	500 ml
FCS	50 ml

Pen/Strep (5000 I.U. / ml)	5 ml
Insulin (40 IU / ml)	320 µl
EGF (20 ng/µl)	500 µl
NEAA (100x)	5 ml
DMSO	10 ml

Cholangiocytic differentiation medium	
William's E Medium	500 ml
FCS	50 ml
Pen/Strep (5000 I.U. / ml)	5 ml
Insulin (40 IU / ml)	320 µl
EGF (20 ng/µl)	500 µl
NEAA (100x)	5 ml
TNFα (15 ng/ul)	500 µl

Trypsin/EDTA	
10 x solution was diluted 1:10 in bidistilled water	Cat. No. L2153, BiochromeAG, Berlin, Germany

2.1.3 Buffers

Buffer	Composition
RIPA buffer	50 mM TRIS-HCL (pH 7,4), 150 mM NaCl, 0.25% DOC, 1 mM EDTA, 1% NP-40 (Igepal)
RLT buffer	Cat. No. 74106, Qiagen, Germany, Hilden
Lysis buffer for protein extraction	RIPA buffer plus Roche complete protease inhibitor cocktail
Lysis buffer for RNA extraction	RLT buffer plus 1% β-mercaptoethanol
SDS-PAGE running gel	8.1% acrylamide mix, 0.375 M Tris (pH 8.8), 1% SDS, 0.1% ammonium persulfate, 0.04% TEMED
Stacking gel	5% acrylamide mix, 0.125 M Tris (pH 8.8), 0.1% SDS, 1% ammonium persulfate, 0.1% TEMED
3x SDS Loading buffer	0.24 M TRIS-CL (pH 6.8), 6% SDS, 30% glycerol, 16% β-mercaptoethanol, 0.6 mg/ml bromphenol blue

10x Electrophoresis buffer	0.25 M TRIS, 1.92 M glycine, 1% SDS, in distilled water
PONCEAU-S	Cat. No. P-3504, Sigma, Steinheim, Germany
TBST	0.01 M TRIS-HCl (pH 8.0), 0.15 M NaCl, 0.05% TWEEN 20
Blocking buffer	5% Skim Milk in TBST
Antibody dilution buffer	5% BSA in TBST
Transfer buffer	0.3% TRIS base, 1.4% glycin, 20% methanol

2.1.4 Cell lines

Cell line	Description
HepG2	human hepatocellular carcinoma cell line
Huh7	human hepatocellular carcinoma cell line
HepaRG	human hepatocellular carcinoma cell line
STK-1	human intrahepatic cholangiocarcinoma cell line
HuCCT1	human intrahepatic cholangiocarcinoma cell line
&&&	Mouse intrahepatic cholangiocarcinoma cell line

2.1.5 Commercial kits

Cell line	Description
CellTiter-Blue® Cell Viability Assay	Promega, Mannheim, Germany
RNeasy Mini Kit	Qiagen, Hilden, Germany
BCA Protein Assay kit	Thermo Scientific, Ulm, Germany
QuantiTect Reverse Transcription Kit	Qiagen, Hilden, Germany
DNA FFPE Tissue Kit	Qiagen, Hilden, Germany
aCGH Kit	Agilent, California, USA

2.1.6 Devices

Device	Manufacturer
Infinite F200 PRO microplate reader	Tecan, Männedorf, Switzerland
Molecular Imager® ChemiDocTM XRS	Bio Rad, München, Germany
-80°C fridge Herafreeze	Heraeus, Hanau, Germany
-20°C fridge	Liebherr, Switzerland
4°C fridge	Bauknecht, Stuttgart, Germany
Biofuge Fresco Microcentrifuge	Heraeus, Hanau, Germany
Megafuge 1.0	Heraeus, Hanau, Germany
Micro centrifuge MiniStar Silverline	VWR, Darmstadt, Germany
Heracell CO2 Incubator	Thermo Scientific, Ulm, Germany
Herasafe Cell Culture Bench	Thermo Scientific, Ulm, Germany
Vortexer Reax 200	Heidolpf, Kelheim, Germany
7900HT Fast Real Time PCR System	Applied Biosystems, Darmstadt, Germany
Nanodrop 2000 Spectrophotometer	Peqlab, Erlangen, Germany
Thermomixer comfort	Eppendorf, Hamburg, Germany
Microscope Axiovert 25	Zeiss, Jena, Germany
Microscope BX53	Olympus, Hamburg, Germany
SCN400 slide scanncer	Leica Microsystems, Wetzlar, Germany
Automatic Ice Machine AF10	Scotsman, USA
PCR-cycler	Biometra, Göttingen, Germany
Water bath	Memmert, Schwabach, Germany

2.1.7 Antibodies

Antibodies for Western blot:

Target	Species	Dilution	Clone	Company
AFP	goat	1:1,000	polyclonal	R&D, Minneapolis, USA
CHOP	rabbit	1:1,000	D46F1	Cell Signaling, Danvers, MA, USA
c-Myc	mouse	1:500	9E10	Santa Cruz Biotechnology, Heidelberg, Germany

Cyclin D1	mouse	1:200	72-13G	Santa Cruz Biotechnology, Heidelberg, Germany
eIF2a	rabbit	1:1,000	polyclonal	Cell Signaling, Danvers, MA, USA
GAPDH	rabbit	1:1,000	14C10	Cell Signaling, Danvers, MA, USA
HDAC2	rabbit	1:200	polyclonal	Cell Signaling, Danvers, MA, USA
HRP-anti-goat Ig	donkey	1:10,000	polyclonal	Dako, Hamburg, Gemany
HRP-anti-mouse Ig	goat	1:4,000	polyclonal	Cell Signaling, Danvers, MA, USA
HRP-anti-rabbit Ig	goat	1:10,000	polyclonal	Cell Signaling, Danvers, MA, USA
HSP60	goat	1:5,000	N-20	Santa Cruz Biotechnology, Heidelberg, Germany
JNK	rabbit	1:1,000	polyclonal	Cell Signaling, Danvers, MA, USA
LC3	rabbit	1:1,000	polyclonal	Mbl, Woburn, MA
p38 MAPK	rabbit	1:1,000	polyclonal	Cell Signaling, Danvers, MA, USA
p-Akt	rabbit	1:1,000	D9E	Cell Signaling, Danvers, MA, USA
PCNA	rabbit	1:1,000	polyclonal	Santa Cruz Biotechnology, Heidelberg, Germany
p-eIF2a	rabbit	1:1,000	119A11	Cell Signaling, Danvers, MA, USA
p-JNK	rabbit	1:1,000	56G8	Cell Signaling, Danvers, MA, USA
p-p38 MAPK	rabbit	1:1,000	D3F9	Cell Signaling, Danvers, MA, USA
p-RelA	rabbit	1:1,000	93H1	Cell Signaling, Danvers, MA, USA
RelA	rabbit	1:1,000	D14E12	Cell Signaling, Danvers, MA, USA

Antibodies for staining:

Target	Species	Dilution	Clone	Company
8OHdG	mouse	1:100	N45.1	Abcam, MA, USA
B220	mouse	1:3,000	RA36B2	BD Biosciences, San Jose, CA, USA
CD3	rabbit	1:300	SP7	Lab Vision / NeoMarkers, Fremont, CA, USA

CD44v6	rabbit	1:100	polyclonal	Millipore, CA, USA
CD68	rat	1:100	FA-11	Serotec, Puchheim, Germany
CHOP	rabbit	1:1,000	D46F1	Cell Signaling, Danvers, MA, USA
c-Jun	rabbit	1:400	polyclonal	Abcam, Cambridge, UK
cleaved-caspase 3	rabbit	1:300	polyclonal	Cell Signaling, Danvers, MA
c-Myc	rabbit	1:100	Y69	Abcam, MA, USA
Collagen IV	rabbit	1:50	polyclonal	Cedarlane, Burlington, Ontario, Canada
F4/80	rat	1:120	BM8	BMA Biomedicals, Augst, Switzerland
Glutamine Synthetase	rabbit	1:500	polyclonal	Abcam, MA, USA
GP73	goat	1:100	polyclonal	Santa Cruz Biotechnology, Heidelberg, Germany
HSP60	goat	1:4,000	N-20	Santa Cruz Biotechnology, Heidelberg, Germany
Ki67	rabbit	1:500	SP6	Lab Vision / NeoMarkers, Fremont, CA, USA
pan-Cytokeratin	rabbit	1:300	polyclonal	Dako, Hamburg, Gemany
p-JNK	mouse	1:250	56G8	Cell Signaling, Danvers, MA
RelA	rabbit	1:500	polyclonal	Lab Vision / NeoMarkers, Fremont, CA, USA
TNFR1	rabbit	1:1,000	C25C1	Cell Signaling, Danvers, MA
TNFα	rabbit	1:100	polyclonal	Abcam, MA, USA

2.1.8 Primers

Primers for mouse genes

Gene symbol	Sequence
HSP60_F	TCTTCAGGTTGTGGCAGTCA
HSP60_R	CCCCTCTTCTCCAAACACTG
CK19_F	GTCCGCGGTGGAAGTTTTAG

CK19_R	CAGCAGCCCATCAGACACAG
Hnf4a_F	GGTTTAGCCGACAATGTGTGG
Hnf4a_R	TCCCGCTCATTTTGGACAGC
CoxIV_F	ATTGGCAAGAGAGCCATTTCTAC
CoxIV-R	CACGCCGATCAGCGTAAGT
Tfam_F	ATTCCGAAGTGTTTTTCCAGCA
Tfam-R	TCTGAAAGTTTTGCATCTGGGT
Trail_F	ATGGTGATTTGCATAGTGCTCC
Trail_R	GCAAGCAGGGTCTGTTCAAGA
CoxI_F	AGCCTGAGCGGGAATAGTG
CoxI_R	ATGGGCAGTTACGATAACATTGT
Pgc1a-F	TATGGAGTGACATAGAGTGTGCT
Pgc1a-R	CCACTTCAATCCACCCAGAAAG
HSP10-F	AGTTTCTTCCGCTCTTTGACAG
HSP10-R	TGCCACCTTTGGTTACAGTTTC
Grp75-F	ATGGCTGGAATGGCCTTAGC
Grp75-R	ACCCAAATCAATACCAACCACTG
Tid1_F	GCTCGGGCATGGAAACTATCA
Tid1_R	TCTGCACCCTGAATGTGACAA
ClpP_F	GCCTTGCCGTGCATTTCTC
ClpP_R	CTCCACCACTATGGGGATGA
Gadd34-F	GAGGGACGCCCACAACTTC
Gadd34-R	TTACCAGAGACAGGGGTAGGT
p58IPK-F	GGCGCTGAGTGTGGAGTAAAT
p58IPK-R	GCGTGAAACTGTGATAAGGCG
Atf3-F	GAGGATTTTGCTAACCTGACACC
Atf3-R	TTGACGGTAACTGACTCCAGC
Trb3-F	GCAAAGCGGCTGATGTCTG
Trb3-R	AGAGTCGTGGAATGGGTATCTG

Cpt1a-F	CTCCGCCTGAGCCATGAAG
Cpt1a-R	CACCAGTGATGATGCCATTCT
Fasl_F	TCCGTGAGTTCACCAACCAAA
Fasl_R	GGGGGTTCCCTGTTAAATGGG
TNFa_F	CGATGGGTTGTACCTTGTC
TNFa_R	CGGACTCCGCAAAGTCTAAG
Sod1_F	AACCAGTTGTGTTGTCAGGAC
Sod1_R	CCACCATGTTTCTTAGAGTGAGG
Sod2_F	CAGACCTGCCTTACGACTATGG
Sod2_R	CTCGGTGGCGTTGAGATTGTT
Sod3_F	CCTTCTTGTTCTACGGCTTGC
Sod3_R	TCGCCTATCTTCTCAACCAGG
Gpx1_F	AGTCCACCGTGTATGCCTTCT
Gpx1_R	GAGACGCGACATTCTCAATGA
Gpx2_F	GCCTCAAGTATGTCCGACCTG
Gpx2_R	GGAGAACGGGTCATCATAAGGG
Gpx3_F	CCTTTTAAGCAGTATGCAGGCA
Gpx3_R	CAAGCCAAATGGCCCAAGTT
Gpx7_F	TCCGAGCAGGACTTCTACGAC
Gpx7_R	TCTCCCTGTTGGTGTCTGGTT
Ucp3_F	CTGCACCGCCAGATGAGTTT
Ucp3_R	ATCATGGCTTGAAATCGGACC
Nqo1_F	AGGATGGGAGGTACTCGAATC
Nqo1_R	AGGCGTCCTTCCTTATATGCTA
Srxn1_F	CCCAGGGTGGCGACTACTA
Srxn1_R	GTGGACCTCACGAGCTTGG
Tmod1_F	TGAGCTAGATGAACTAGACCCTG
Tmod1_R	CGGTCCTTAAATTCCTTCGCTTG
Slc41a3_F	CTCAGCCTTGAGTTCCGCTTT

Slc41a3_R	GCAGGATAGGTATGGCGACC
Ncf2_F	GCTGCGTGAACACTATCCTGG
Ncf2_R	AGGTCGTACTTCTCCATTCTGTA
TNFR1_F	ACCAAGTGCCACAAAGGAAC
TNFR1 r	CACGCACTGGAAGTGTGTC
PKR_F	ACGCCAGGTTTAACAGCGAT
PKR_R	TTCTGCCAGCGCTTGTACTT
CHOP_F	GCGACAGAGCCAGAATAACA
CHOP_R	GATGCACTTCCTTCTGGAACA
GRP78_F	CTGAGGCGTATTTGGGAAAG
GRP78_R	TCATGACATTCAGTCCAGCAA
s-XBP-1_F	TGACGAGGTTCCAGAGGTG
s-XBP-1_R	TGCACCTGCTGCGGACTCAG
u-XBP-1_F	GCAGCACTCAGACTATGT
u-XBP-1_R	GGTCCAACTTGTCCAGAATGCCC
ERO-1_F	GCGTCCAGATTTTCAGCTCT
ERO-1_R	TCGAAGTGCAAAGGAAATGA
CyclinD1_F	GGGCACCTGGATTGTTCT
CyclinD1_R	CACCGGAGACTCAGAGCA
Sox9_F	AGTACCCGCATCTGCACAAC
Sox9_R	ACGAAGGGTCTCTTCTCGCT
HNF1β_F	CAAGCTCCTCTCCACCCAAC
HNF1β_R	GTGATCTGCATTTTACTGTCAGG
ALDH2_F	AGGGAGCTGGGCGAGTATG
ALDH2_R	TGTGTGGCGGTTTTTCTCAGT
AFP_F	TTTAAACGCCCAAAGCATCAC
AFP_R	GCCTGAACTGACAGAGGAGGA
Aktip_F	AACCCTTTGTGGAGCATGTCT
Aktip_R	CGCTATGGGTAGAGCATTTTTGG

APC_F	CTTGTGGCCCAGTTAAAATCTGA
APC_R	CGCTTTTGAGGGTTGATTCCT
bcl2_F	ATGCCTTTGTGGAACTATATGGC
bcl2_R	GGTATGCACCCAGAGTGATGC
bcl3_F	CCGGAGGCCCTTTACTACCA
bcl3_R	GGAGTAGGGGTGAGTAGGCAG
bcl6_F	CCGGCACGCTAGTGATGTT
bcl6_R	TGTCTTATGGGCTCTAAACTGCT
catenin 1b_F	ATGGAGCCGGACAGAAAAGC
catenin 1b_R	CTTGCCACTCAGGGAAGGA
c-myc_F	TAGAAGGCACAGTCGAGG
c-myc_R	CACCGCCTACATCCTGTCCATTCAAGC
ets1_F	ACAGACTACTTTCGGATCAAGCA
ets1_R	ACGCTCTCAAAAGAGTCCTGG
Fgf10_F	TTTGGTGTCTTCGTTCCCTGT
Fgf10_R	TAGCTCCGCACATGCCTTC
Fgfr_F	GCAGAGCATCAACTGGCTG
Fgfr_R	GGTCACGCAAGCGTAGAGG
Fgfr4_F	TTGGCCCTGTTGAGCATCTTT
Fgfr4_R	GCCCTCTTTGTACCAGTGACG
Fgr_F	CGGCTGAAGAACGCTATTACC
Fgr_R	GGGCGACGAATATGGTCACTC
fos_F	CGGGTTTCAACGCCGACTA
fos_R	TTGGCACTAGAGACGGACAGA
Fyn _F	GAAACCACCAAAGGTGCCTA
Fyn _R	AACTACTAGGCGGCAGCAGA
Hras_F	ATGTGACCCAGCGGCCCTCA
Hras_R	CCGGGACGGGCACAAAGGAC
Ikbkb_F	ACAGCCAGGAGATGGTACG

Ikbkb_R	CGGACTTTGCTACAGGCGAT
Insr_F	ATGGGCTTCGGGAGAGGAT
Insr_R	GGATGTCCATACCAGGGCAC
Jun_F	CCTTCTACGACGATGCCCTC
Jun_R	GGTTCAAGGTCATGCTCTGTTT
JunB_F	TCACGACGACTCTTACGCAG
JunB_R	CCTTGAGACCCCGATAGGGA
Jund_F	GAAACGCCCTTCTATGGCGA
Jund_R	CAGCGCGTCTTTCTTCAGC
kras_F	CAAGAGCGCCTTGACGATACA
kras_R	CCAAGAGACAGGTTTCTCCATC
Lyn_F	GTGACATTGTGGTGGCCTTAT
Lyn_R	ACCATTCCCCATGCTCTTCTA
MAPK_F	TTCAATCATGCAAGATTTGGCTG
MAPK_R	AGTGTAGATCCATAGACTGCCC
mdm2_F	ATCTGCCAGGGGCGGCCTAA
mdm2_R	GCACACTGGGCAGGGCTTGT
myb_F	AGACCCCGACACAGCATCTA
myb_R	CAGCAGCCCATCGTAGTCAT
Mycl1_F	TTCTACGACTATGACTGCGGA
Mycl1_R	TGATGGAAGCATAATTCCTGCC
mycn_F	ACCATGCCGGGGATGATCT
mycn_R	ATCTCCGTAGCCCAATTCGAG
Net1_F	CGGCGAACGAGAGATGCTC
Net1_R	CTCCTTCAAATCAAGGCTGCTA
nras_F	ACTGAGTACAAACTGGTGGTGG
nras_R	TCGGTAAGAATCCTCTATGGTGG
Ntrk1_F	GCACCGTCTCTGCGCTGGTT
Ntrk1_R	GGCTGATTGAGGCGCAGGCA

Ntrk2_F	CTGGGGCTTATGCCTGCTG
Ntrk2_R	AGGCTCAGTACACCAAATCCTA
p53_F	GCTCACTCCAGCCTCCAGCC
p53_R	GGCAGCAGAAGGGACCGGGA
Rab20_F	GGGAGCAGTTTCATGGTCTGG
Rab20_R	GCAGTCATTGTTGGCTGTTTC
Rab24_F	GTGGACGTTAAGGTGGTTATGC
Rab24_R	CCCGATGGTGTTCTGATAGGG
Rab2a_F	GCGACACAGGTGTTGGTAAAT
Rab2a_R	CATCAATCGTTATCATCCGAGCA
Rab3a_F	GTGGGCAAAACCTCGTTCCT
Rab3a_R	TCCTCTTGTCGTTGCGGTAGA
Rab3b_F	CCTCCTTCCTTTTCCGCTATG
Rab3b_R	TCACACGCTTCTCATGGCG
raf1_F	TGGACTCAAAGATGCGGTGTT
raf1_R	AAAACCCGGATAGTATTGCTTGT
Rala_F	ATGGCTGCAAACAAGCCCA
Rala_R	TCCTCTACAAACTCGTCGTACAT
rsu1_F	CCAGCTTGGCGTCTCCCACG
rsu1_R	GGCTGCTAGGGGTTTCCGGC
Ski_F	CAAAACAGACGACACTTCCTCA
Ski_R	CAGCCGAGGCTCTTATTGGAG
src_F	GAACCCGAGAGGGACCTTC
src_R	GAGGCAGTAGGCACCTTTTGT
Thrb _F	CCATTCTGATGTGTGCAAGG
Thrb _R	AAGGCCATGGAAAGGAAAGT
Tfdp1_F	TTGAAGCCAACGGAGAACTAAAG
Tfdp1_R	TGGACTGTCCGAAGGTTTTTG
Tom1_F	CAACGGATCGAGAAAGCTACAG

Tom1_R	CATGTTTCCAAGACCGTAAGGG
tsc2_F	GAGCTGATTAACTCGGTGGTC
tsc2_R	GGCCAGGTCCCTTTCTTCC
Usp4_F	CCTGGGGCCTGCAATGGCTC
Usp4_R	GCCTCTTGTGCCTCGGCTGG
Vav3 _F	CGCCCGCTCCAGAAAGGCAA
Vav3 _R	TGAGCGCACTGCTTCCACGG

Primers for human genes

Gene symbol	Sequence
CD133_F	AGTCGGAAACTGGCAGATAGC
CD133_R	GGTAGTGTTGTACTGGGCCAAT
CK19_F	CAGCCACTACTACACGACCA(20)
CK19_R	GCATTGTCGATCTGCAGGACA(21)
HNF1b_F	AAGGGCACCCCTATGAAGAC
HNF1b_R	AGCTGATCCTGACTGCTTTTGT
HNF4a_F	CGAAGGTCAAGCTATGAGGACA
HNF4a_R	ATCTGCGATGCTGGCAATCT
EpCAM_F	TGATCCTGACTGCGATGAGAG
EpCAM_R	CTTGTCTGTTCTTCTGACCCC

2.2 Methods

2.2.1 Animal housing conditions

Mice were maintained under specific pathogen-free conditions, and experiments were conducted in accordance with the guidelines of the Germany Animal Protection Law and were approved by government of Bavaria (licenses 55.2-1-54-2532-134-14). C57BL/6J mice were purchased from Harlan or obtained from own breedings. R26R-Confetti mice were purchased from Jackson. Tnfr1KO mice (??) and Alb-Cre mice (Haybaeck et al., 2009) were bred in house. We analyzed between 3 and 6 mice per condition in each

experiment. All procedures and protocols were approved by the MGH Subcommittee on Research Animal Care in accordance with NIH guidelines. Injury models…?

2.2.2 Histology and immunohistochemistry

Liver tissue samples were fixed overnight in 4% paraformaldehyde, embedded in paraffin. Paraffin sections were subjected to hematoxylin-eosin or immunohistochemistry staining as previously described (Wolf et al., 2014). Briefly, paraffin sections (2 µm) and frozen sections (5 µm) of livers were used for automated staining performed in the ?? system (bornmax) using the DAB detection kit (bornmax). The following primary antibodies were used: mouse anti-8-OHdG (1:1000 dilution, Abcam); goat anti-AFP (1:1000 dilution, R&D); rabbit anti-CHOP (1:1000 dilution, Cell Signaling); rabbit anti-c-Jun (1:1000 dilution, Cell Signaling); rabbit anti-cleaved Caspase-3 (1:1000 dilution, Cell Signaling); rabbit anti-Collagen Type IV (1:1000 dilution, Cedarlane); rabbit anti- Cytokeratin (1:1000 dilution, Dako); rat anti-F4/80 (1:1000 dilution, BioLegend); rabbit anti- Glutamine Synthetase (1:1000 dilution, Abcam); goat anti-HSP60 (1:4000 dilution, Santa Cruz); rabbit anti-Ki67 (1:200 dilution, NeoMarkers); rat anti-Ly6G (1:1000 dilution, BD); rabbit anti-RelA (1:200 dilution NeoMarkers); rabbit anti-TNFa (1:1000 dilution, Abcam); rabbit anti-c-Myc (1:1000 dilution, Abcam); rat anti-CK19 (1:100 dilution, Developmental Studies Hybridoma Bank). Paraffin-embedded tissue sections were used for staining with 0.1% Sirius red dissolved in saturated picric acid. Oval cell proliferation was detected by A6 staining (1:50), kindly provided by Dr. Valentina Factor. TUNEL assays were performed using the Fluorescein cell death detection kit (Clontech).

2.2.3 RNA isolation from liver tissue

Total RNA from mouse liver samples was isolated using RNeasy Mini kit (Qiagen). The quantity and quality of the RNA was determined spectroscopically using a nanodrop (Thermo Scientific). Purified RNA was reversely transcribed into cDNA using Quantitect Reverse Transcription Kit (Qiagen) according to the manufacturer’s instructions.

2.2.4 Real-time PCR

For mRNA expression analysis quantitative real-time PCR was performed in triplicates in 384-well plates using Fast Start SYBR Green Master Rox (Roche) on a 7900 HT qRT-PCR system (Applied Biosystems, Life Technologies Darmstadt, Germany). Relative mRNA levels were calculated according to the ΔΔCt relative quantification method and were normalized to at least two house-keeping genes (HPRT; RHOT2; GAPDH) levels.

2.2.5 Immunofluorescence microscopy

Deparaffinized and rehydrated slides were subjected to microwave antigen retrieval in 25mM citrate buffer (pH 6.0) and allowed to cool to room temperature. Slides were blocked in TBS containing 0.1% Triton X-100 and 2% serum from the species that the secondary antibody was raised in at room temperature for two hours. After blocking, primary antibodies diluted in TBS with 0.1% Triton X-100 and 2% blocking serum were added overnight at 4°C. After extensive washing, slides were incubated with the secondary antibody in TBS with 0.1% Triton X-100 and 2% blocking serum for 2 hours at room temperature in dark and counterstaining with DAPI. Slides were mounted with Fluoromount-G (SouthernBiotech, Birmingham, Alabama, USA) and images were captured with Olympus FV10i confocal Microscope (Olympus, Germany).

Cells grown on 4-well-glass slide (Lab-Tek II, Fisher Scientific - Germany, Schwerte, Germany) were fixed with 4% paraformaldehyde (PFA) in PBS pH 7.4 for 10 min at room temperature and permeabilized with 0.5% Triton X-100. The staining procedure is as described above for paraffin sections.

2.2.6 RNA in-situ hybridization

Probes for TNFR1, the housekeeping gene ubiquitin C (positive control), the bacterial gene dapB (negative control), and the hybridization kit (RNAscope 2.0 FFPE Assay) were purchased from Advanced Cell Diagnostics. RNA in-situ hybridization was performed using the RNAscope 2.0 technology according to the manufacturer instructions. Briefly, 2 µm paraffin sections were pretreated with heat at 75°C in EZprep buffer for 20 minutes and protease at 37°C for 30 minutes. TNFR1 specific probe pairs (Advanced Cell Diagnostics) were then hybridized at 48°C for 2 hours, followed by a

series of signal amplification and washing steps. Hybridization signals were detected by DAB staining, followed by counterstaining with hematoxylin. Stained slides were scanned into digital images using a Leica SCN400 scanner (Leica) at ×40 magnification.

2.2.7 Measurement of serum parameters

The analysis for AST, ALT, AP, bilirubin, cholesterol, triglycerides and bile acid was performed with mouse serum on a Roche Modular System (Roche Diagnostics) with a commercially available automated colorimetric system at the Klinikum Isar (?) using a Hitachi P-Modul (Roche).

2.2.8 ELISA

TNFα protein levels from liver homogenates were measured using a Quantikine-Elisa-Kit from R&D Systems (Oxon, UK). The procedures closely followed the manufacturer's instructions. The detection limit was 16 pg/ml. The homogenization buffer was tested as a negative control.

2.2.9 Immunoblot analysis

Liver homogenates were prepared by mechanical grinding in RIPA buffer (50 mM Tris; 1% NP40; 0.25% Deoxycholic acid sodium salt; 150 mM NaCl; 1 mM EGTA) containing Halt Protease and Phosphatase Inhibitor Cocktail (Thermo Scientific), and quantified with a BCA protein assay kit (Thermo Scientific) according to the manufacturer's manual. 50 µg protein were denatured in Laemmli buffer containing 5% β-mercaptoethanol and separated by gel electrophoresis and blotted by wet blotting onto nitrocellulose membranes (Bio Rad). Membranes were blocked in 5% milk/TBS-T for at least 1hr at RT. Primary antibodies against HSP60 (Santa Cruz), gp73 (Santa Cruz), cJun (Abcam), p-JNK, JNK, p-Erk1/2, Erk1/2, CHOP, p-p38MAPK, p38MAPK, p-Akt, Akt, GAPDH and PCNA (all Cell Signaling) were incubated at 4°C overnight under shaking conditions. Incubation with the secondary antibody (HRP-anti rabbit IgG, 1:10000, HRP-anti mouse IgG, 1:10000, Jackson; HRP-anti Goat IgG, 1:10000, Dako) was performed under shaking conditions for 1 hr. Detection was achieved with Clarity Western ECL Substrate (Bio Rad) using Stella 3200 imaging system (Bio Rad). To assure equal loading,

membranes reprobed with anti-GAPDH antibody (Cell Signaling) and detected as described above.

2.2.10 Counting proliferating hepatocytes

For quantification of Ki67 staining, slides were scanned using a SCN400 slide scanner (Leica). The total number of Ki67+ hepatocytes was counted at the screen (20x). For each mouse 5 fields were counted.

2.2.11 Isolation, culture and differentiation of hepatoblasts

Isolation of fetal livers (C57BL/6J) at gestation stage E14.5 was done by a modified MACS based immune-isolation protocol [253]. Briefly, fetal livers were dissected, freed of adherent tissue, shredded and subsequently incubated with dispase II (1.6 U/ml) (Sigma) for 1hour at 37°C. Liver specimen were further dispersed by pipetting and filtered three times through a 100 µm Nylon cell strainer (Falcon). The cell suspension was further centrifuges for 10 min at 800 rpm, washed twice using Hepes-buffered (20 mM) (Sigma) DMEM (Dulbecco's Modified Eagle Medium; Gibco) with 0.01% DNase (Roche), and subsequently re-suspended in Hepes-buffered (20mM) (Sigma) DMEM (Dulbecco's Modified Eagle Medium; Gibco) supplemented with 10% FBS (Biochrom) and 1x PenStrep (Life Technologies). Purification of E-Cadherin positive hepatoblasts were performed as described previously [30, 254] using the rat anti-mouse E-Cadherin antibody (clone Decma-1, Merck Millipore). Briefly, anti-rat IgG microbeads were incubated with Decma-1 antibody for 45 min at room temperature on a Intelli-mixer (LTF Labortechnik) and the complexes of primary and secondary antibody were subsequently washed twice times with DMEM (Dulbecco's Modified Eagle Medium; Gibco) supplemented with 10% FBS (Biochrom) and 1x PenStrep (Life Technologies) using a table centrifuge for 10min at 13 rpm. Following the incubation of the cell suspension with the complexed microbeads, the cells were purified using the MACS columns (MS, Milteny Biotec). Cells were washed and afterwards eluded in Hepes-buffered (20mM) (Sigma) DMEM (Dulbecco's Modified Eagle Medium; Gibco).

Isolated hepatocytes were plated onto rat tail type I collagen (Sigma) coated plates. Cells were kept in an undifferentiated state in basal medium composed of Williams' Medium E supplemented with 10% FCS, 10mM nicotinamide, 20 ng/ml mouse EGF

(Roche Diagnostics), and 40 IU / ml insulin (Sigma Chemical Company). After 3 days, 0.5% DMSO or 10 ng/ml of recombinant murine TNFα was added into the basal medium to induce differentiation. For JNK inhibition in presence of TNFα, 10 μM of SP600125 (abcam) was added. Cells were kept in basal medium or differentiation medium for another 7 days until harvest, changing the culture medium daily.

2.2.12 Statistical Analysis

Statistical analyses were performed with Prism software (Graphpad Prism version 5.0a). The standard error of the mean was calculated from the average of at least 3 independent samples per condition. To evaluate statistical significance, data was subjected to Student's t-test (unpaired, two-tailed test). Human specimens were compared using the chi-square test. A p-value of less than 0.05 was considered significant.

3. RESULTS

3.1 Mitochondrial defects in hepatocytes cause cholangiolar hyper-proliferation via Kupffer cell-mediated paracrine TNFα signaling

3.1.1 HSP60 deficiency leads to acute liver damage, hepatic proliferation and cholangiolar hyperplasia

To study the role of mitochondria defect in the liver, we generated mice carrying hepatocyte-specific deletion of *HSP60* (designated HSP60$^{\Delta Hep}$) by crossing Alb-Cre transgenic mice [255] with mice bearing *HSP60* with floxed exon 4 to 8 (Figure 5A). Polymerase chain reaction (PCR) analysis of livers and tails from newborn HSP60$^{\Delta Hep}$ mice confirmed that excision of *HSP60* exons was complete and specific (Figure 5B, C). Quantitative PCR (qPCR) and Western blot analysis revealed loss of *HSP60* transcript and protein in 6-week old livers (Figure 5D).

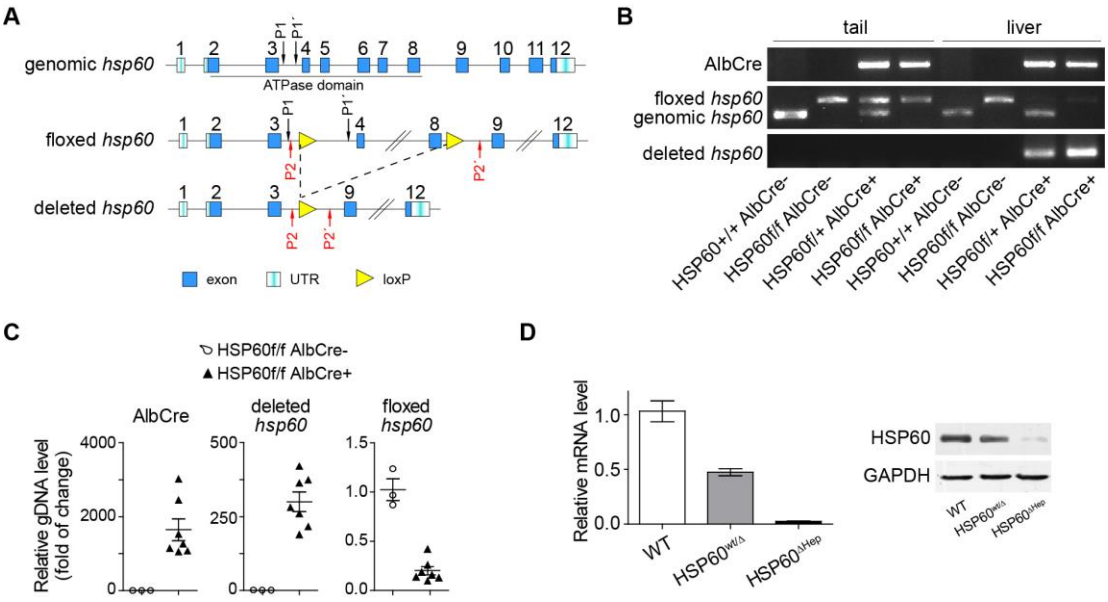

Figure 5. Efficient deletion of HSP60 in hepatocytes of HSP60$^{\Delta Hep}$ mice.

(A) Schematic representation of genomic *hsp60* (top), floxed *hsp60* and deleted *hsp60* (bottom) alleles. Exons are represented by blue boxes. The primer pairs detecting the floxed alleles (P1 and P1') and the deleted alleles (P2 and P2') are shown.

(B) Genotypes were determined by PCR using tail genomic DNA and liver genomic DNA from the mice as indicated.

(C) Relative DNA levels of *cre*, floxed *hsp60* alleles and deleted *hsp60* alleles were determined by qPCR with liver genomic DNA from HSP60f/f AlbCre^{-} mice and HSP60f/f AlbCre^{+} mice.

(D) qPCR and Western blot of whole liver lysates from 6-week-old HSP60$^{\Delta Hep}$ mice, HSP60$^{\Delta Hep/+}$ mice and control littermates (WT).

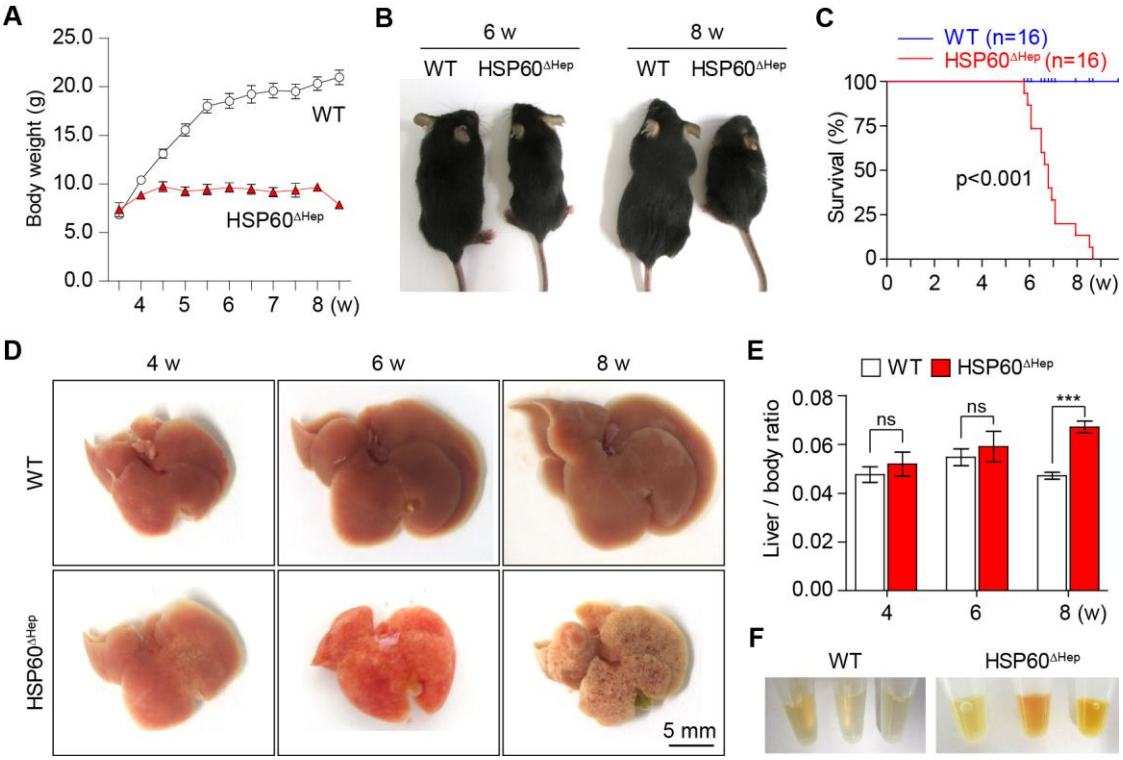

Figure 6. Chronic liver damage and cholestasis in HSP60$^{\Delta Hep}$ mice.

(A) Body weights of HSP60$^{\Delta Hep}$ mice and control littermates were measured.

(B) Representative photograph of 6- and 8-week-old HSP60$^{\Delta Hep}$ mice and WT littermates.

(C) Kaplan-Meier survival curve of HSP60$^{\Delta Hep}$ mice and WT mice.

(D) Macroscopic appearance of livers from postnatal 4-week-old (4 w), 6-week-old (6 w) and 8-week-old (8 w) HSP60$^{\Delta Hep}$ mice and control littermates (WT).

(E) Liver weight to body weight ratios of 4-, 6- and 8-week-old HSP60$^{\Delta Hep}$ mice and WT littermates.

(F) Representative images of serum from 8-week-old HSP60$^{\Delta Hep}$ mice and WT littermates.

At later stages of postnatal development (6 to 8 w), the overall behavior of HSP60$^{\Delta Hep}$ mice changed tremendously, as indicated by weakness and loss of body weight from the age of 6 weeks (Figure 6A, B). 8-week old HSP60$^{\Delta Hep}$ mice had to be euthanized due to the severe body weight loss (Figure 6C). We then characterize in more detail why animals die on HSP60 disruption. On dissection, signs of focal macroscopic liver

necrosis were evident as early as at postnatal week 4 (4 w) in HSP60$^{\Delta Hep}$ mice (Figure 6D). At 8 weeks of age, pale livers were evident, with significantly higher liver to body ratio and yellow colored serum indicative of cholestasis (Figure 6D~F).

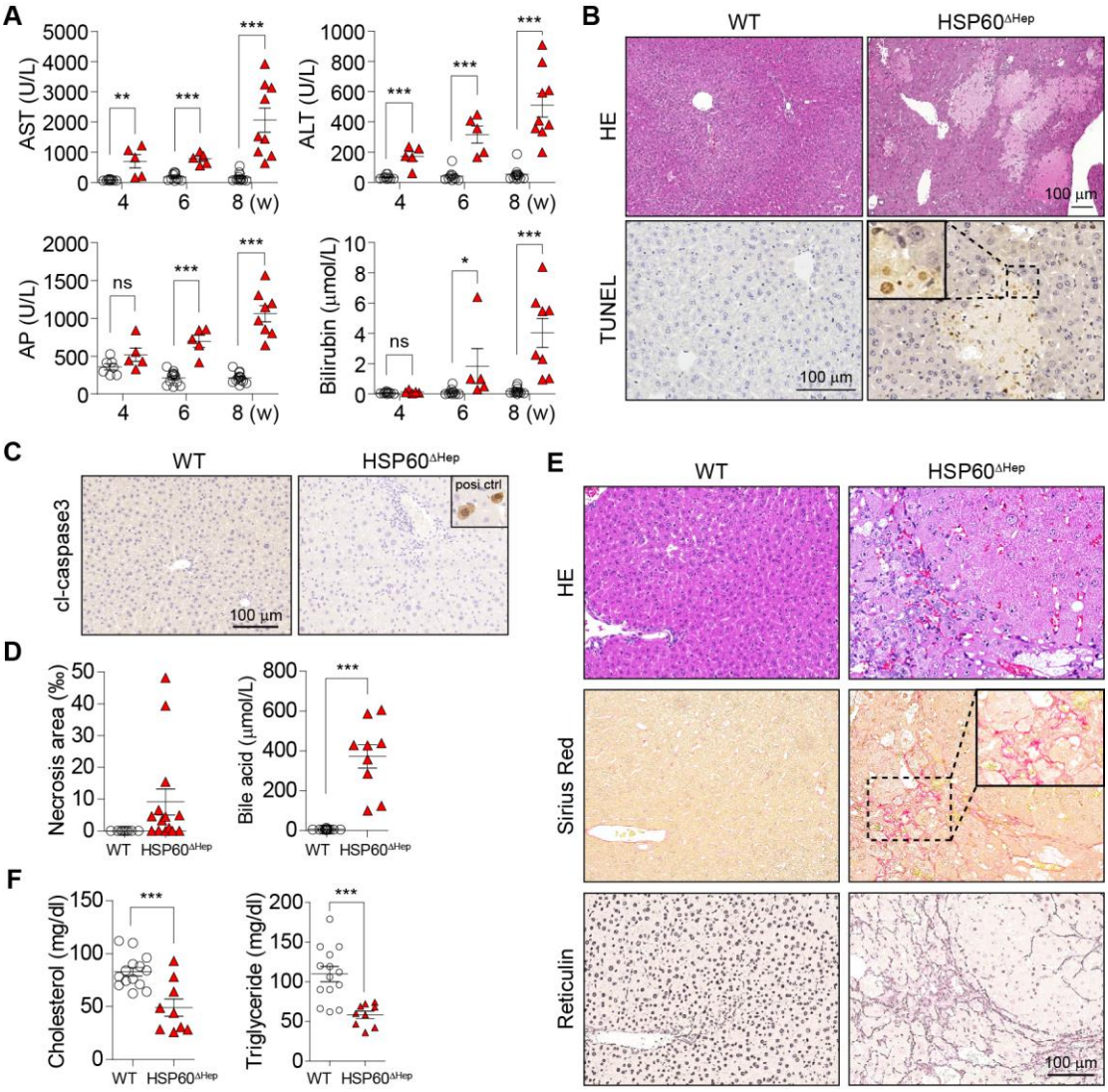

Figure 7. Hepatocyte cell death, fibrosis and disruption of liver functions in HSP60$^{\Delta Hep}$ mice.

(A) Serum levels of AST, ALT, AP and Bilirubin in 4-, 6- and 8-week-old HSP60$^{\Delta Hep}$ mice and control littermates.

(B) Hematoxylin-eosin and TUNEL staining of liver sections from 8-week-old HSP60$^{\Delta Hep}$ mice and WT littermates.

(C) Cleaved-caspase3 (cl-caspase3) staining of liver sections from 8-week-old HSP60$^{\Delta Hep}$ mice and WT littermates.

(D) Left: Quantification of necrotic areas in HSP60$^{\Delta Hep}$ mice and WT littermates. Right: Serum levels of cholesterol in HSP60$^{\Delta Hep}$ mice and WT littermates.

(E) Sirius red and reticulin staining of liver sections from 8-week-old HSP60$^{\Delta Hep}$ mice and WT littermates.

(F) Serum levels of cholesterol and triglyceride in 8-week-old HSP60$^{\Delta Hep}$ mice and control littermates.

Analysis of biochemical parameters showed progressive increase of aspartate and alanine aminotransferase (AST and ALT), alkaline phosphatase (AP) and bilirubin levels in the serum (Figure 7A), indicating hepatocyte cell death and obstruction of the biliary ducts in livers of HSP60$^{\Delta Hep}$ mice. Hematoxylin eosin (HE) staining and terminal deoxynucleotidel transferase (TdT)-mediated dUTP nick end labelling (TUNEL) revealed widespread hepatocyte cell death (Figure 7B). Immunohistochemistry staining against cleaved caspase-3 showed no obvious staining, indicating that the HSP60 defective hepatocytes mainly underwent necrosis but not apoptosis (Figure 7C, D). In addition, fibrillary collagen deposition was detected by Sirius red staining and reticulin silver staining at week 8 postnatal, highly resembling fibrotic livers (Figure 7E). Hepatocyte death and bile duct defect correlated with the disruption of liver functions, as indicated by reduced levels of cholesterol and triglyceride, and elevated bile acid level (Figure 7D, F).

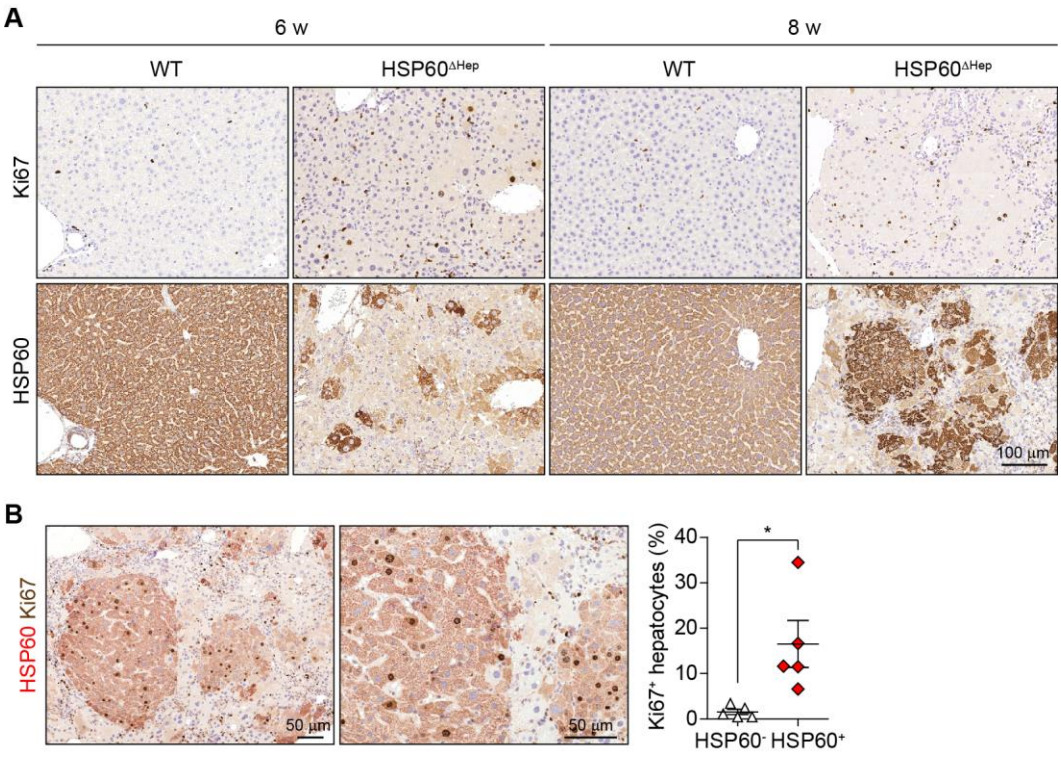

Figure 8. Focal areas of liver regeneration in HSP60$^{\Delta Hep}$ mice.

(A) Representative immunohistochemistry staining of consecutive liver sections from 6- and 8-week-old HSP60$^{\Delta Hep}$ mice and WT littermates with Ki67 and HSP60 antibodies.

(B) Double staining of HSP60 (red) and Ki67 (brown) of liver sections from 8-week-old HSP60$^{\Delta Hep}$ mice and WT littermates. Quantification of Ki67^{+} hepatocytes is shown in the right panel.

Notably, focal areas of liver regeneration were observed (Figure 8A). Immunohistochemistry demonstrated that the Ki67^{+}, proliferating hepatocytes, which further formed regenerative nodules in livers of 8-week-old HSP60$^{\Delta Hep}$ mice (Figure 8B), were positive for HSP60 protein expression, while the other HSP60 negative hepatocytes were seldomly positive for Ki67 (Figure 8C).

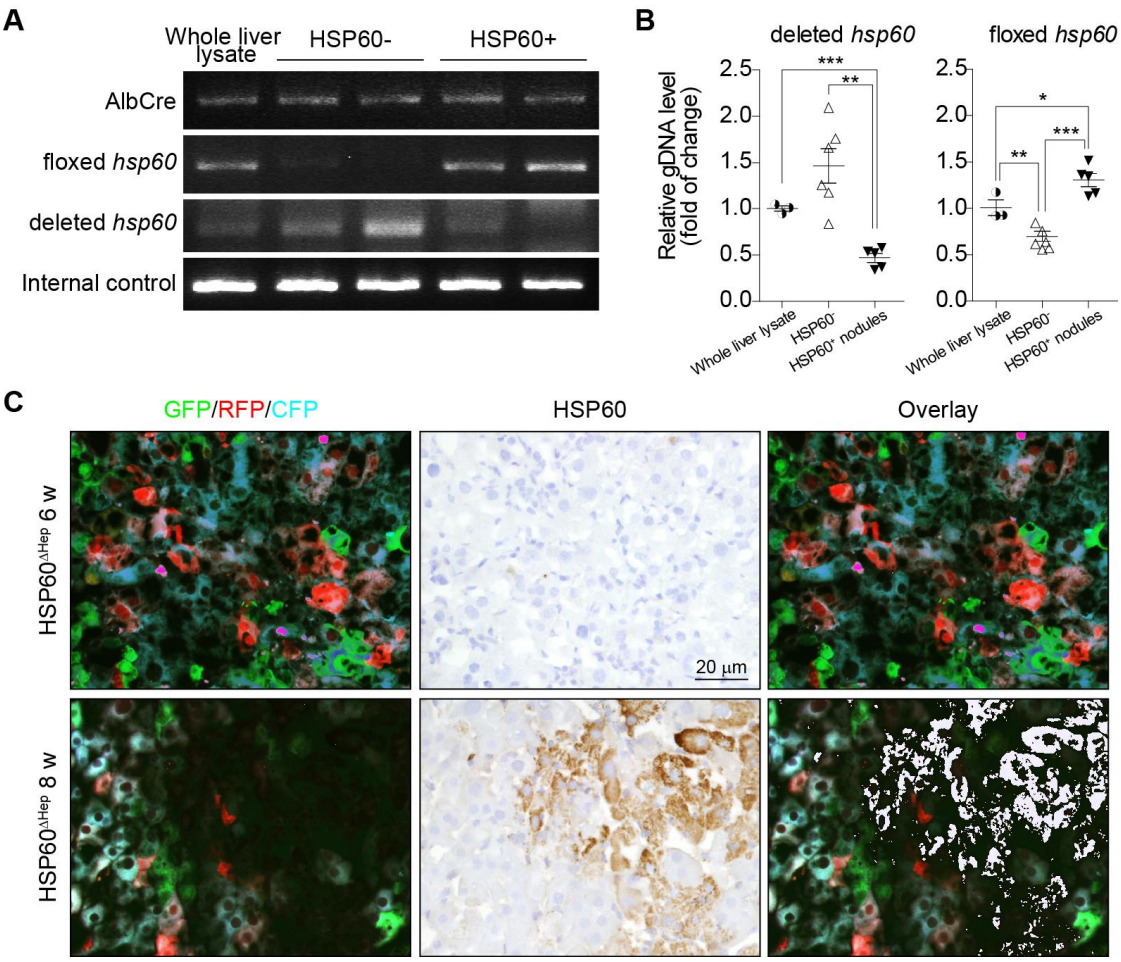

Figure 9. Lack of Cre-mediated recombination event in HSP60^{+} hepatocytes.

(A) Genotypes were determined by PCR using genomic DNA from HSP60^{+} areas and HSP60^{-} areas of the 8-week-old HSP60$^{\Delta Hep}$ livers.

(B) Relative DNA levels of floxed *hsp60* alleles and deleted *hsp60* alleles were determined by qPCR with genomic DNA indicated as in (K).

(C) Representative microscopy of liver sections from 6- and 8-week-old HSP60$^{\Delta Hep}$ -confetti mice. Unlabelled hepatocytes in 8-week-old HSP60$^{\Delta Hep}$-confetti liver stained positive with HSP60.

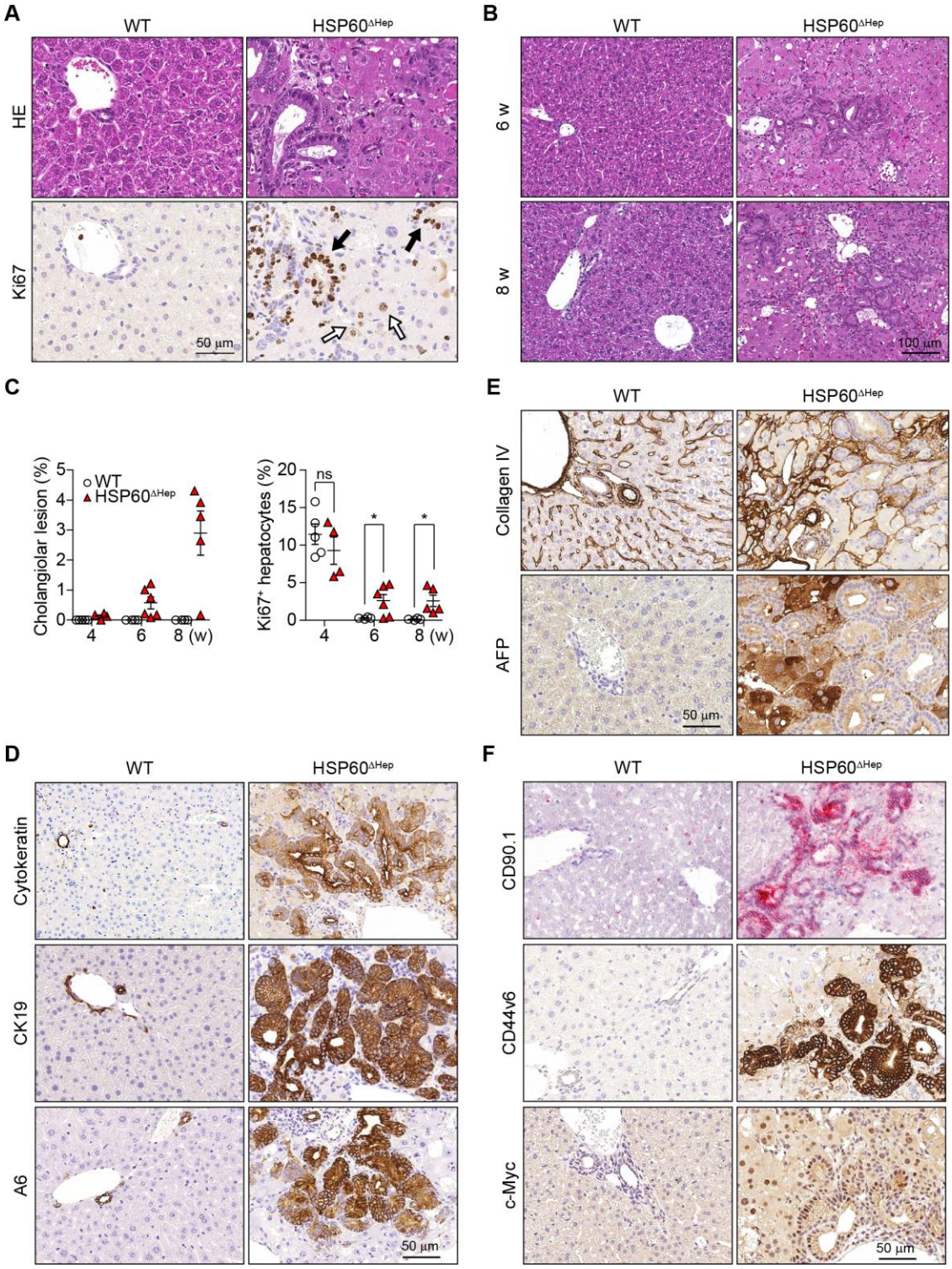

Figure 10. Cholangiolar hyperproliferation in HSP60$^{\Delta Hep}$ mice.

(A) Hematoxylin-eosin and corresponding Ki67 staining of liver sections from 8-week-old HSP60$^{\Delta Hep}$ mice and WT littermates. Ki67^{+} cholangiocytes are indicated with black arrows, while Ki67+ hepatocytes are indicated with white arrows.

(B) Hematoxylin-eosin staining of liver sections from 6- and 8-week-old HSP60$^{\Delta Hep}$ mice and WT littermates.

(C) Quantification of cholangiolar overgrowth areas and Ki67^{+} hepatocytes over time in HSP60$^{\Delta Hep}$ mice and WT littermates.

(D) Immunohistochemistry analysis of biliary lineage markers cytokeratin, CK19 and A6 in liver sections from 8-week-old WT and HSP60$^{\Delta Hep}$ mice.

(E) Collagen IV and AFP stainings of liver sections from 8-week-old HSP60$^{\Delta Hep}$ mice and WT littermates.

(F) Immunohistochemistry analysis of cancer initiating cell markers CD90.1, CD44, and oncogene c-Myc in liver sections from 8-week-old WT and HSP60$^{\Delta Hep}$ mice.

We dissected tissues containing regenerative nodules as well as the surrounding HSP60 negative hepatocytes. Genotyping by PCR analysis and qPCR analysis revealed that the *HSP60* alleles were almost intact in the regenerative hepatocytes, while the excision of *HSP60* exons was complete in HSP60 negative regions (Figure 9A, B). To further determine that the Ki67 positive hepatocytes originated from Cre- negative escaper cells, we crossed the HSP60$^{\Delta Hep}$ mice with Confetti mice, a stochastic multicolor Cre recombinase reporter of multiple fluorescent proteins [256]. The HSP60^{-} hepatocytes were labelled with multi-colored fluorescent proteins, whereas the HSP60^{+} haptatocytes in 8-week-old HSP60$^{\Delta Hep}$ mice were unlabeled, further supporting the lack of Cre-mediated recombination event in these cells (Figure S1M). The re-emergence of HSP60 positive hepatocytes was in line with the previous reports that Cre- recombinase mediated excision was inefficient in LPC-derived regenerative livers resulting in the above described phenotype [257-259].

In parallel with the Ki67^{+}, proliferating hepatocytes, marked expansion of cholangiolar cells was observed, with strands or trabeculae of cells with scant cytoplasm and hyperchromatic nuclei by 7~8 weeks of age (Figure 10A~C). The glandular areas showed immune-reactivity for A6 and CK19, and were negative for α-fetoprotein (AFP), reflecting biliary differentiation of these cells (Figure 10D, E). Furthermore, these glandular areas co-stained for the validated cancer progenitor markers CD44 and CD90.1, and oncogene c-Myc, and had a collagen IV (Col-IV) positive stromal reaction like the human intrahepatic cholangiocarcinoma (Figure 10E, F).

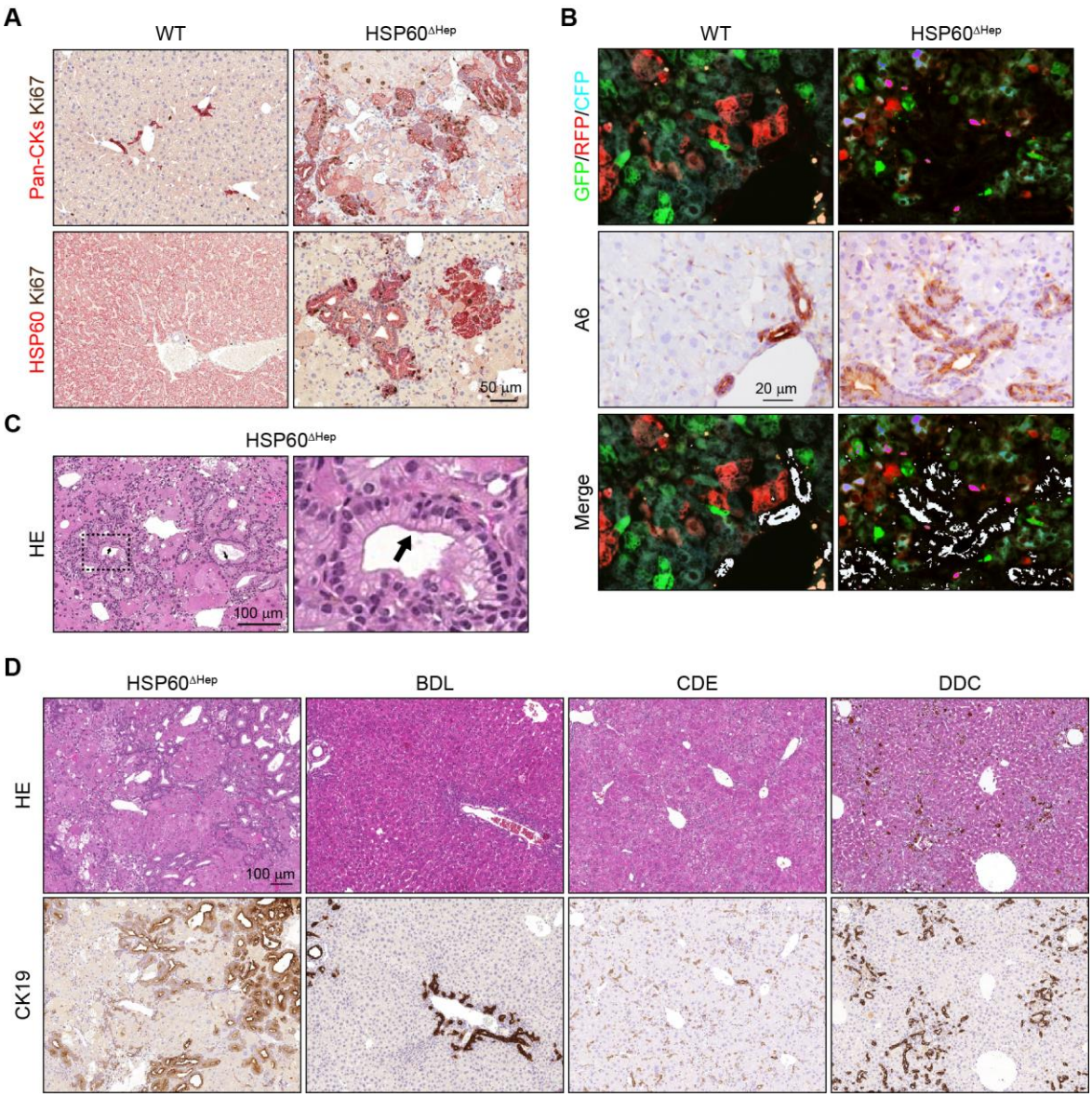

Figure 11. HSP60^{+} Cholangiocytes originate from LPCs in HSP60$^{\Delta Hep}$ mice.

(A) Upper: Double staining of pan-cytokeratin (red) and Ki67 (brown) of liver sections from 8-week-old HSP60$^{\Delta Hep}$ mice and WT littermates; Lower: Double staining of HSP60 (red) and Ki67 (brown) of liver sections from mice as indicated above.

(B) Fluorescence microscopy and A6 staining of liver sections from 8-week-old WT and HSP60$^{\Delta Hep}$ -confetti mice. Unlabelled cholangiocytes stained positive with A6 antibody.

(C) Representative hematoxylin-eosin staining of liver sections from HSP60$^{\Delta Hep}$ mice. Black arrow indicates cholangiocytes with nuclei mis-location.

(D) Hematoxylin-eosin and CK19 staining of liver sections from different mouse liver injury models as indicated.

These cholangiolar cells were highly proliferative and positive for HSP60 (Figure 11A). Tracing with Confetti-HSP60$^{\Delta Hep}$ mice further proved the lack of Cre- recombinase activity in these cells, as well as in the progenitor cells around the ductal plates, indicative of their true LPC origin (Figure 11B). Notably, premalignant cholangiolar lesions, featured by irregular glands, loss of polarity, nuclear atypia and frequent mitosis, were evident in 9-week-old HSP60$^{\Delta Hep}$ livers (Figure 2E). These foci resembled human biliary intraepithelial neoplasia (BilIN), the premalignant condition which ICC arises from, suggesting an initiation of the multistep carcinogenesis progression of ICC in this model [260-262]. Particularly, such cholangiolar lesions was absent in other liver injury models, including DDC or CDE diet model, bile duct ligation (BDL) model (Figure 11D), or genetically engineered mouse models like CYLD knockout mice or Survivin knockout mice [42, 257].

Altogether, these results indicate that livers of HSP60$^{\Delta Hep}$ mice undergo severe hepatocyte death, compensatory hepatic proliferation and cholangiolar hyperproliferation, which was not seen in other liver injury models.

3.1.2 Oxidative stress induces a pro-carcinogenic environment in HSP60$^{\Delta Hep}$ livers

Given the essential function of HSP60 in the transportation and refolding of mitochondrial proteins [263, 264], we then sought to address the role of mitochondrial dysfunction and oxidative stress in the progression of liver damage and cholangiolar hyperplasia. Indeed, ultrastructural analysis revealed severely disrupted mitochondria in HSP60 deficient livers, as evidenced by either fragmented or enlarged, swollen appearance (Figure 12A). Mitochondria in double-membrane autophagosomes or autolysomes, known as mitophagy, were detected (Figure 12A). Several genes implicated in mitochondria homeostasis or mitochondrial respiratory chain, such as mitochondrial transcription factor A (TFAM) and cytochrome c (CytC) oxidase or complex IV (CoxIV), were upregulated (Figure 12B). Consistently, all the mitochondrial stress markers we examined were elevated in HSP60 knockout livers compared to WT, including Grp75, Hsp10, Tid1, CHOP, Gadd34 and ClpP (Figure 12C). In comparison, most of the ER stress associated genes remained unchanged, indicating mtUPR is primarily responsible for HSP60 deficiency (Figure 12C).

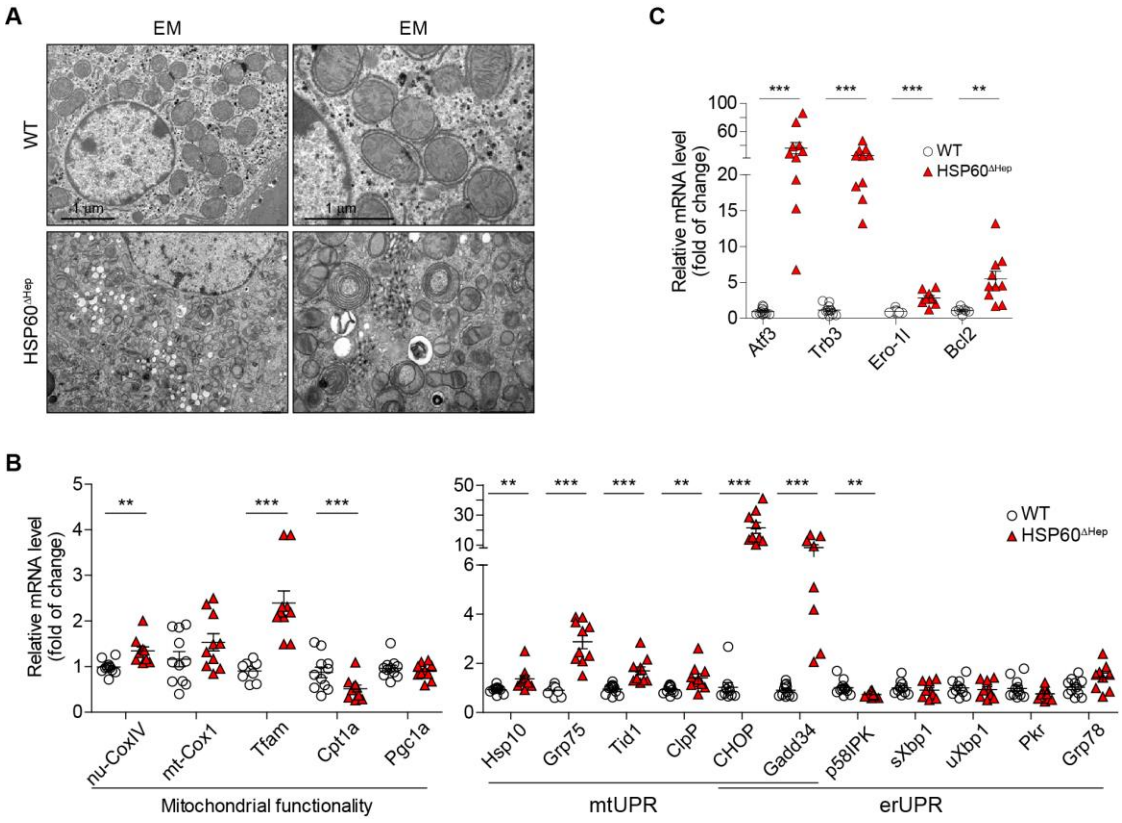

Figure 12. HSP60 deficiency leads to mitochondrial dysfunction and mitochondrial UPR.

(A) Electron microscopy of hepatocytes from 8-week-old WT and HSP60$^{\Delta Hep}$ mice.

(B, C) qRT-PCR of whole liver lysates from 8-week-old HSP60$^{\Delta Hep}$ mice and control littermates for the indicated genes.

Impaired mitochondrial function induces oxidative stress through production of ROS, such as O_2^- and H_2O_2, which consequently upregulate the expression of antioxidant enzymes [265]. As expected, a large panel of antioxidant enzymes, such as superoxide dismutase 3 (SOD3), glutathione peroxidase 2, 3 and 7 (Gpx2/3/7), NAD(P)H dehydrogenase 1 (Nqo1), Sulfiredoxin 1 (Srxn1), was strongly upregulated in HSP60 deficient livers (Figure 13A, B). Oxidized protein level was also much higher upon HSP60 knockout, as determined by oxyblot (Figure 13C). In addition, staining with 8-hydroxy-2-deoxyguanosine (8-OHdG), an indicator of secondary metabolite subsequent to oxidative DNA damage, extensively labelled HSP60 negative hepatocytes (Figure 3D). By Western blot analysis, we further confirmed the early upregulation of phosphorylated eIF2a (p-eIF2a) and CHOP in HSP60$^{\Delta Hep}$ livers from 4 weeks on (Figure 13E).

Increased abundance of LC3 conjugated to phosphatidylethanolamine (LC3-II) was also observed, supporting the ultrastructural evidence of mitophagy in HSP60 deficient hepatocytes (Figure 13E).

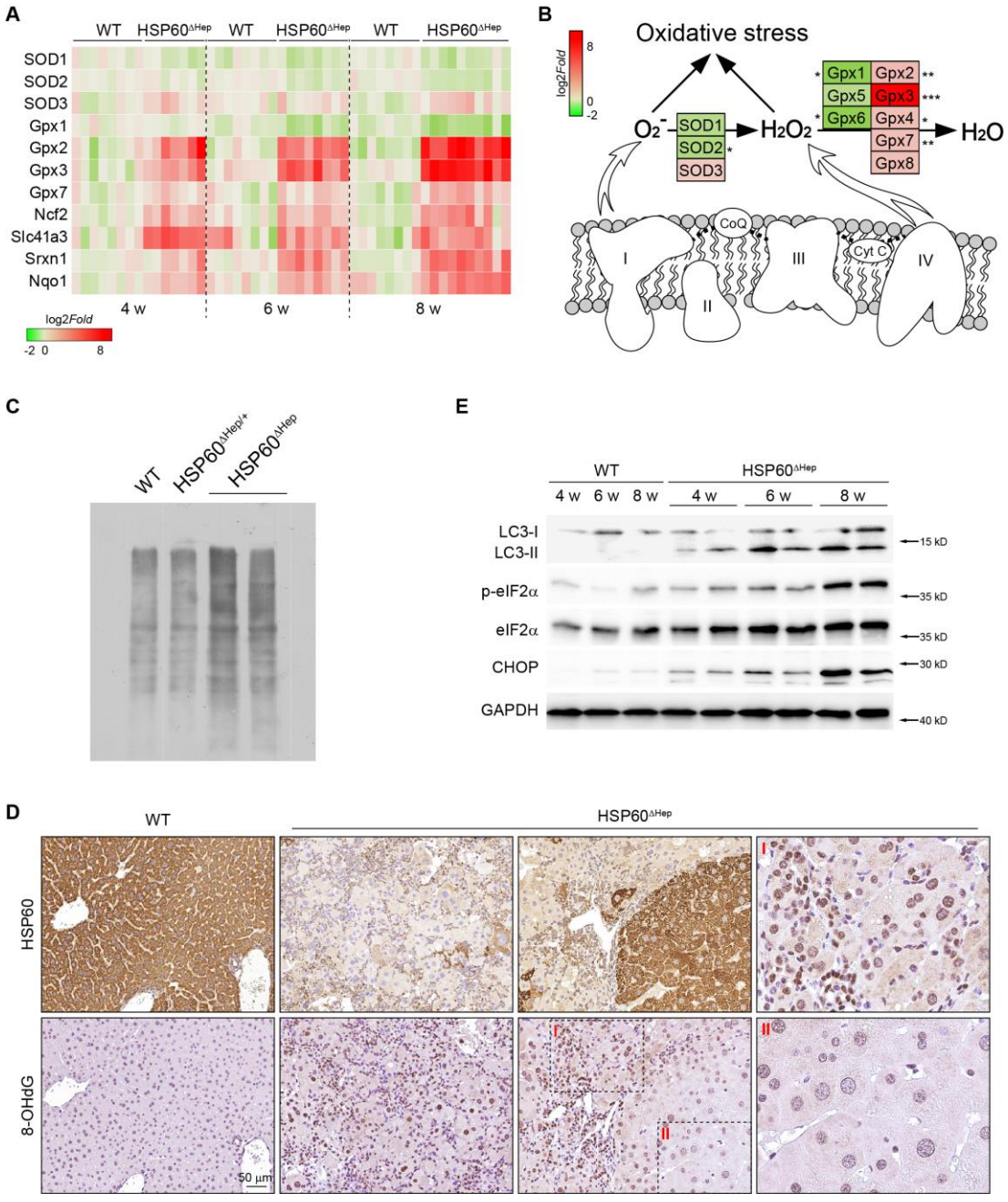

Figure 13. HSP60 deficiency leads to oxidative stress.

(A) Heat map of antioxidant genes in HSP60$^{\Delta Hep}$ livers in comparison with WT livers over time. Gene expression levels by qRT-PCR were present in a color code: red:upregulated, green:downregulated.
(B) Schematic representation of the expression of genes encoding antioxidant enzymes (SOD and Gpx families) in HSP60 KO livers relative to WT livers. Gene expression levels by qRT-PCR were present in a color code: red=upregulated, green=downregulated.
(C) OxyBlot of whole liver extracts from mice indicated.
(D) 8-OHdG staining of liver sections from 8-week-old HSP60$^{\Delta Hep}$ mice and WT littermates.
(E) Whole liver lysates were prepared from HSP60$^{\Delta Hep}$ and WT livers at different ages. Western blot was performed with indicated antibodies.

Prolonged increase of ROS is often associated with activation a variety of stress and oncogenic pathways, including JNK, Erk1/2 and p38 MAPK [266-268]. We next investigated which signaling pathway(s) and oncogene(s) are activated downstream of ROS accumulation in HSP60$^{\Delta Hep}$ livers. Phosphorylation of JNK and Erk1/2, along with the liver cancer markers AFP and GP73, was elevated in livers upon HSP60 knockout from week 4 and onward (Figure 14A). Similar to a previously reported mouse liver injury model induced by CYLD knockout [42], activation of p38 MAPK was absent in HSP60$^{\Delta Hep}$ livers (Figure 14A). Staining of the consecutive sections with HSP60 antibody and p-JNK antibody revealed that most of p-JNK positive cells were HSP60 negative (Figure 14B). Activation of JNK was confirmed by a similar, time dependent upregulation of c-Jun. Besides c-Jun, screening of oncogenes that usually deregulated in liver cancer identified c-Myc, Ras and Src mRNA as most upregulated oncogenes in HSP60$^{\Delta Hep}$ livers (Figure 14C). Staining of c-Jun, c-Myc, Src and AFP by immunohistochemistry further confirmed that the activation of these oncogenic pathways was restricted within HSP60 negative areas and could also be corroborated on protein level (Figure 14D~F). Interestingly, it was recently reported that JNK activation triggered by ROS acts as an environmental factor to promote tumor progression in a cell non-autonomous manner [268]. Therefore, we hypothesized that ROS driven by HSP60 loss induces a regenerative/carcinogenic microenvironment to stimulate the growth of the surrounding wild-type cells.

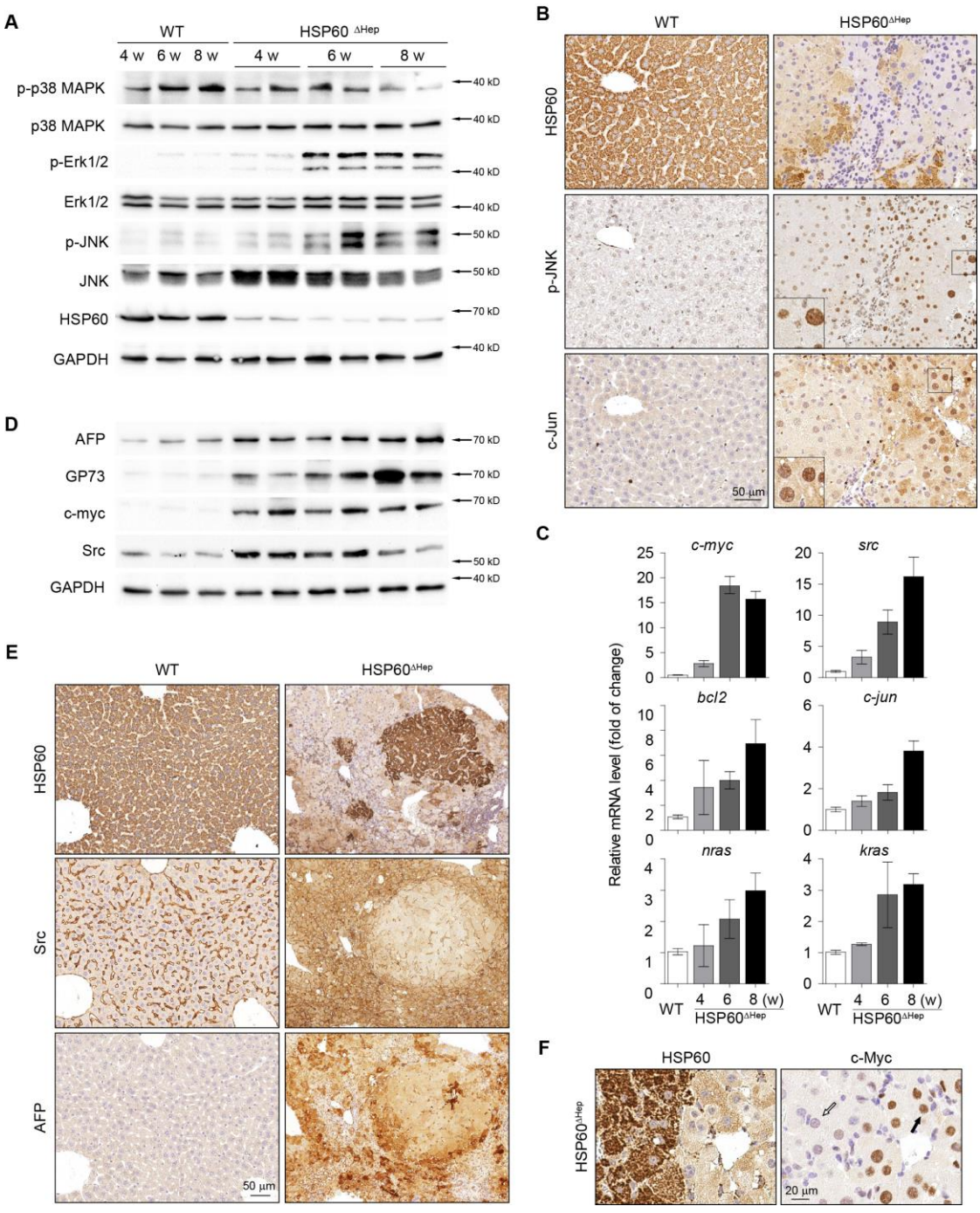

Figure 14. Oncogenic signals in HSP60$^{\Delta Hep}$ livers.

(A) Whole liver lysates were prepared from HSP60$^{\Delta Hep}$ and WT livers at different ages. Western blot was performed with indicated antibodies.

(B) Immunohistochemistry analysis of HSP60, p-JNK and c-Jun in consecutive liver sections from 8-week-old WT and HSP60$^{\Delta Hep}$ mice.

(C) qRT-PCR of whole liver lysates from HSP60$^{\Delta Hep}$ mice and control littermates (WT).

(D) Whole liver lysates were prepared from HSP60$^{\Delta Hep}$ and WT livers at different ages. Western blot was performed with indicated antibodies.
(E) Immunohistochemistry analysis of HSP60, p-JNK and c-Jun in consecutive liver sections from 8-week-old WT and HSP60$^{\Delta Hep}$ mice.
(F) Immunohistochemistry analysis of HSP60 and c-Myc in consecutive liver sections from 8-week-old WT and HSP60$^{\Delta Hep}$ mice.

3.1.3 Anti-oxidant BHA diet attenuates ROS accumulation and cholangiolar hyperplasia

Having implicated the ROS-driven carcinogenic microenvironment in the HSP60$^{\Delta Hep}$ livers, we next examined whether it is functionally significant for the progression of liver injury and cholangiolar overgrowth by feeding HSP60$^{\Delta Hep}$ mice with the antioxidant butylated hydroxyanisole (BHA) containing chow from 4 weeks old on. BHA administration reduced 8-OHdG staining (Figure 15A) and ROS-scavenging enzymes such as GPX3 and SOD3 in HSP60$^{\Delta Hep}$ livers (Figure 15B), indicating an efficient blockade of ROS production and accumulation of secondary ROS metabolites. Remarkably, treatment of HSP60$^{\Delta Hep}$ mice with BHA strongly attenuated liver injury and prevented the early lethality (Figure 15C~E). At 8 weeks of age, hepatocyte cell death was significantly reduced upon BHA treatment as revealed by histological analysis (Figure 15F). Serum levels of ALT, AST and Bilirubin and AP were also reduced in mice fed with BHA-containing diet compared to those with normal diet (Figure 15G).

Moreover, although consumption of BHA-containing diet showed no effect on hepatocyte proliferation or *cyclin d1* mRNA level (Figure 16A), it almost completely blocked the overt proliferation of cholangiolar cells, as revealed by immunohistochemistry staining of A6, and CSC markers CD90.1 and CD44 (Figure 16B, C). Accordingly, *ck19* level was suppressed and hepatocyte nuclear factor 4 alpha (*hnf4α*) and *aldh2* levels were partially rescued at 8 weeks of age (Figure 16D, E). Compensatory proliferation of wild-type hepatocytes kept repopulating the whole liver and the knockout animals finally recovered from the body weight loss at around 18 to 20 weeks (Figure 16F). The rescued mice were kept as long as half a year old and showed no abnormalities compared to wild-type mice, without any proliferation of either hepatocytes or cholangiocytes (Figure 16G). Thus, mitochondrial deficiency induced by HSP60 loss enhances hepatocyte cell death and cholangiolar hyperplasia through a mechanism dependent of ROS accumulation.

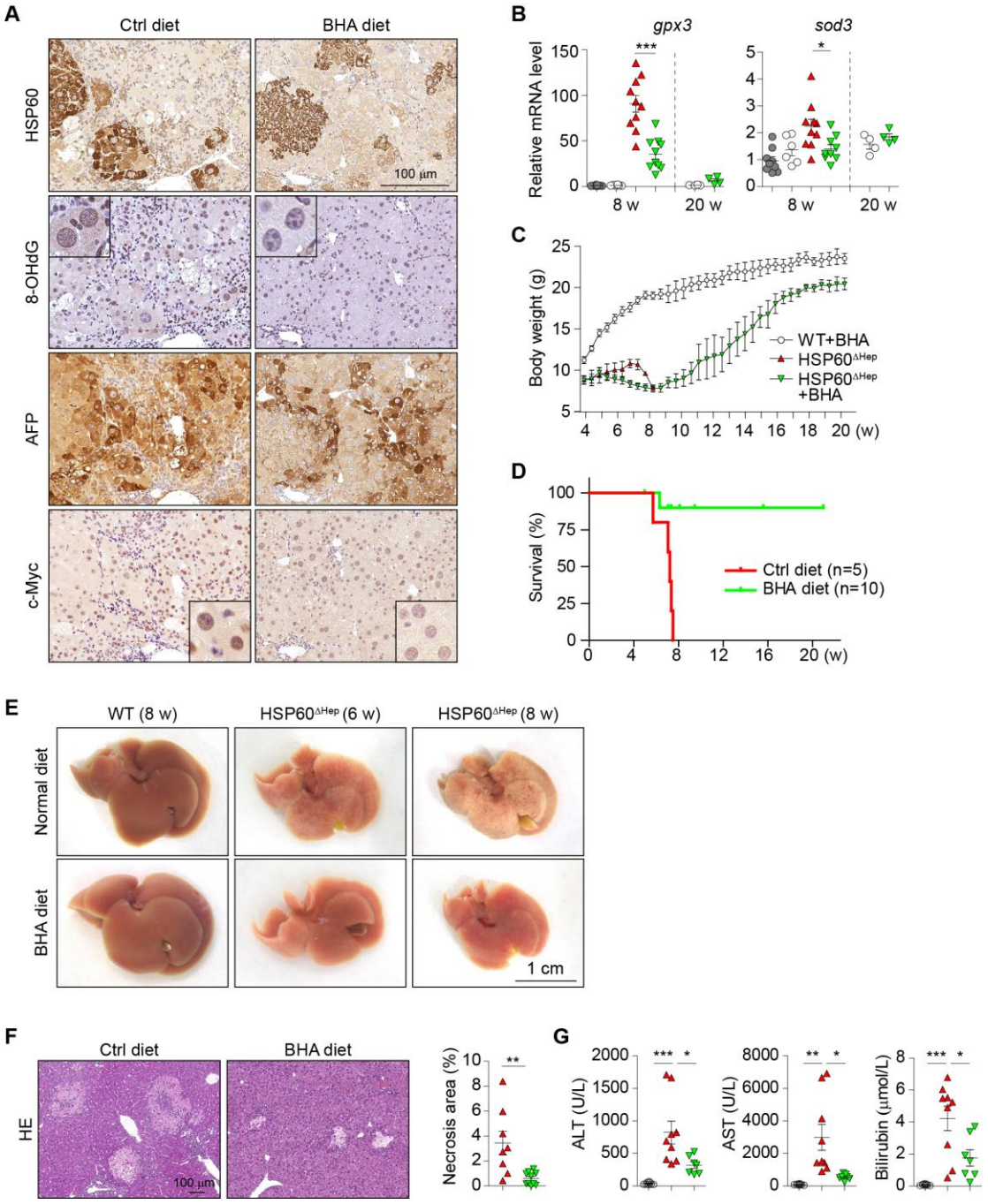

Figure 15. BHA-containing diet rescued HSP60$^{\Delta Hep}$ mice.

(A) Immunohistochemistry staining of HSP60, 8-OHdG, AFP and c-Myc in consecutive liver sections from 8-week-old HSP60$^{\Delta Hep}$ mice fed with normal diet or BHA-containing diet.

(B) qRT-PCR of whole liver lysates from 8- and 20-week-old HSP60$^{\Delta Hep}$ mice fed with normal diet or BHA-containing diet for *gpx3* and *sod3*.

(C) Body weight curve of HSP60$^{\Delta Hep}$ mice fed with normal diet or BHA-containing diet. WT mice fed with BHA-containing diet were used as reference.

(D) Survival plot for HSP60$^{\Delta Hep}$ mice fed with normal diet (red line) or BHA-containing diet (green line).

(E) Macroscopic appearance of livers from 6- and 8-week-old HSP60$^{\Delta Hep}$ mice fed with normal diet or BHA-containing diet. Livers from 8-week-old WT mice were shown as control.

(F) Hematoxylin-eosin staining of liver sections from 8-week-old HSP60$^{\Delta Hep}$ mice fed with normal diet or BHA-containing diet. Quantification of necrotic areas was shown in the right panel.

(G) Serum levels of AST, ALT and Bilirubin in 8-week-old HSP60$^{\Delta Hep}$ mice fed with normal diet or BHA-containing diet.

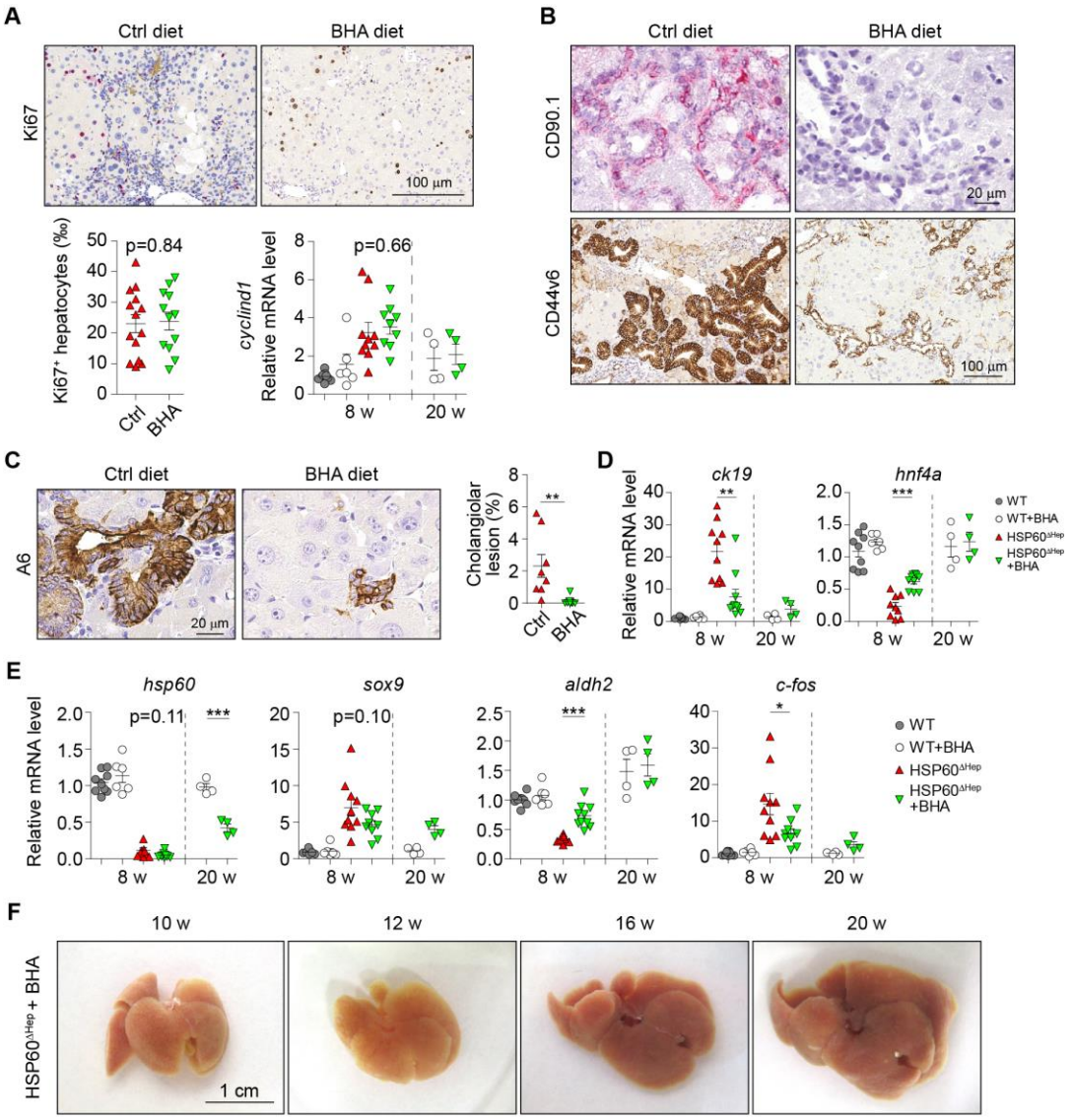

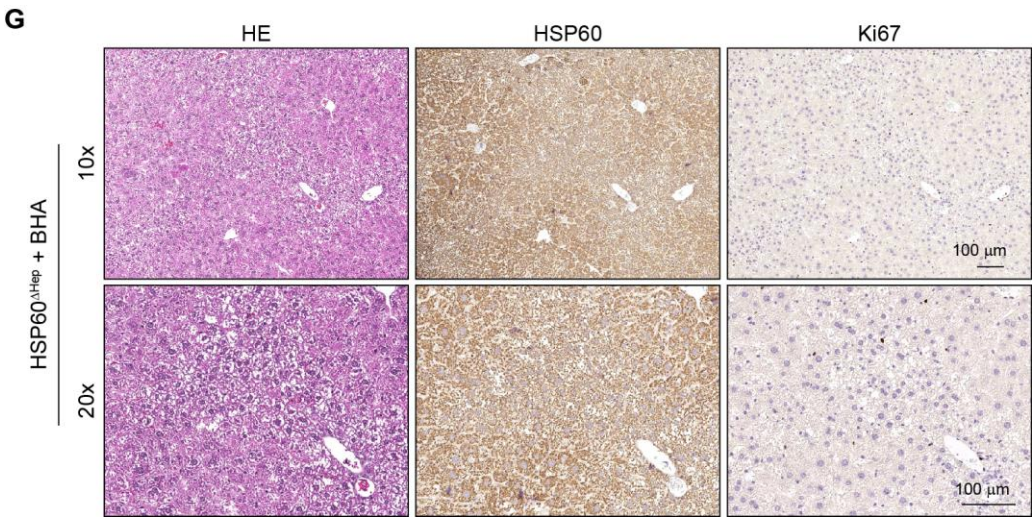

Figure 16. BHA-containing diet attenuated cholangiolar overgrowth in HSP60$^{\Delta Hep}$ mice.

(A) Ki67 staining of liver sections from 8-week-old HSP60$^{\Delta Hep}$ mice fed with normal diet or BHA-containing diet. Quantification of Ki67^{+} hepatocytes and qRT-PCR for *cyclin d1* were shown in lower panels.

(B) Immunohistochemistry staining of CD90.1 and CD44v6 in liver sections from 8-week-old HSP60$^{\Delta Hep}$ mice fed with normal diet or BHA-containing diet.

(C) Immunohistochemistry staining of A6 in liver sections from 8-week-old HSP60$^{\Delta Hep}$ mice fed with normal diet or BHA-containing diet. Quantification of cholangiolar overgrowth areas were shown in the right panel.

(D) qRT-PCR of whole liver lysates from 8- and 20-week-old HSP60$^{\Delta Hep}$ mice fed with normal diet or BHA-containing diet for *ck19* and *hnf4α*.

(E) qRT-PCR of whole liver lysates from 8- and 20-week-old HSP60$^{\Delta Hep}$ mice fed with normal diet or BHA-containing diet for indicated genes.

(F) Macroscopic appearance of livers from HSP60$^{\Delta Hep}$ mice fed with BHA-containing diet at indicated ages.

(G) Hematoxylin-eosin staining and Immunohistochemistry staining of HSP60 and Ki67 in liver sections from half a year old HSP60$^{\Delta Hep}$ mice fed with BHA-containing diet.

We further assessed the effects of the anti-oxidant treatment on the downstream oncogenic signaling. First, phosphorylation of JNK was attenuated upon BHA administration (Figure 17A~C), while the other kinases we analyzed such as Erk1/2, p38 MAPK and eIF2a were not affected (Figure 17A), consistent with the previous results that sustained JNK activation is an important contributor to acute liver failure downstream of ROS production [41]. Second, BHA containing diet strongly reduced levels of oncogenes

including AFP, c-Myc and c-fos (Figure 17D, 16E). However, CHOP expression was even more extensive upon BHA treatment (Figure 17A, C). This was possibly due to the toxicity of the compound itself because wild-type mice fed by BHA-containing diet also showed elevated levels of CHOP expression (Figure 17A, E). Nonetheless, BHA administration did not attenuate *grp75* upregulation and eIF2a phosphorylation (Figure 17A, D), indicating the presence of mtUPR under this circumstance. These results indicated that anti-oxidant treatment protected HSP60$^{\Delta Hep}$ mice via inhibiting ROS and its downstream oncogenic signaling pathways, but not via mtUPR signaling (Figure 17F), which is reasonable because BHA is not likely to compensate the roles of folding proteins.

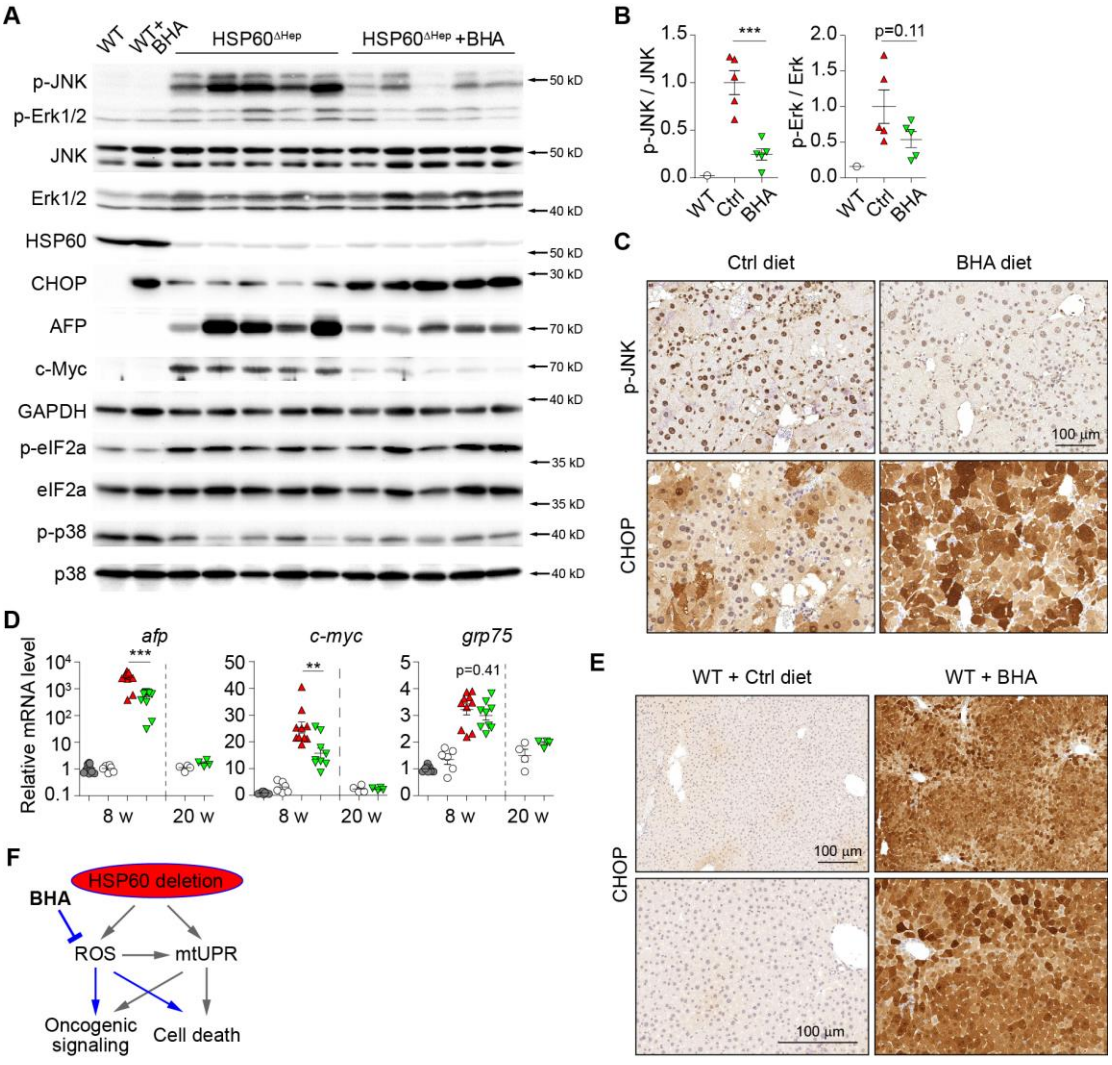

Figure 17. BHA-containing diet reduced oncogenic signals by abolishing ROS accumulation in HSP60$^{\Delta Hep}$ mice.

(A) Whole liver lysates were prepared from 8-week-old HSP60$^{\Delta Hep}$ mice fed with normal diet or BHA-containing diet. Western blot was performed with indicated antibodies.
(B) Quantifications of the ratio of p-JNK to total JNK and the ratio of p-Erk1/2 to total Erk1/2 from (A).
(C) Immunohistochemistry staining of p-JNK and CHOP in consecutive liver sections from 8-week-old HSP60$^{\Delta Hep}$ mice mice fed with normal diet or BHA-containing diet.
(D) qRT-PCR of whole liver lysates from 8- and 20-week-old HSP60$^{\Delta Hep}$ mice fed with normal diet or BHA-containing diet for *afp*, *c-myc* and *grp75*.
(E) Immunohistochemistry staining of CHOP in liver sections from 8-week-old WT mice fed with normal diet or BHA-containing diet.
(F) A schematic diagram depicting the action of BHA in HSP60$^{\Delta Hep}$ mice. BHA reduces oncogenic signaling and cell death by attenuating ROS accumulation in HSP60 deficient livers.

3.1.4 TNFα from Kupffer cells promotes cholangiolar hyperplasia

Next, we sought to identify the molecular and cellualar pathways which link within the carcinogenic niche and the neoplastic phenotype. As various cytokines/ligands are known to mediate the lineage commitment and/or the malignant transformation of the LPCs (Figure 18A, ref [269, 270]), we measured the expression of their mRNA levels in HSP60$^{\Delta Hep}$ livers. Widespread changes in cytokine expression were apparent in the livers of HSP60$^{\Delta Hep}$ mice (Figure 18A). Strikingly, we observed rapid and robust induction of mRNA encoding TNFα, whose levels far exceeded the other cytokines/ligands such as TGFβ, Jag1, HGF and FGF10 (Figure 18A). We confirmed the upregulation of TNFα protein by ELISA (Figure 18B). Consistent with the rescuing effect of BHA on HSP60$^{\Delta Hep}$ mice, TNFα production was strongly attenuated compared to the mice with normal diet (Figure 18B, C). Immunohistochemistry analysis further localized TNFα to F4/80 positive Kupffer cells (Figure 18D), whose number was more extensively increased in HSP60$^{\Delta Hep}$ livers compared to T, B cells and neutrophils (Figure 18E).

To determine whether TNFα can directly act on biliary lineage cells, we addressed whether LPCs and cholangiolar cells expressed TNFR1. Immunofluorescence analysis and *in situ* hybridization confirmed enrichment of TNFR1 in bile duct cells and cholangiolar hyperplasia compared to the surrounding hepatocytes (Figure 19 A~C), demonstrating the capability of these cells to react to TNFα. Therefore, we postulated that Kupffer cell produced TNFα linked ROS production with cholangiolar hyperplasia in HSP60$^{\Delta Hep}$ mice.

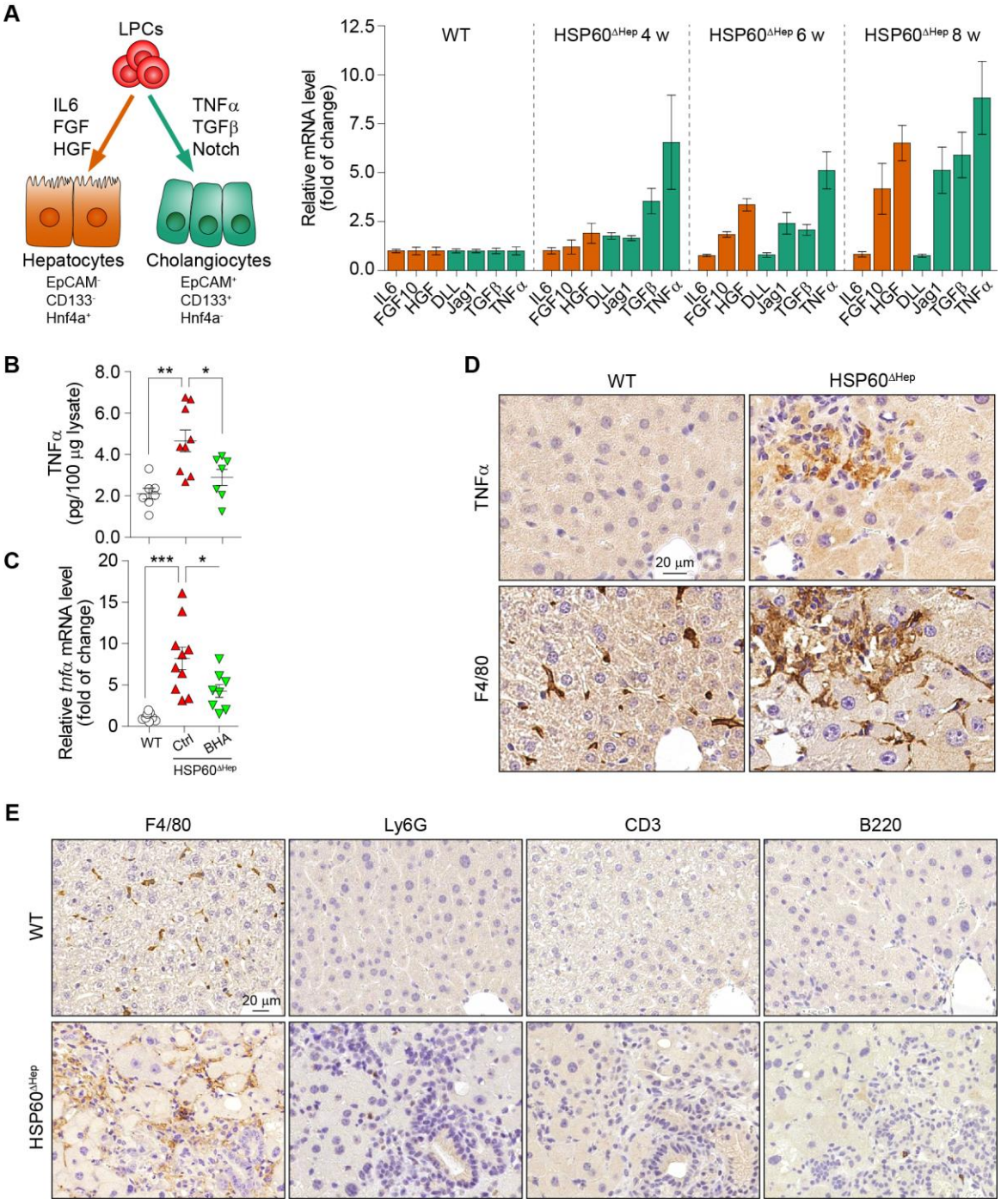

Figure 18. Activated Kupffer cells produced TNFα in HSP60$^{\Delta Hep}$ mice.

(A) Left: schematic diagram of possible key signals in regulation of LPC differentiation. Right: mRNA levels of the key ligands were measured by qRT-PCR in whole liver lysates from HSP60$^{\Delta Hep}$ mice at different ages.

(B) Concentration of TNFα in whole liver lysates from WT mice and 8-week-old HSP60$^{\Delta Hep}$ mice fed with normal diet or BHA-containing diet by ELISA.

(C) qRT-PCR for *tnfα* in whole liver lysates from WT mice and 8-week-old HSP60$^{\Delta Hep}$ mice fed with normal diet or BHA-containing diet by ELISA.

(D) Immunohistochemistry staining of TNFα and F4/80 in consecutive liver sections from 8-week-old HSP60$^{\Delta Hep}$ and WT mice.

(E) Immunohistochemistry staining of F4/80, Ly6G, CD3 and B220 in liver sections from 8-week-old HSP60$^{\Delta Hep}$ and WT mice.

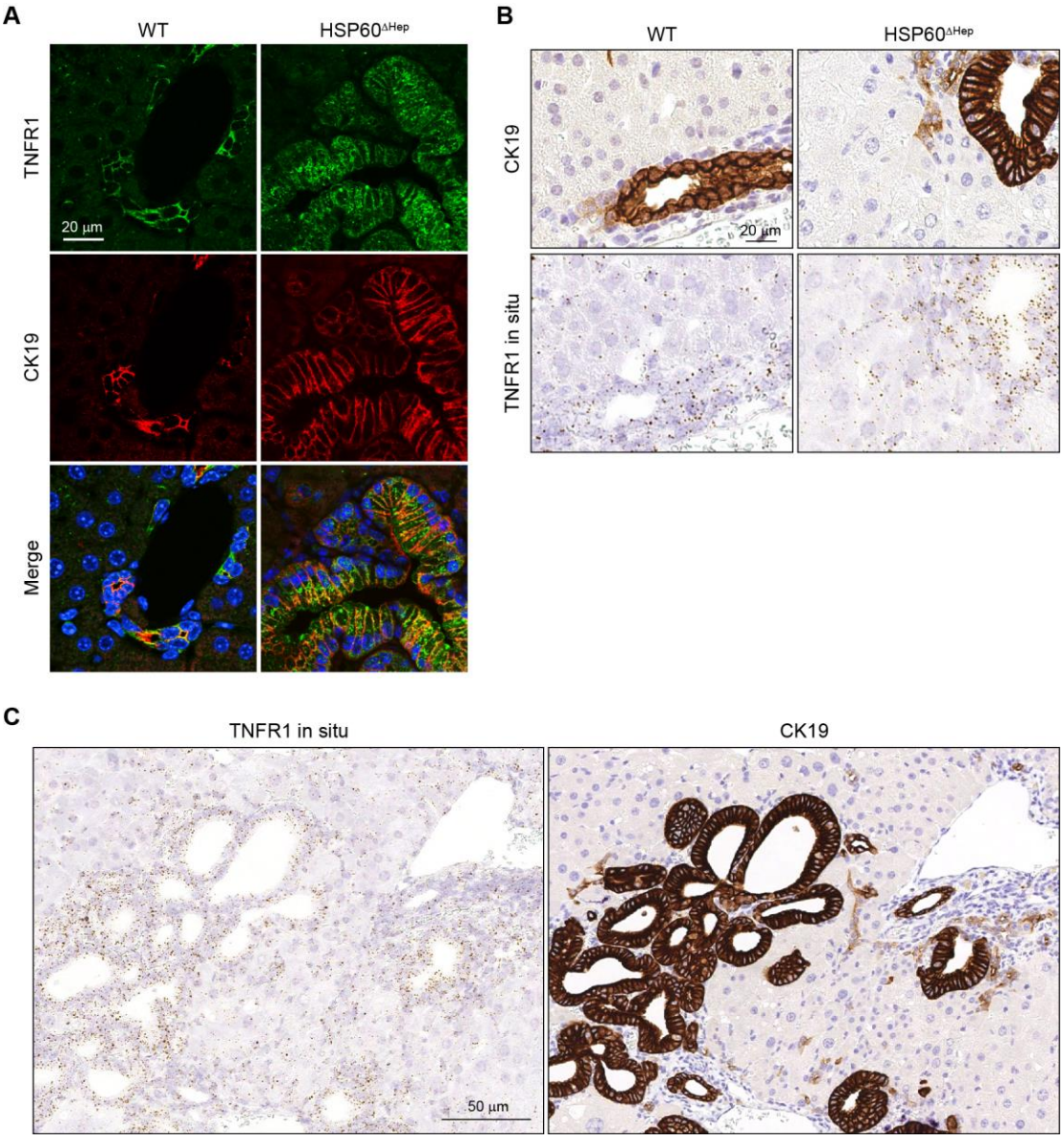

Figure 19. Cholangiocytes express high level of TNFR1.

(A) Doulbe staining of TNFR1 (green) and CK19 (red) in liver sections from 8-week-old HSP60$^{\Delta Hep}$ and WT mice.

(B) Immunohistochemistry staining of CK19 and in situ hybridization of TNFR1 in consecutive liver sections from 8-week-old HSP60$^{\Delta Hep}$ and WT mice.

(C) Lower magnification of (B). Immunohistochemistry staining of CK19 and in situ hybridization of TNFR1 in consecutive liver sections from 8-week-old HSP60$^{\Delta Hep}$ mice.

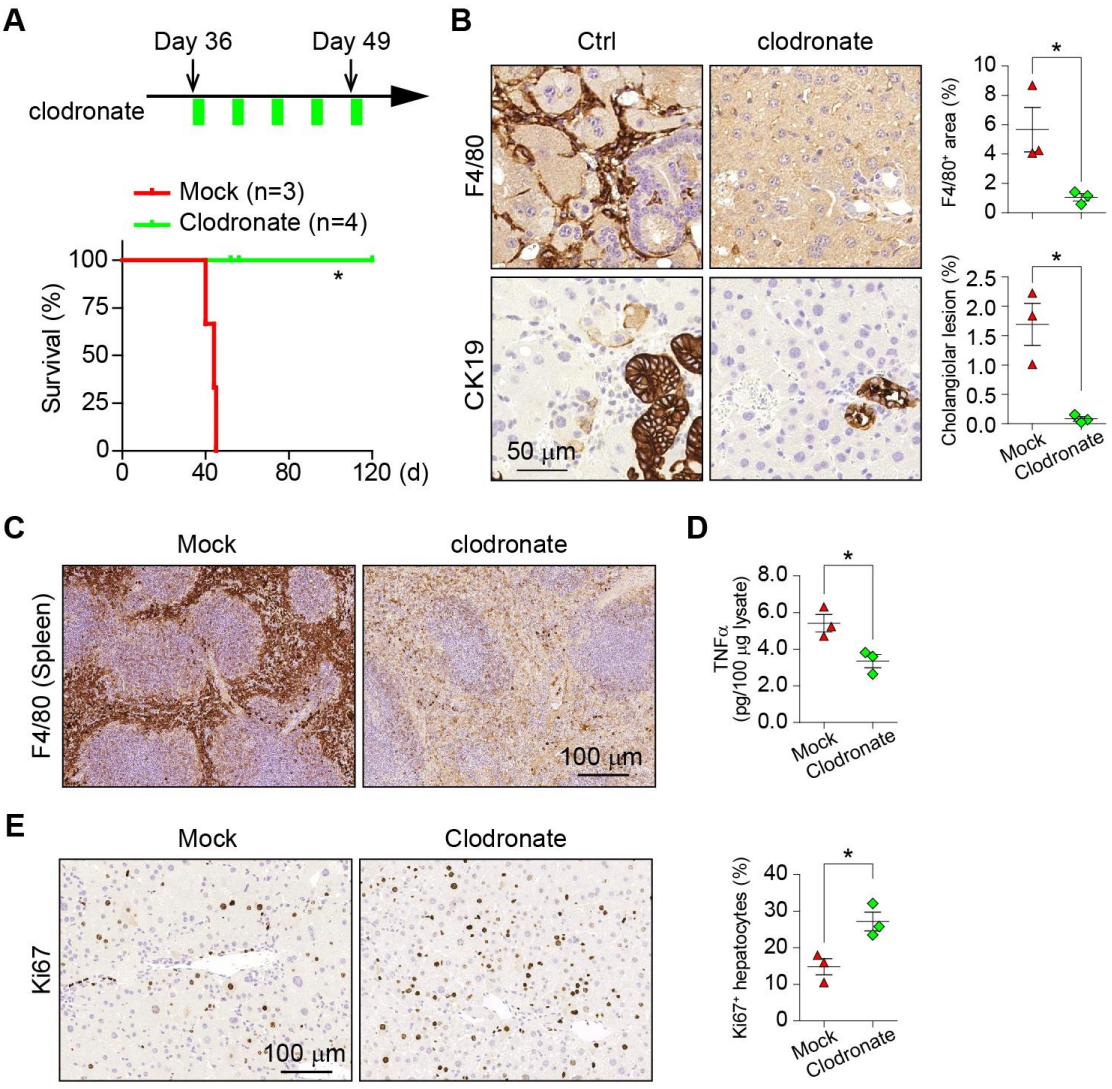

Figure 20. Clodronate treatment reduced cholangiolar overgrowth.

(A) Upper: time line of clodronate administration on HSP60$^{\Delta Hep}$ mice. Lower: survival plot for HSP60$^{\Delta Hep}$ mice treated with mock (red line) or liposomal clodronate (green line).

(B) Immunohistochemistry staining of F4/80 and CK19 in consecutive liver sections from 8-week-old HSP60$^{\Delta Hep}$ mice treated with mock or liposomal clodronate. Quantification of each staining was shown in the right panels.

(C) Immunohistochemistry staining of F4/80 in spleen sections from 8-week-old HSP60$^{\Delta Hep}$ treated with mock or liposomal clodronate.

(D) Concentration of TNFα in whole liver lysates from 8-week-old HSP60$^{\Delta Hep}$ mice treated with mock or liposomal clodronate by ELISA.

(E) Ki67 staining in liver sections from 8-week-old HSP60$^{\Delta Hep}$ mice treated with mock or liposomal clodronate. Quantification of Ki67^{+} hepatocytes was shown in the right panel.

If increase of TNFα-producing Kupffer cells is crucial for triggering cholangiolar hyperplasia, depletion of Kupffer cells around the times of cholangiolar proliferation should protect HSP60$^{\Delta Hep}$ mice similar to BHA treatment. To test this hypothesis, we performed liposomal clodronate injection in HSP60$^{\Delta Hep}$ mice once every 3 days from week 6 to 8 (Figure 20A) [271, 272]. One day after the liposomal clodronate injection, efficient and significant Kupffer cell depletion in liver as well as in spleen was confirmed by immunohistochemistry of F4/80 (Figure 20B, C). Administration of liposomal encapsulated clodronate significantly reduced TNFα levels in HSP60$^{\Delta Hep}$ livers (Figure 20D). Correspondingly, we found that the cholangiolar hyperproliferation was almost entirely abolished, while Ki67^{+} hepatocytes increased up to 1.84 fold (from 14.7% to 27.1%) when Kupffer cells were depleted (Figure 20B, E).

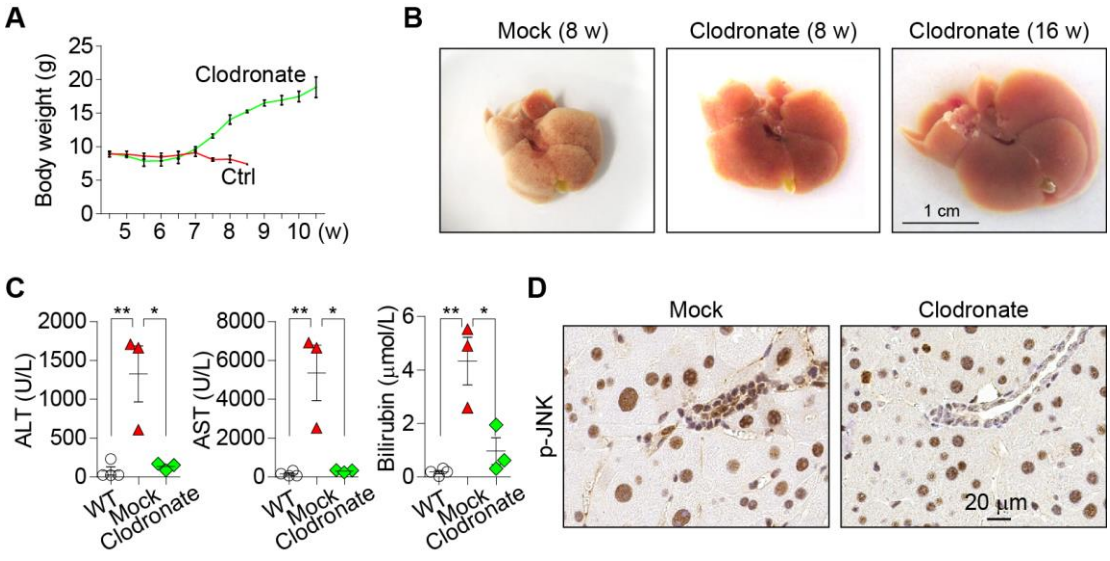

Figure 21. Clodronate treatment rescued HSP60$^{\Delta Hep}$ mice.

(A) Body weight curve of HSP60$^{\Delta Hep}$ mice treated with mock or liposomal clodronate.

(B) Macroscopic appearance of livers from 8-week-old HSP60$^{\Delta Hep}$ mice treated with liposomal clodronate.
(C) Serum levels of AST, ALT, AP and Bilirubin in 8-week-old HSP60$^{\Delta Hep}$ mice treated with mock or liposomal clodronate.
(D) Immunohistochemistry staining of p-JNK in liver sections from 8-week-old HSP60$^{\Delta Hep}$ mice treated with mock or liposomal clodronate.
(E) Macroscopic appearance of livers from 16-week-old HSP60$^{\Delta Hep}$ mice treated with clodronate for two weeks.

Clodronate-treated HSP60$^{\Delta Hep}$ mice began to restore body weight from day 42 (Figure 21A), and 8-week-old mice displayed significantly rescued liver architecture and decreased levels of liver enzymes (Figure 21B, C), indicative of an accelerated liver regeneration. Contrary to the previously reported models, depletion of Kupffer cells resulted in no significant reduction of p-JNK in HSP60$^{\Delta Hep}$ mice (Figure 21D), suggesting that JNK activation in HSP60 deficient hepatocytes was independent of the paracrine pro-inflammatory signal. Clodronate-treated HSP60$^{\Delta Hep}$ mice were kept under surveillance until they were 4 months old, without displaying any abnormalities (Figure 21B). These findings indicate that the enhanced cholangiolar growth in HSP60$^{\Delta Hep}$ mice is associated with TNFα signaling, and that Kupffer cells are the major source of TNFα in response to hepatocytic mitochondrial dysfunction and oxidative stress.

3.1.5 TNFR1 signaling on LPCs promotes biliary differentiation

TNFα was recently reported in two independent work to be a main contributor during retro-differentiation of tumor-derived hepatocyte-like cells [270] and trans-differentiation of rat hepatocytes into ductal cells [273]. To invest the effect of TNFα signaling on lineage commitment of LPCs in vitro, we isolated hepatoblasts from E14.5 liver using immunomagnetic bead extraction with antibodies recognizing the extracellular epitopes of E-Cadtherin [254, 274]. Undifferentiated hepatoblasts clonally proliferated on collagen I coated plates (Figure 22A). Immunofluorescence staining confirmed their double positivity for A6 and Hnf4α, indicative of the bipotential feature (Figure 22B). To induce hepatocytic differentiation, hepatoblasts were maintained in the basal medium supplemented with 0.5% DMSO for 7 days. Under this condition, the cells downregulated cholangiolar lineage marks A6, CK19 and Sox9, while Hnf4α and Hnf1β were highly

expressed (Figure 22A~C). Strikingly, when hepatoblasts were cultured in the basal medium supplemented with 10 ng/ml recombinant murine TNFα for the same period, the cells adopted a ductal morphology (Figure 22A~C). Molecular characterization indicated strong expression of A6, CK19 and Sox9 and repressed or even entirely abolished expression of Hnf4α and Hnf1β, suggesting that TNFα can indeed act on hepatoblasts to promote their biliary differentiation (Figure 22B, C). We again treated HepRG, a human bipotential liver cancer cell line, with TNFα. This resulted in significant upregulation of biliary lineage markers Epcam, CK19 and CD133 and downregulation of hepatocytic markers hnf4α and hnf1β (Figure 22D). All of these data suggest that TNFα directly affects LPC lineage commitment *in vitro*.

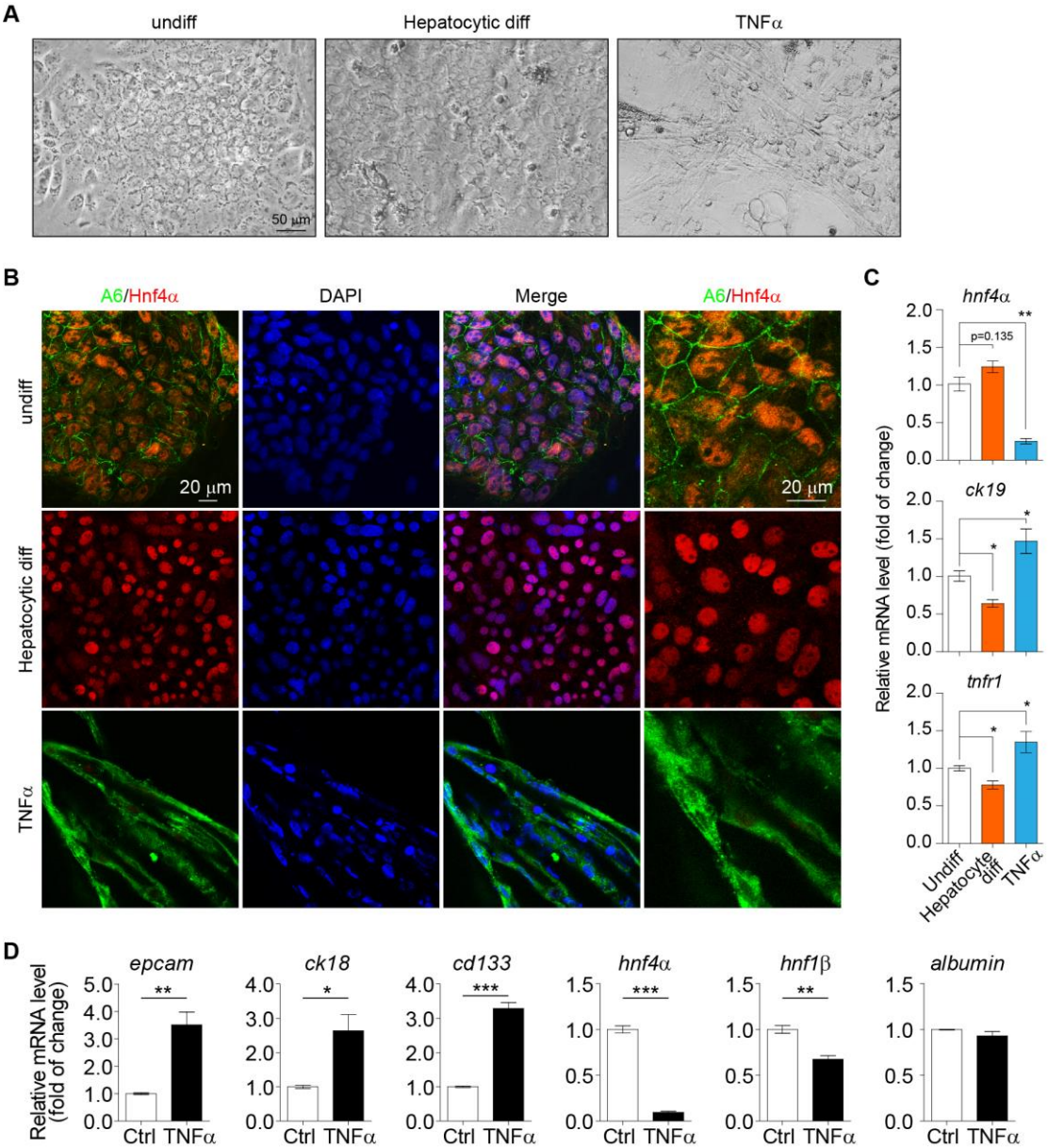

Figure 22. TNFα promoted biliary differentiation of LPCs in vitro.

(A) Phase contrast images of hepatoblasts kept in undifferentiated medium (basal medium), hepatocytic differentiation medium (basal medium + DMSO) or cholangiocytic differentiation medium (basal medium + TNFα) for 7 days.

(B) Hepatoblasts were kept in undifferentiated medium (basal medium), hepatocytic differentiation medium (basal medium + DMSO) or cholangiocytic differentiation medium (basal medium + TNFα). Double staining of A6 (green) and Hnf4α (red) was performed.

(C) qRT-PCR of the cell extracts from (B) for indicated genes.

(D) qRT-PCR of the HepRG cells cultured with or without TNFα for 3 days.

To investigate the role of TNFα signaling in cholangiolar hyperplasia in HSP60$^{\Delta Hep}$ animals, we generated HSP60$^{\Delta Hep}$ TNFR1-/- double knockout mice. Genetic ablation of TNFR1 in HSP60$^{\Delta Hep}$ mice prevented the early lethality, coincident with reduced liver damage at 8 weeks old (Figure 23A~C). Interestingly, while most HSP60$^{\Delta Hep}$ TNFR1+/- mice were also rescued, 4 out of 18 mice showed dramatic body weight loss between week 8 to 10 and were sacrificed, indicating a dose-dependent effect of TNFα signaling (Figure 23A, C). The rescued phenotype was not dependent on the pro-survival or pro-apoptotic role of TNFR1 because equal levels of cell necrosis were observed in HSP60$^{\Delta Hep}$ mice as well as in the double knockout mice at 6 weeks old (Figure 23D, E). Consistently, there was no obvious difference in serum amounts of ALT, AST, AP and bilirubin between HSP60$^{\Delta Hep}$ TNFR1-/- mice and HSP60$^{\Delta Hep}$ mice by week 6 (Figure 23F). However, we observed significant reduction of their levels in the double knockout mice at week 8 (Figure 23F), the time point when HSP60$^{\Delta Hep}$ mice displayed robust cholangiolar hyperplasia.

Consistent with the idea that TNFα signaling contributes to the lineage commitment of LPCs, the emergence of cholangiolar dysplasia was blocked, as revealed by A6, CK19, CD90.1 and CD44 staining (Figure 23D, 24A). Importantly, Ki67 positive hepatocytes increased significantly in 8 weeks old livers by 2 fold in double knockout mice (Figure 23D, 24B). The preference of hepatocytic proliferation but not cholangiocytic proliferation in double knockout mice was also evident by elevated *hnf4α* expression and reduced *ck19* expression by qRT-PCR (Figure 24C). This phenotype indicated that the differentiation of LPCs was shifted towards hepatocytic lineage under the circumstance of TNFR1 deletion. The increased hepatocyte differentiation and proliferation prevented the worsening of the liver damage and fully restored liver functions at around 16 weeks old. The double knockout mice were kept as long as 1 year old and we did not see any

abnormalities in their livers, as indicated by immunohistochemistry of Ki67 and CK19 (Figure 24D). Together with the *in vitro* data, these results demonstrated that TNFα signaling is an important mediator of cholangiolar lineage commitment of LPCs.

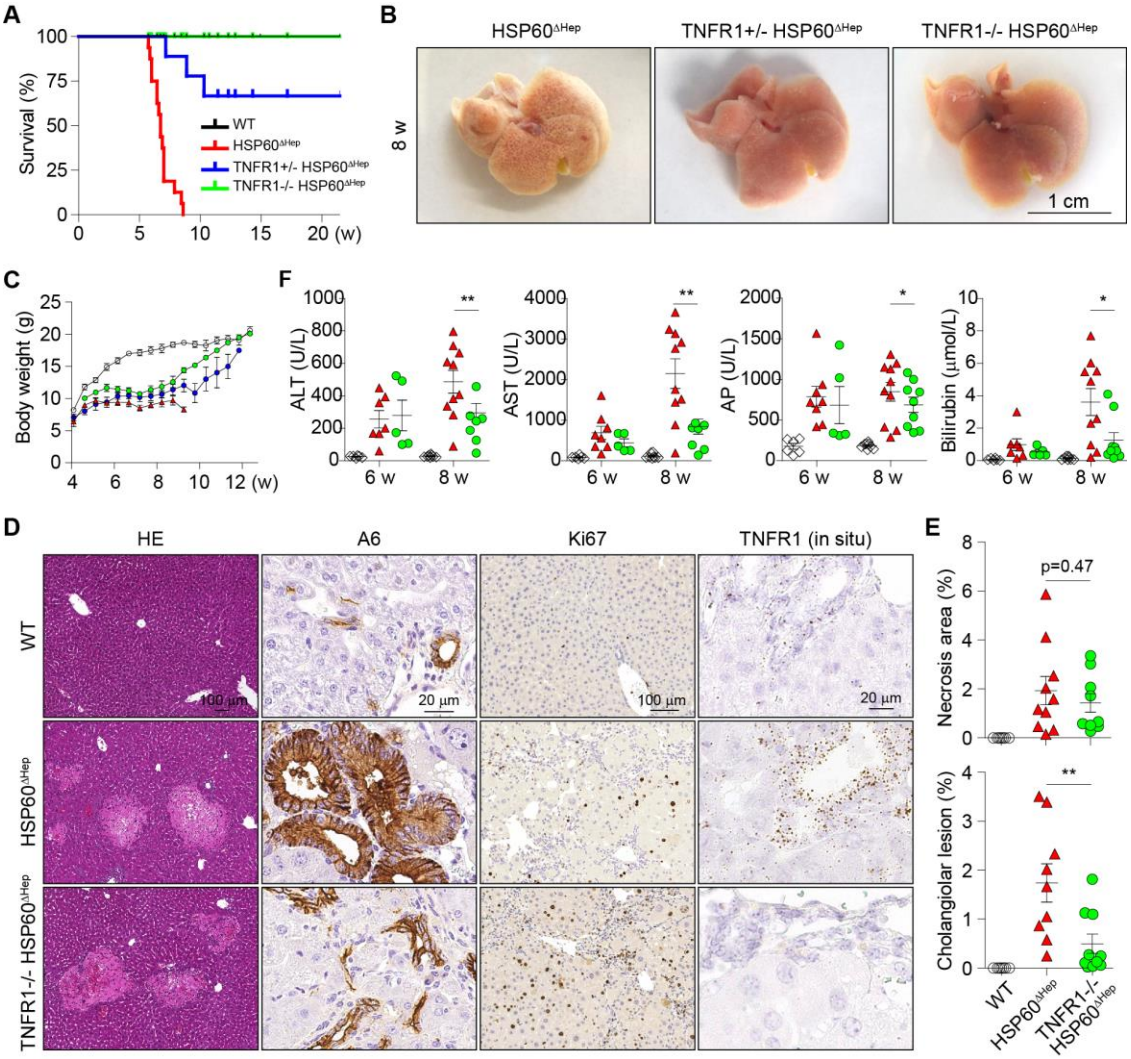

Figure 23. TNFR1 deletion rescued HSP60$^{\Delta Hep}$ mice.

(A) Survival analysis for HSP60$^{\Delta Hep}$, HSP60$^{\Delta Hep}$ TNFR1$^{+/-}$ and HSP60$^{\Delta Hep}$ TNFR1$^{-/-}$ mice.

(B) Macroscopic appearance of livers from 8-week-old HSP60$^{\Delta Hep}$, HSP60$^{\Delta Hep}$ TNFR1$^{+/-}$ and HSP60$^{\Delta Hep}$ TNFR1$^{-/-}$ mice.

(C) Body weight curves for WT, HSP60$^{\Delta Hep}$, HSP60$^{\Delta Hep}$ TNFR1$^{+/-}$ and HSP60$^{\Delta Hep}$ TNFR1$^{-/-}$ mice.

(D) Hematoxylin-eosin staining, immunohistochemistry staining for A6 and Ki67, and in situ hybridization for TNFR1 of liver sections from 8-week-old WT, HSP60$^{\Delta Hep}$ and HSP60$^{\Delta Hep}$ TNFR1$^{-/-}$ mice.

(E) Quantification of necrosis areas (upper) and cholangiolar overgrowth areas (lower) in WT, HSP60$^{\Delta Hep}$ and HSP60$^{\Delta Hep}$ TNFR1$^{-/-}$ mice.

(E) Serum levels of AST, ALT, AP and Bilirubin in 6- and 8-week-old WT, HSP60$^{\Delta Hep}$ and HSP60$^{\Delta Hep}$ TNFR1$^{-/-}$ mice.

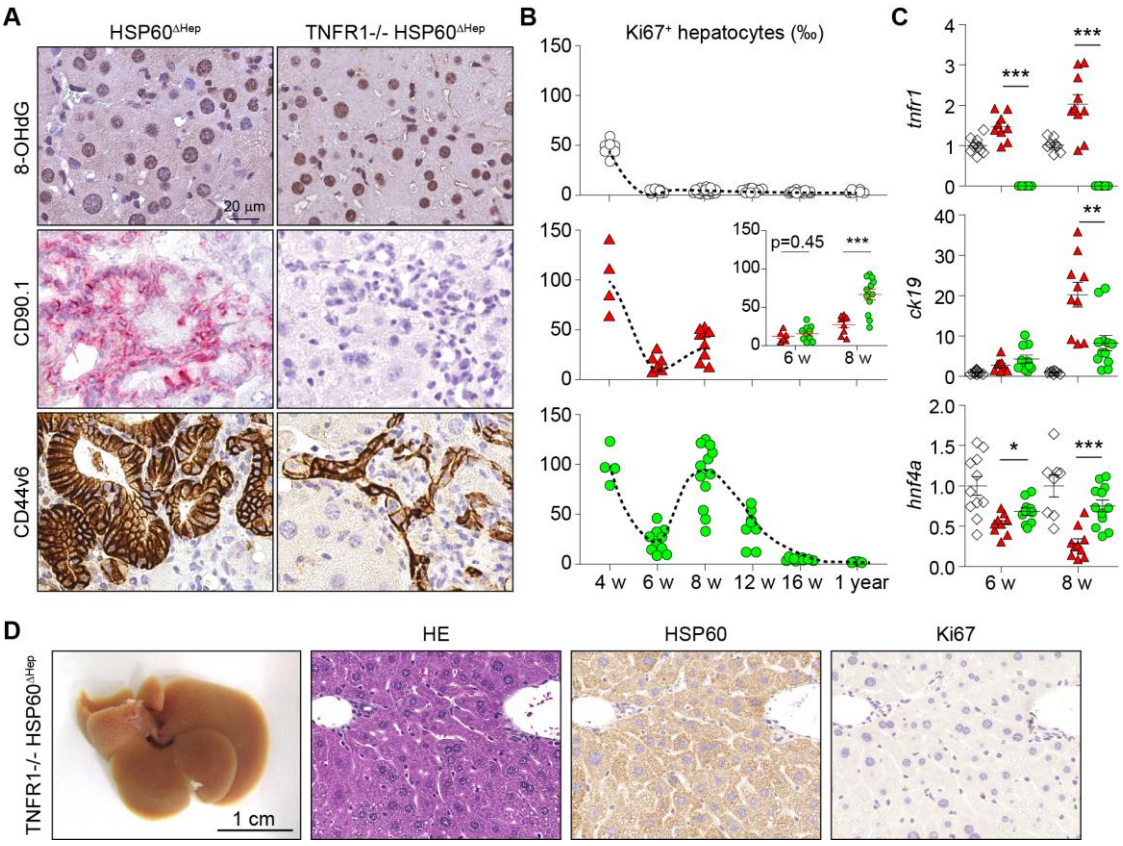

Figure 24. TNFR1 deletion promoted hepatocytic proliferation but not cholangiocytic proliferation.

(A) Immunohistochemistry staining for 8-OHdG, CD90.1 and CD44 of liver sections from 8-week-old HSP60$^{\Delta Hep}$ and HSP60$^{\Delta Hep}$ TNFR1$^{-/-}$ mice.

(B) Quantification of Ki67^{+} hepatocytes in WT, HSP60$^{\Delta Hep}$ and HSP60$^{\Delta Hep}$ TNFR1$^{-/-}$ livers.

(C) qRT-PCR of whole liver extracts from 6- and 8-week-old WT, HSP60$^{\Delta Hep}$ and HSP60$^{\Delta Hep}$ TNFR1$^{-/-}$ mice for indicated genes.

(D) Macroscopic appearance of liver from 1-year-old HSP60$^{\Delta Hep}$ TNFR1$^{-/-}$ mouse. Hematoxylin-eosin staining and immunohistochemistry staining for HSP60 and Ki67 were shown.

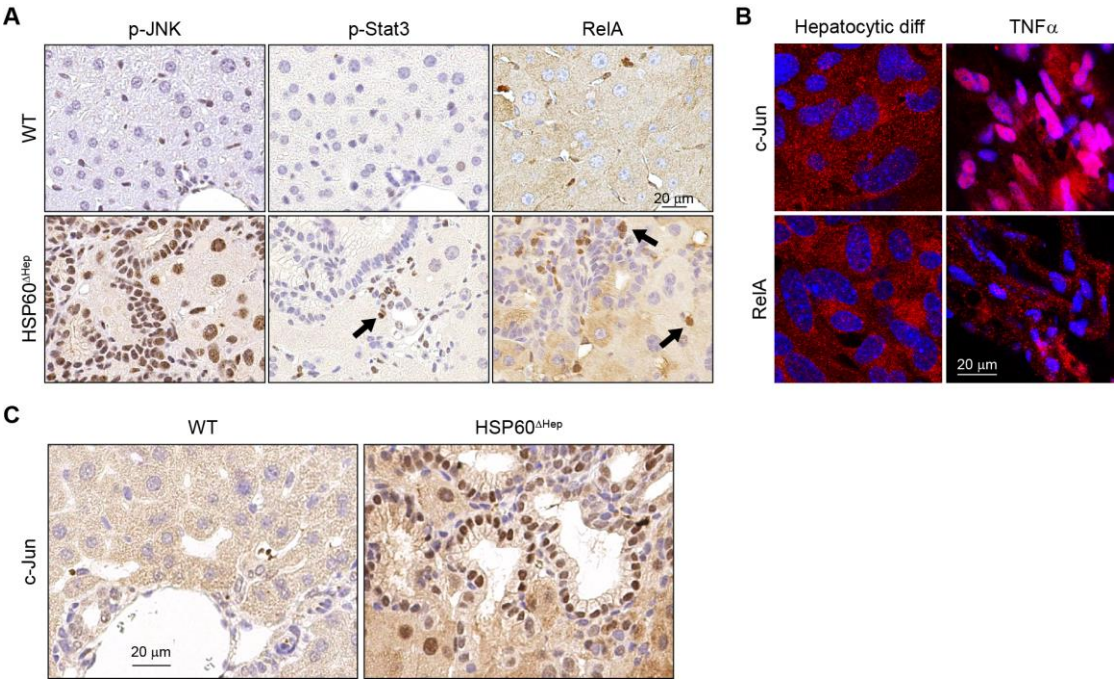

Figure 25. JNK/c-Jun activation in cholangiocytes.

(A) Immunohistochemistry staining of p-JNK, p-Stat3 and RelA in liver sections from 8-week-old WT and HSP60$^{\Delta Hep}$ mice. Black arrows indicate the positive staining of the indicated protein in the non-parenchyma cells.

(B) Immunofluorescent staining of RelA and c-Jun in hepatoblasts cultured in hepatocytic differentiation medium with or without TNFα.

(C) Immunohistochemistry staining for c-Jun of liver sections from 8-week-old WT and HSP60$^{\Delta Hep}$ mice.

3.1.6 JNK/c-Jun activation is required for biliary differentiation

Next we focused on the molecular mechanisms underlying the TNFR1-mediated lineage specification. Depending on cellular context, TNFα/TNFR1 signaling has been shown to involve a diverse set of signaling molecules, including RelA, Stat3, and JNK [275]. To determine on which downstream signaling TNFα mediated biliary differentiation depends, nuclear translocation of several signaling factors (including the above mentioned) was investigated by immunohistochemistry. We observed nuclear p-JNK staining in cholangiolar cells, whereas RelA and Stat3 positivity was localized to the non-parenchyma cells (Figure 25A). In parallel, c-Jun activation was also evidenced by its nuclear localization in cholangiolar cells (Figure 25B). Similarly, primary hepatoblasts cultured in basal medium supplemented with TNFα for 3 days showed nuclear staining of

c-Jun but not RelA (Figure 25C). The involvement of JNK signaling, but not RelA or Stat3, was consistent with a most recent report that JNK is the major contributor during TNFα induced ductular trans-differentiation of rat hepatocytes [273].

To test the effects of JNK signaling inhibition on cholangiolar hyperplasia in HSP60$^{\Delta Hep}$ mice, SP600125 (50 mg/kg) or the same volume of vehicle was administrated intraperitoneally daily for a total period of 2 weeks beginning at day 36 (Figure 26A). JNK inhibition reduced cholangiolar hyperplasia, resulting into benign regeneration and eventually functional livers with wild-type hepatocytes at week 16 (Figure 26A~C). Additionally, the cholangiolar cells in the glandular structure of SP600125 treated HSP60$^{\Delta Hep}$ mice were not proliferating as determined by Ki67 staining (Figure 26D), whereas the hepatocytic proliferation was not influenced (Figure 26E). However, since JNK phosphorylation was also present in the surrounding HSP60^{-} hepatocytes, SP600125 might also exert its role by attenuating the hepatocyte injury and/or the carcinogenic niche. Indeed, we observed less necrosis and marked reduction of ALT and AST levels in SP600125 treated HSP60$^{\Delta Hep}$ mice compared to mock treated mice (Figure 26F, G).

To directly assess the role of JNK signaling on LPC lineage commitment, we treated hepatoblasts with SP600125 during the in vitro differentiation process. Culture of hepatoblasts in hepatocytic differentiation medium supplemented with 10 ng/ml of TNFα as well as 10 μM of SP600125 abolished c-Jun activation, as revealed by the absence of its nuclear localization (Figure 27A). Meanwhile, biliary differentiation of hepatoblasts was also suppressed, with reduced ductular morphogenesis and decreased expression of biliary lineage marker A6 (Figure 27B, C).

In summary, the in vivo and in vitro results strongly suggest that JNK/c-Jun signaling is activated by TNFα and is required for biliary differentiation.

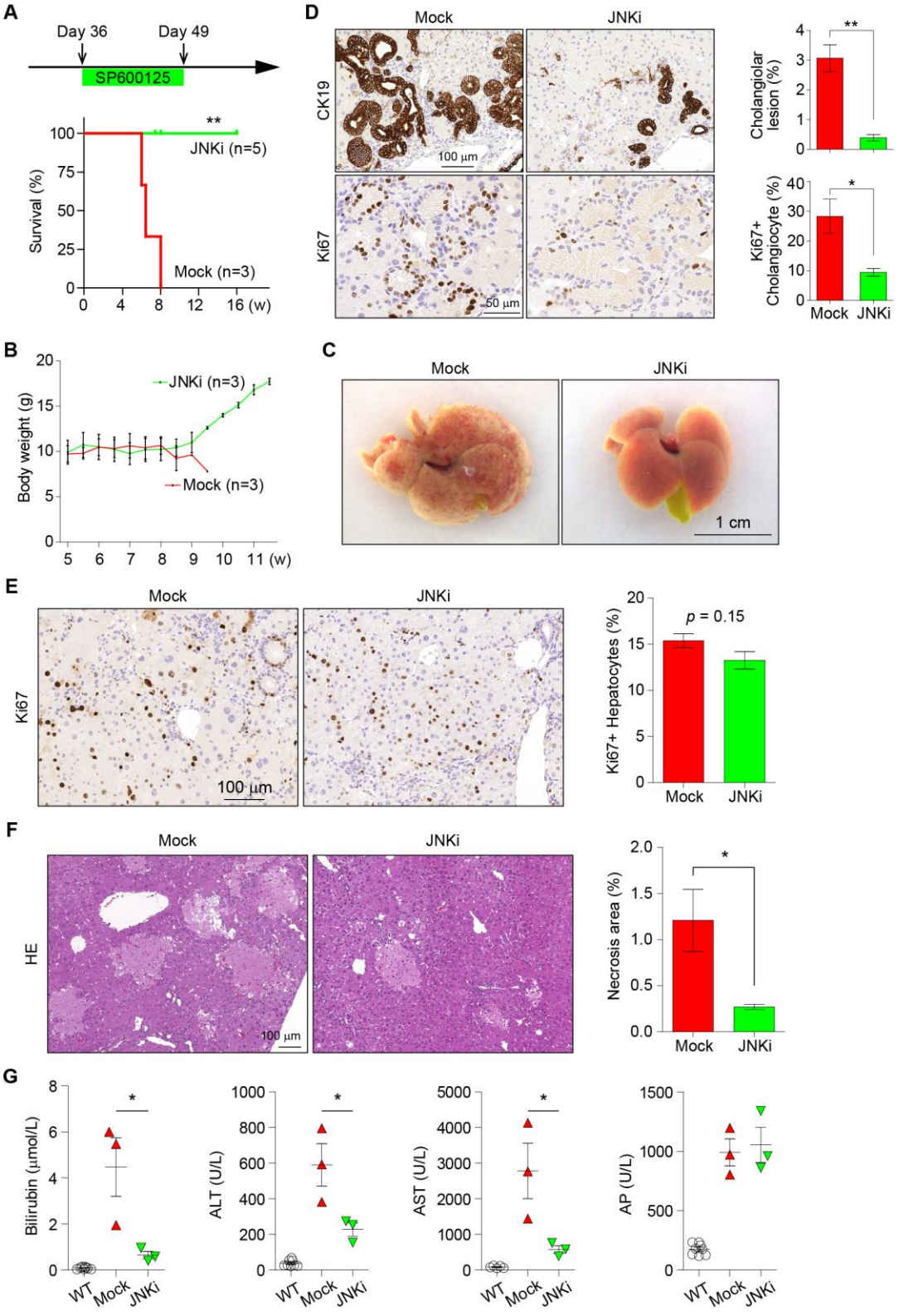

Figure 26. JNK inhibition rescued HSP60$^{\Delta Hep}$ mice.

(A) Upper: time line of SP600125 administration on HSP60$^{\Delta Hep}$ mice. Lower: survival plot for HSP60$^{\Delta Hep}$ mice treated with mock (red line) or SP600125 (green line).

(B) Body weight curves for HSP60$^{\Delta Hep}$ mice treated with mock (red line) or SP600125 (green line).

(C) Macroscopic appearance of liver from 8-week-old HSP60$^{\Delta Hep}$ mice treated with mock or SP600125.

(D) Immunohistochemistry staining of CK19 and Ki67 in liver sections from 8-week-old HSP60$^{\Delta Hep}$ mice treated with mock or SP600125. Quantification of cholangiolar lesion areas and Ki67^{+} cholangiocytes in relative to total cholangiocytes were shown in the right panels.

(E) Ki67 staining in liver sections from 8-week-old HSP60$^{\Delta Hep}$ mice treated with mock or SP600125. Quantification of Ki67^{+} hepatocytes was shown in the right panel.

(F) Hematoxylin-eosin staining in liver sections from 8-week-old HSP60$^{\Delta Hep}$ mice treated with mock or SP600125. Quantification of necrotic areas was shown in the right panel.

(G) Serum levels of AST, ALT, AP and Bilirubin in 8-week-old WT mice and HSP60$^{\Delta Hep}$ mice treated with mock or SP600125.

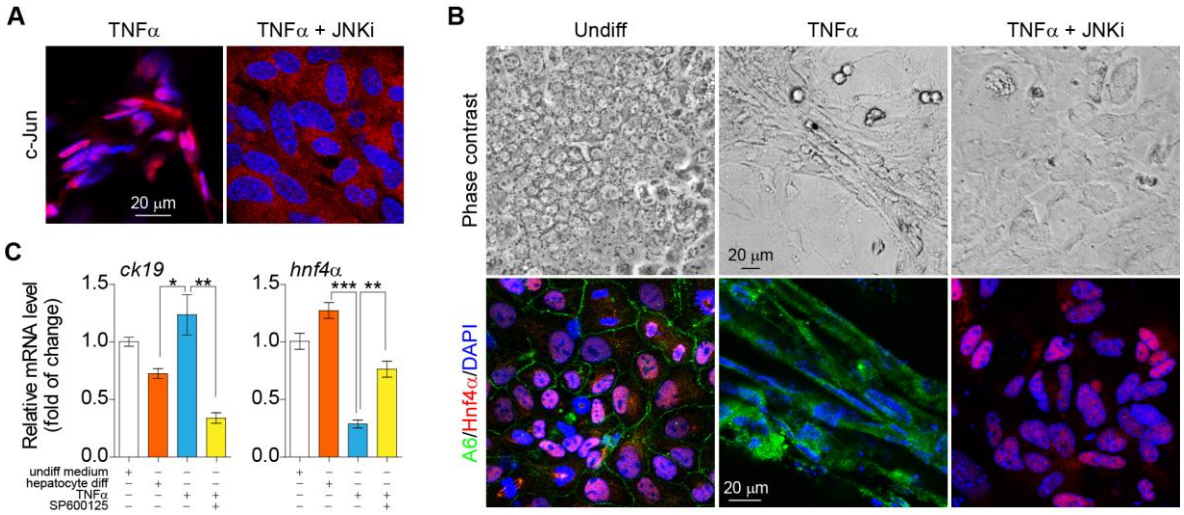

Figure 27. JNK inhibition impaired biliary differentiation of LPCs in vitro.

(A) Immunofluorescent staining of c-Jun in hepatoblasts cultured in TNFα-containing differentiation medium with or without SP600125.

(B) Phase contrast images and double staining of A6 and Hnf4α of hepatoblasts kept in undifferentiated medium or TNFα-containing differentiation medium with or without SP600125 for 7 days.

(C) qRT-PCR of the cell extracts from (B) for indicated genes.

3.1.7 Pharmacological inhibition of JNK reduced ICC cell grow in vivo and in vitro

Comprehensive genomic profiling of human HCC and ICC samples by next generation sequencing reveals distinct genomic traits of these two different pathological entities and implies different therapeutic targets [49, 50]. To examine the clinical relevance of our findings, we analyzed human liver tumor specimens from patients with HCC (n=14), from patients with ICC (n=16), and from patients with colon cancer hepatic metastasis (CHM) (n=10), for TNFα and p-JNK expression by immunohistochemistry (Figure 28). TNFα immunohistochemistry exhibited positive staining only in 20% of CHM and 21.4% in HCC, whereas 62.5% of ICC tissues showed positive TNFα expression ($p=0.0285$, Figure 28A, B). Consistently, p-JNK was exclusively expressed in ICC cells ($p<0.001$) (Figure 28A). Our results are also in line with the most recent report that malignant hepatocytes of human HCC specimen are mostly negative for p-JNK [276], together demonstrating that TNFα is preferentially secreted in human ICC's niches and ICC cells possess higher levels of p-JNK.

The above findings prompted an analysis of pharmacological sensitivities of well-characterized ICC and HCC cell lines to JNK inhibition. Human HCC cell lines Huh-7 and HepG2, human ICC cell lines ETK-1 and HuCCT-1 as well as an ICC cell line derived from murine ICC model were used (Ref). HCC cell lines and ICC cell lines were exposed with JNK inhibitor SP600125 at a range of concentration for 3 days. Inhibition of JNK activity by administration of SP600125 impaired cell proliferation in a dose-dependent manner (Figure 29A, B). All the three ICC cell lines showed more sensitivity to SP600125 than ICC cell lines (Figure 29A, B). ICC cell lines also showed higher degree to which maximal growth inhibition was achieved by JNK inhibition (Figure 29B). The effect of JNK inhibition on tumor formation was further investigated in vivo. mICC cells were subcutaneously injected into C57BL/6 mice. 50 mg/kg of SP600125 or mock control was administrated by i.p. injection once per day starting from day 1 post-operation. In the absence of SP600125 administration, the ICC cells resulted in tumor formation and aggressive growth (Figure 29C). Treatment with 50 mg/kg SP600125 inhibited tumor formation, as revealed by the decreased tumor mass weight (Figure 29C). The subcutaneous tumors formed by murine ICC cells expressed biliary lineage markers CK19 and A6, and displayed similar histological features to primary tumors in human ICC patients (Figure 29D). Collectively, these data suggested that targeted inhibition of JNK signaling in ICC may have therapeutic value.

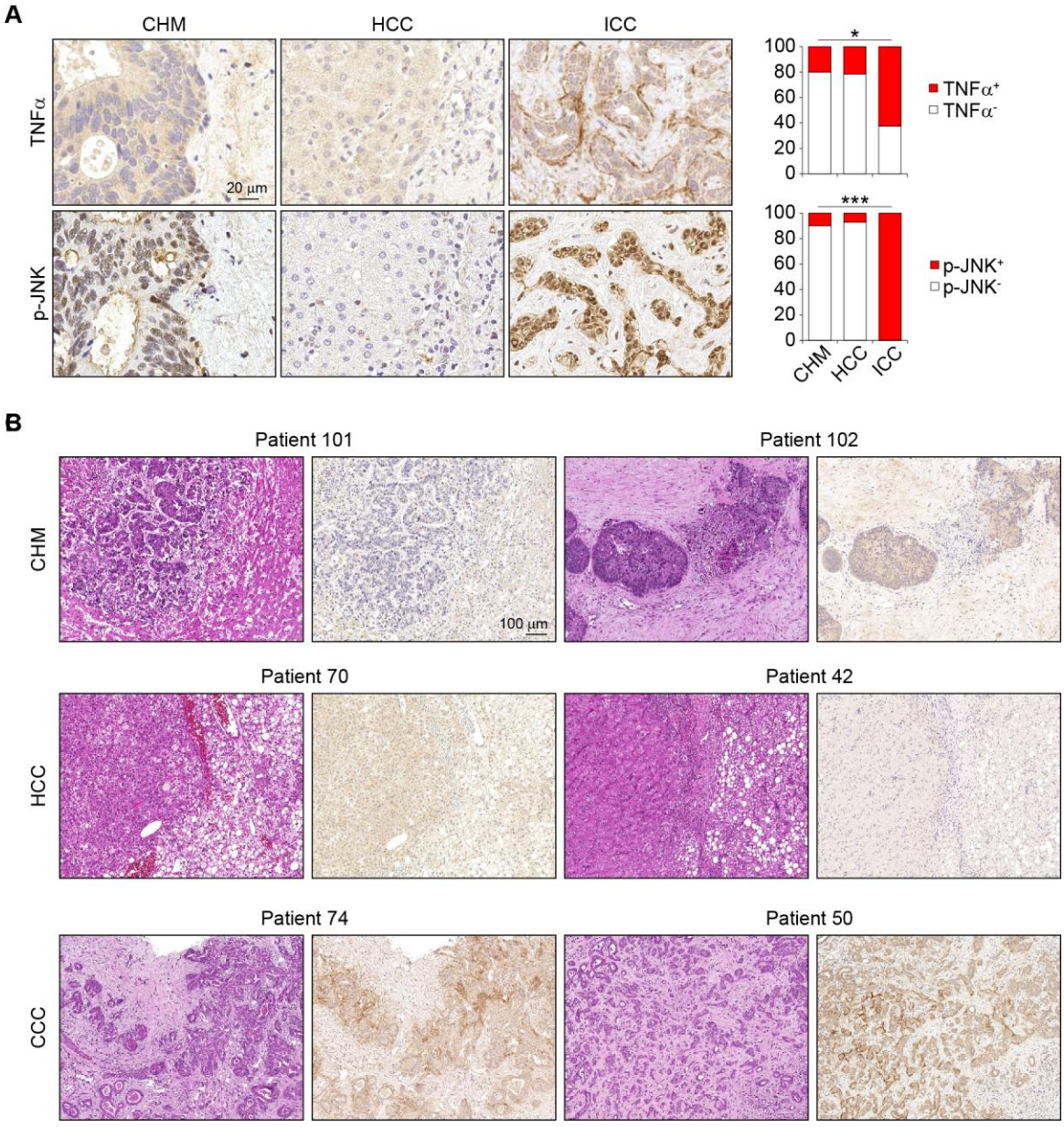

Figure 28. TNFα and p-JNK are specifically upregulated in ICC patient specimens.

(A) Immunohistochemistry staining of TNFα and p-JNK in consecutive liver sections from human patient samples. Quantifications of TNFα status and p-JNK status were shown in the right panels. (B) Representative hematoxylin-eosin staining and immunohistochemistry staining of TNFα in consecutive liver sections from human patient samples.

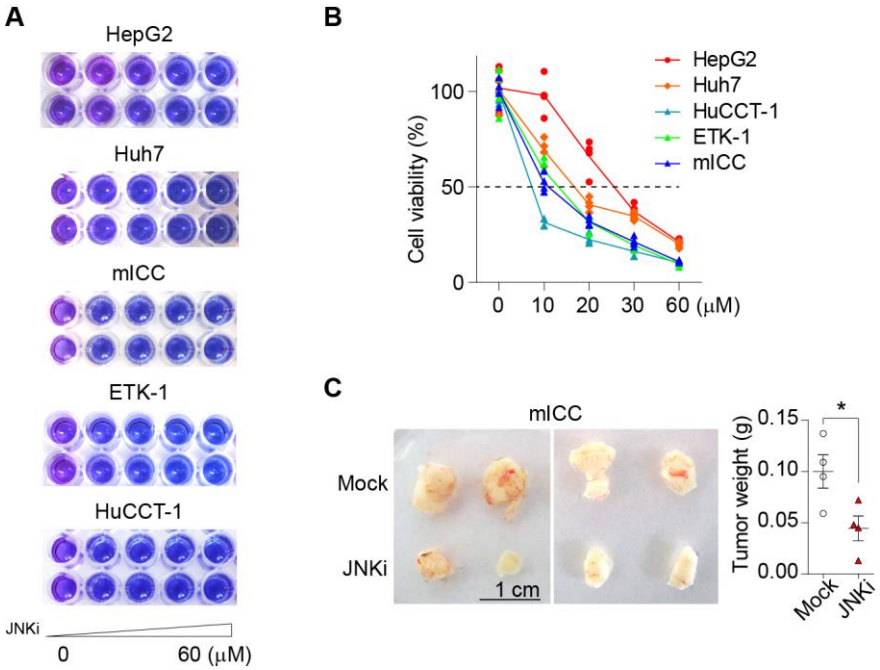

Figure 29. Pharmacological inhibition of JNK attenuates ICC cell growth in vitro and in vivo.

(A~B) Cell viability was measured using CellTiter-Blue assay in presence or absence of SP600125 for 3 days with gradients of concentrations as indicated in the x axis in human HCC cell lines HepG2, Huh7, human ICC cell lines HuCCT-1, ETK-1 and mouse ICC cell line. Data represent percentage of viable cells relative to untreated controls. Representative images of cell plates after CellTiter-Blue incubation were shown in (A).

(C) Mouse ICC cells were subcutaneously injected to C57BL/6 mice. Mice were treated with vehicle or SP600125 (50 mg/kg). Mice were sacrificed 2 weeks after the implantation and tumor weights were measured (n=5).

(D) Hematoxylin-eosin staining and immunohistochemistry staining of Ki67, CK19 and A6 in subcutaneous tumors formed by mouse ICC cell line.

3.2 HDAC2 deficiency in hepatocytes leads to HCC development

3.2.1 Specific and efficient deletion of HDAC2 in hepatocytes

To study the functions of HDAC2 in hepatocytes, we crossed mice with floxed *hdac2* alleles to the Alb-Cre mouse line [255]. The Alb-Cre HDAC2$^{f/f}$ mice were referred to as HDAC2$^{\Delta Hep}$ mice. Western blot analysis of whole liver extracts from adult mice revealed strongly reduced HDAC2 expression (Figure 30A). In agreement with recently published study, the mRNA levels of HDAC1 and 3, the HDACs sharing the highest similarity with HDAC2, were unchanged as determined by qRT-PCR (Figure 30B). Immunohistochemistry staining further confirmed the deletion of HDAC2 in hepatocytes, but not in other non-parenchyma cells, suggesting that Cre- driven excision of floxed exons was hepatocyte-specific.

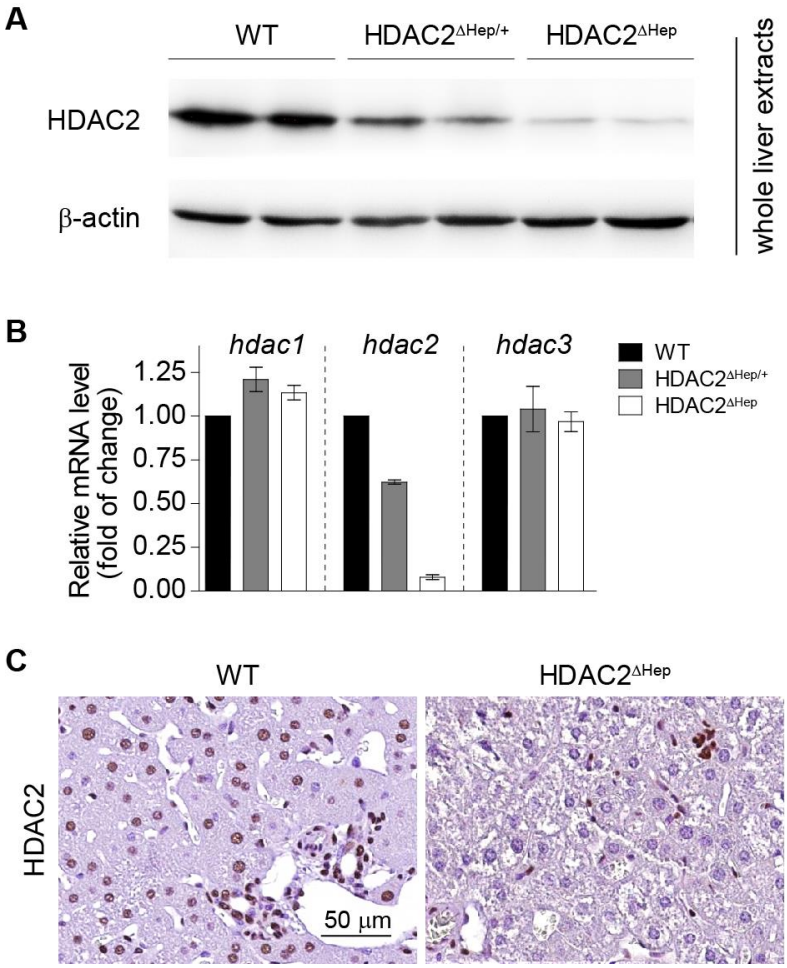

Figure 30. Specific deletion of HDAC2 in hepatocytes of HDAC2$^{\Delta Hep}$ mice.

(A) Western blot of whole liver lysates from 20-week-old HDAC2$^{\Delta Hep}$ mice, HDAC2$^{\Delta Hep/+}$ mice and control littermates (WT).

(B) qPCR of whole liver lysates from 20-week-old HDAC2$^{\Delta Hep}$ mice, HDAC2$^{\Delta Hep/+}$ mice and WT littermates.

(C) Immunohistochemistry staining of HDAC2 in liver sections from 20-week-old WT and HDAC2$^{\Delta Hep}$ mice.

3.2.2 No obvious liver damage was observed in HDAC2$^{\Delta Hep}$ mice

We analyzed the effects of hepatocyte specific HDAC2 deletion for liver homeostasis. No behavioral abnormalities were observed between HDAC2$^{\Delta Hep}$ mice and WT mice from 0~12 months of age. There were no statistically significant differences in terms of either the body weight or the ratio of liver weight to body weight between two groups (Figure 31A). Serum levels of liver enzymes were also monitored. Aspartate and alanine aminotransferase (AST and ALT) values, indicators of hepatocyte injury, were not changed in HDAC2$^{\Delta Hep}$ mice compared to control littermates (Figure 31C). There were no obvious differences in AP levels or bilirubin levels between two groups, demonstrating that liver function was not impaired (Figure 31C). Liver metabolisms such as cholesterol and triglyceride were not changed either (Figure 31C).

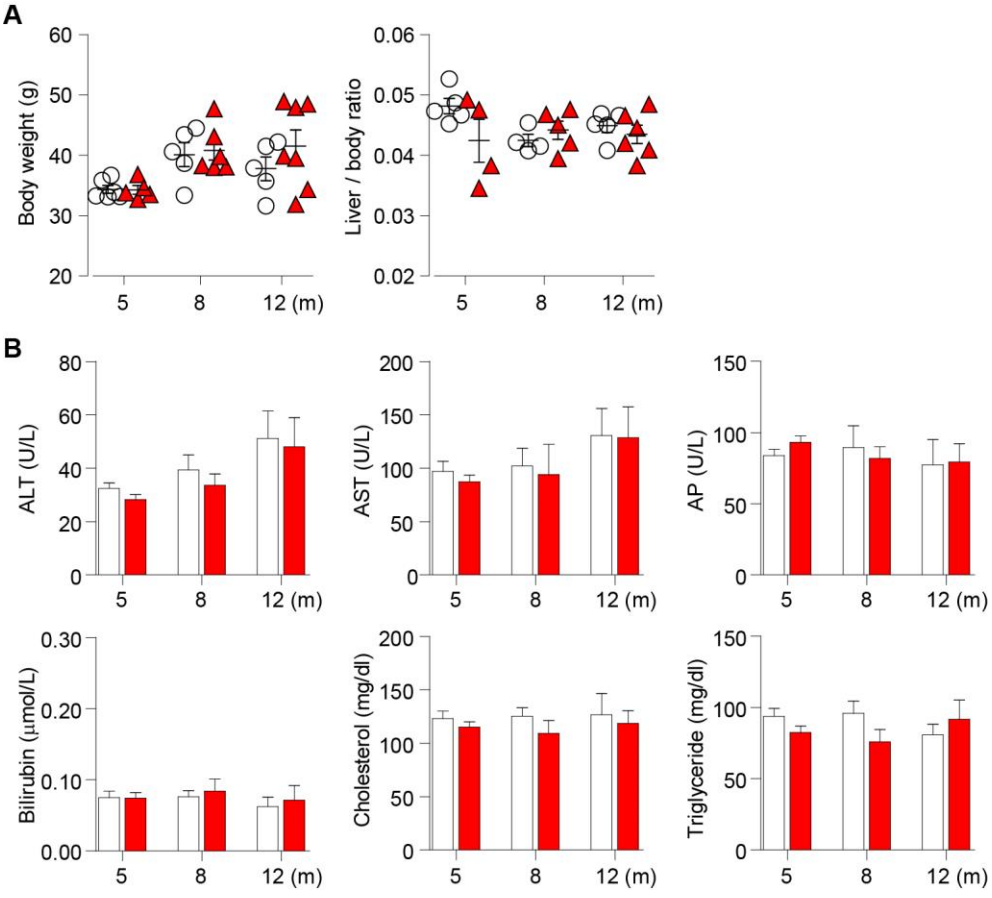

Figure 31. No obvious liver injury was detected in HDAC2$^{\Delta Hep}$ mice.

(A) Left: body weight of WT mice and HDAC2$^{\Delta Hep}$ mice. Right: Liver / body weight ratio of WT and HDAC2$^{\Delta Hep}$ mice was determined.
(B) Serum levels of AST, ALT, AP, bilirubin, cholesterol and triglyceride in WT mice and HDAC2$^{\Delta Hep}$ mice.

Most of the livers from 1-year-old HDAC2$^{\Delta Hep}$ mice exhibited normal macroscopic appearance as the WT livers (Figure 32A). Immunohistochemistry analysis of p53 and cleaved-caspase 3, which are often expressed in liver damage models, were stained negatively in HDAC2$^{\Delta Hep}$ mice (Figure 32B).

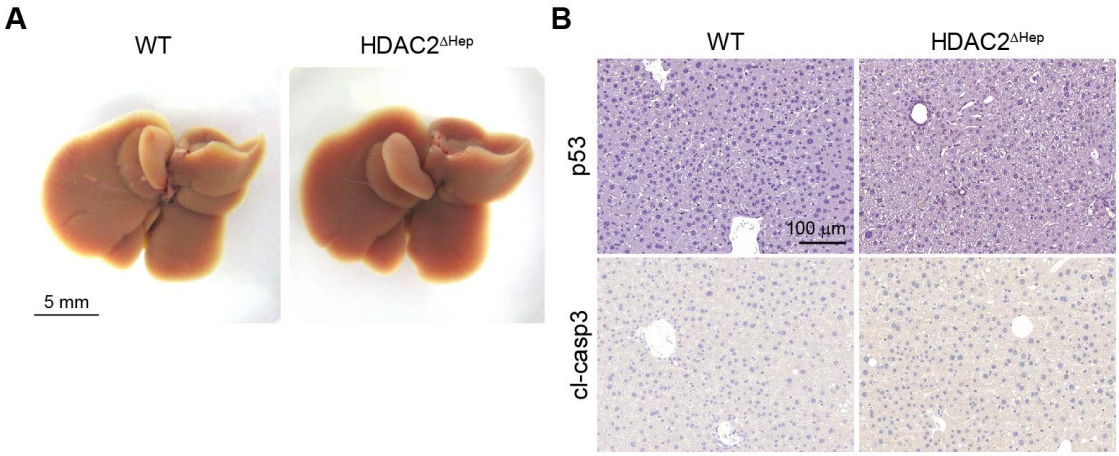

Figure 32. Livers of 1-year-old HDAC2$^{\Delta Hep}$ mice show normal architecture.
(A) Macroscopic appearance of liver from 1-year-old WT and HDAC2$^{\Delta Hep}$ mice.
(B) Immunohistochemistry staining of p53 and cleaved-caspase 3 in liver sections from 1-year-old WT and HDAC2$^{\Delta Hep}$ mice.

3.2.3 Low incidence of HCC formation in HDAC2$^{\Delta Hep}$ mice

Although most of 1-year-old HDAC2$^{\Delta Hep}$ mice didn't show sign of disease, 17.1% (6/35 mice) developed tumors on the liver surface. Liver tumors ranged from ~1 mm to 5 mm in diameter (Figure 33A, B). Histologically, most of tumors were similar to human steatohepatitic HCC characterized by with ballooning cancer cells and inflammatory cell infiltration (Figure 33C), a special morphologic variant of HCC associated with metabolic risk factors [277].

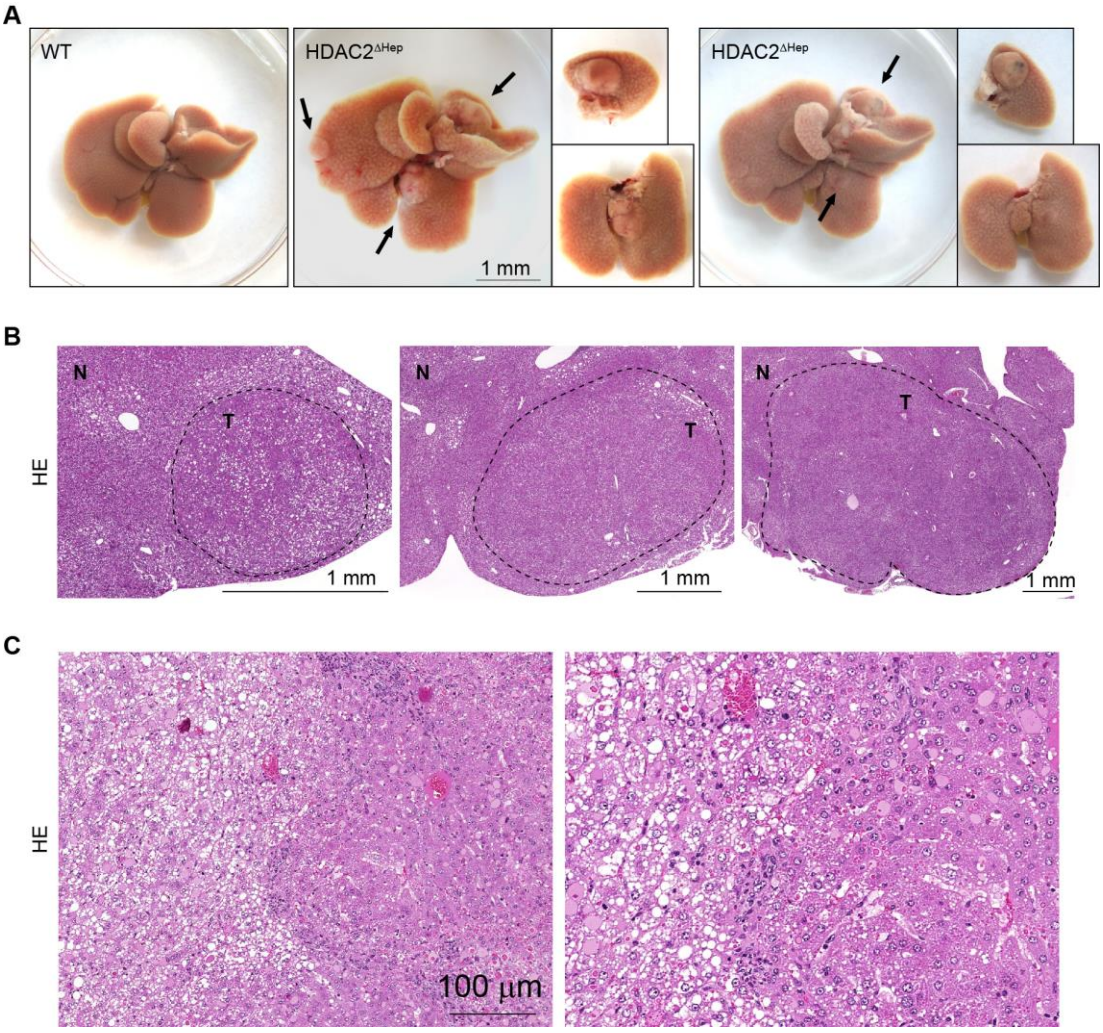

Figure 33. Development of liver tumors in HDAC2$^{\Delta Hep}$ mice.

(A) Macroscopic appearance of liver from 1-year-old WT and HDAC2$^{\Delta Hep}$ mice.

(B) Representative hematoxylin-eosin staining of liver sections with HCC ranging from small nodules to large tumors.

(C) Representative hematoxylin-eosin staining of steatohepatitic HCC in 1-year-old HDAC2$^{\Delta Hep}$ mice.

3.2.4 Histological characterization of HCC in HDAC2$^{\Delta Hep}$ mice

To determine whether the tumors in HDAC2$^{\Delta Hep}$ mice originated from HDAC2 deficient hepatocytes or a minute subset of HDAC2 positive hepatocytes due to an inefficient Cre-recombinase mediated excision, immunohistochemistry analysis of tumor sections was performed with HDAC2 antibody. The results showed that the tumor cells were

negatively stained, suggesting that tumors in HDAC2$^{\Delta Hep}$ mice originated from HDAC2 deficient hepatocytes (Figure 34A).

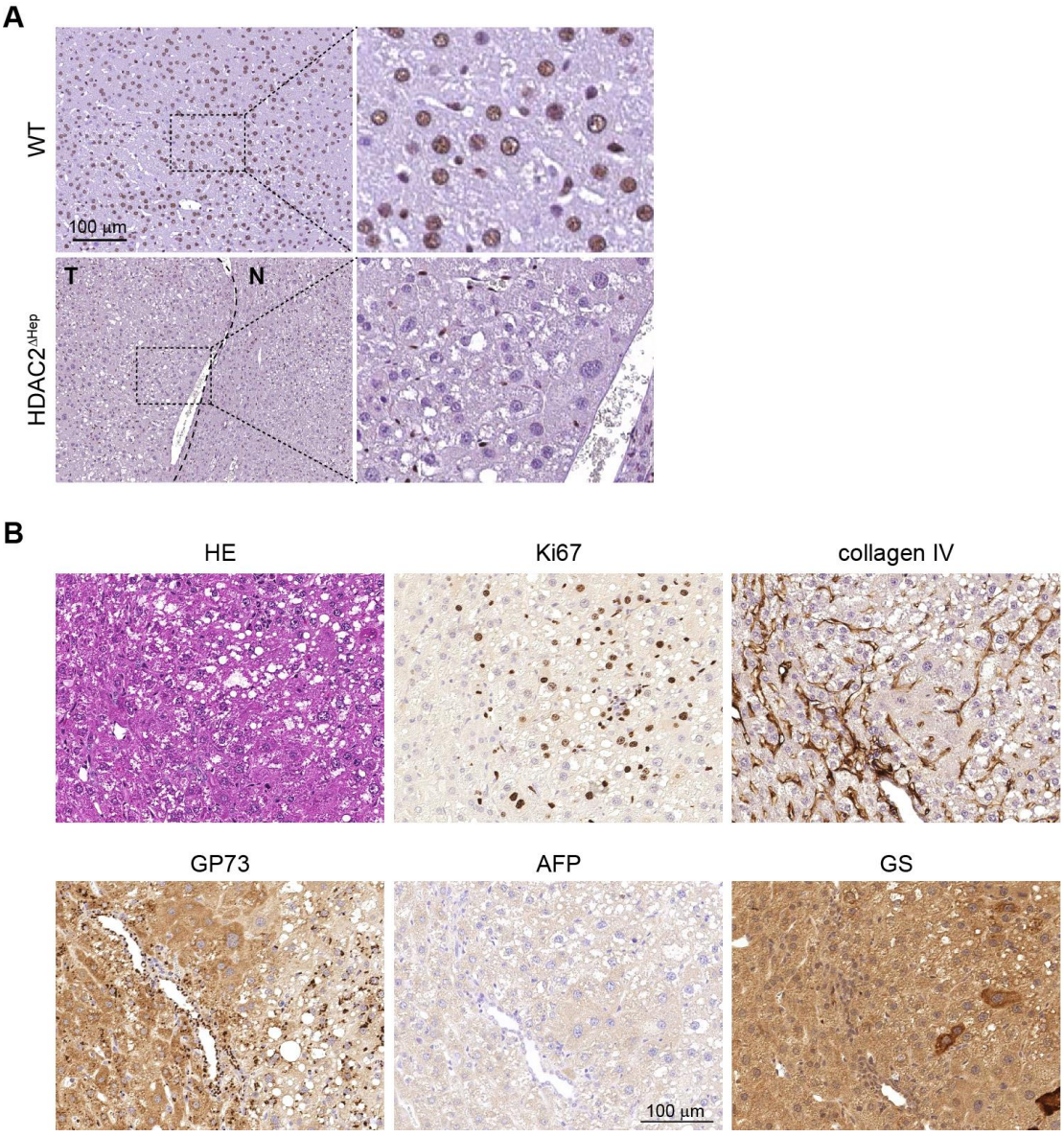

Figure 34. Histological characterization of HCC in HDAC2$^{\Delta Hep}$ mice.

(A) Immunohistochemistry staining of HDAC2 in liver sections from 1-year-old WT and HDAC2$^{\Delta Hep}$ mice.

(B) Representative hematoxylin-eosin staining and immunohistochemistry staining of Ki67, collagen IV, GP73, AFP and glutamine synthetase (GS) of liver sections with tumors in HDAC2$^{\Delta Hep}$ mice.

HDAC2 deficient tumors showed higher rate of proliferation than the surrounding non-tumor areas, as revealed by Ki67 staining, and disordered ECM network by collagen IV staining (Figure 34B). In addition, tumors in HDAC2$^{\Delta Hep}$ mice displayed strong immunoreactivity for GP73 (Figure 34B). However, most HDAC2 deficient tumors were negatively stained for AFP and glutamine synthetase (GS) (Figure 34B). These patterns might provide clues for exploring mechanism of how HDAC2 deficiency leads to cancer development.

3.3 Inflammatory micro-niche promotes HCC development with crucial survival and growth factors.

3.3.1 Persistent activation of IKK in hepatocytes induces HCC

ROSA26-LSL-IKKβ(EE) mice [278] was bred with Albumin-Cre mice by our collaborator, Dr. Finkin and Prof. Pikarsky to assess the outcome of aberrant IKK-NF-κB activation in hepatocytes. Their preliminary work has shown that 100% of IKKβ(EE) mice spontaneously developed HCC at 20 months of age compared to 8% of control Albumin-Cre mice. Treating IKKβ(EE) mice with the hepatic carcinogen diethylnitrosamine (DEN) accelerated appearance of HCCs as early as 9 months of age (data from Shlomi). We performed histological analysis to further characterize the liver tumors in IKKβ(EE) mice. Immunostaining for the proliferation marker Ki67, the matrix associated collagen IV, and the HCC markers GP73 and GS confirmed that these were aggressive HCCs (Figure 35A, B). Quantification of $Ki67^{+}$ hepatocytes showed that hepatocytes in IKKβ(EE) mice are more proliferative than those in WT mice (Figure 35C).

3.3.2 Molecular characterization of HCCs in IKKβ(EE) mice

Cairo and colleagues defined a set of 16 genes that characterizes HCC aggressiveness [279], composed of a proliferation signature (associated with an aggressive phenotype) and a differentiation signature (associated with a mild phenotype). I measured expression of these 16 genes, using real time PCR, in spontaneously-developed IKKβ(EE) HCCs (n=10), DEN-treated IKKβ(EE) HCCs (n=10) and DEN-treated WT mice HCCs (n=10) that served as controls. Both classical HCC and CCC/HCC morphologies from IKKβ(EE) were included in this analysis. Also included in the analysis were RNA samples prepared from normal WT liver parenchyma (n=4) and from highly aggressive c-myc/p53-/- HCCs (n=3) (REF). I then performed unsupervised clustering of the tumors (Figure 36). HCCs from DEN treated WT mice tended to cluster with the WT livers while HCCs from IKKβ(EE) mice clustered with the aggressive c-myc/p53-/- HCCs (7 out of 10 compared with 2 out of 20, p=0.002, Fisher's exact test). Tumors displaying the CCC/HCC morphology, which were only detected in the IKKβ(EE) mice and not found in control DEN treated ones, showed a worse expression pattern than those with classical HCC morphology (Figure 36). Of note, I did not detect a difference in the gene expression pattern between spontaneous and DEN induced HCCs in IKKβ(EE) mice.

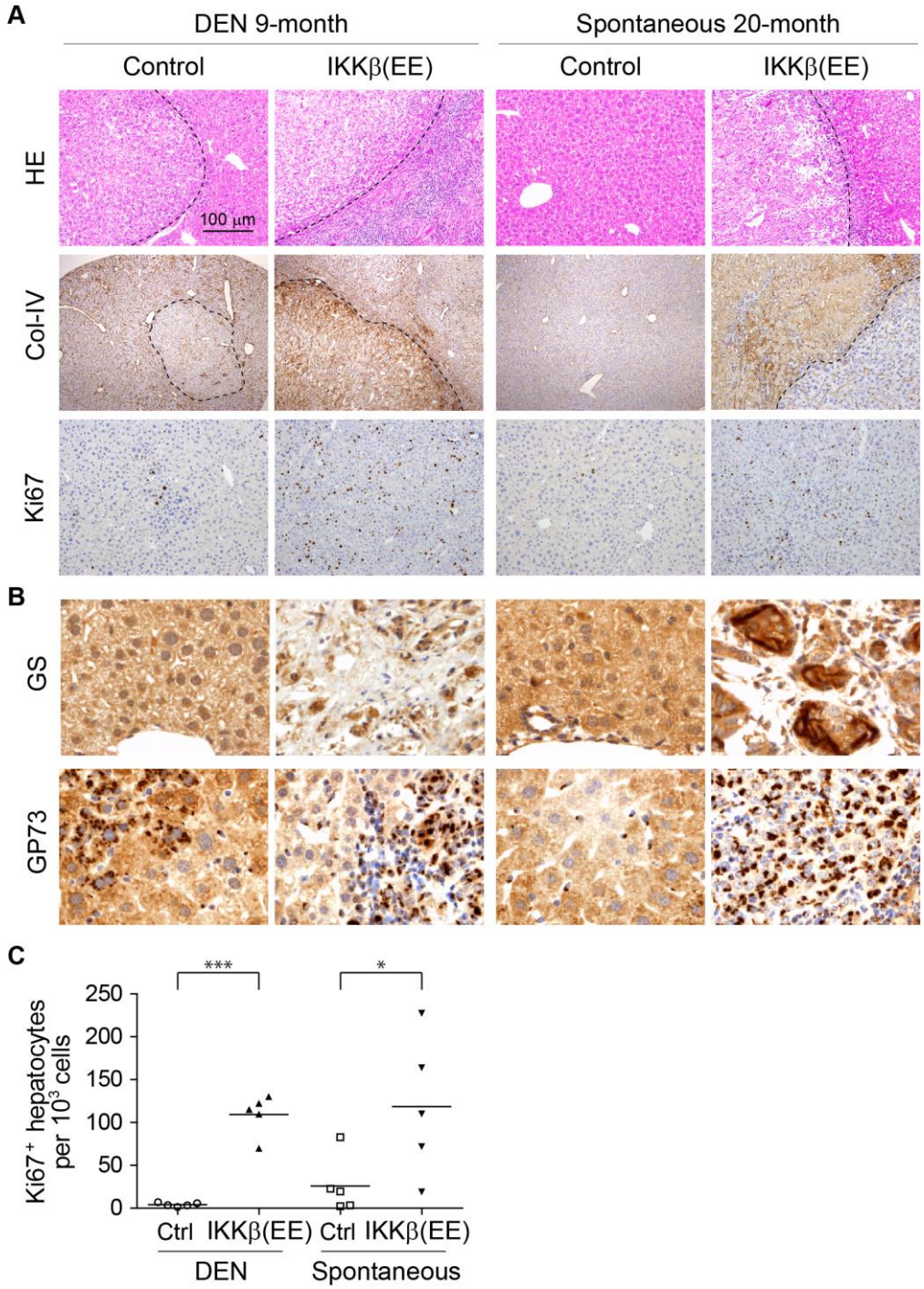

Figure 35. Histological characterization of HCC in IKKβ(EE) mice.

(A) Hematoxylin-eosin staining and immunohistochemistry staining of col-IV, Ki67 in liver sections from mice as indicated.

(B) Immunohistochemistry staining of GS and GP73 of liver sections from (A).

(C) Quantification of Ki67^{+} hepatocytes from (A).

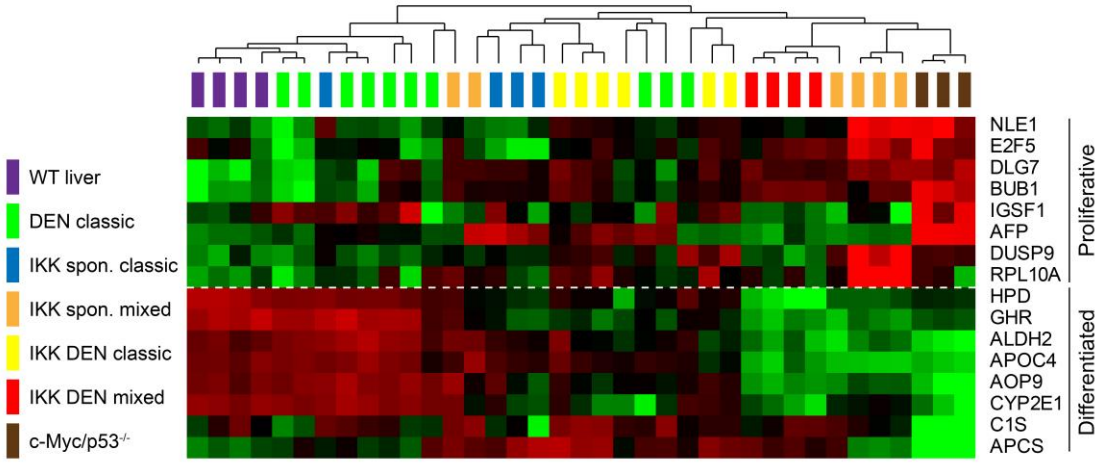

Figure 36. Molecular characterization of HCCs in IKKβ(EE) mice by 16-gene HCC signature. Heat map representation of relative mRNA expression of a 16-gene HCC proliferation/differentiation signature in WT liver parenchyma or HCCs derived from the indicated mice. Clusters were determined by an unsupervised clustering.

To further confirm the neoplastic nature of the tumors we performed array comparative genomic hybridization (aCGH) of genomic DNA isolated from HCCs derived from either DEN-treated Alb-Cre control (n=12), DEN-treated IKKβ(EE) mice (n=11) and 20-months old IKKβ(EE) mice (n=13). aCGH revealed chromosomal aberrations in all HCC samples, confirming their neoplastic nature (Figure 37). Amplifications and deletions of chromosomal regions ranged from <1 megabase (MB) to 193 MB. Of note, the complexity of the genomic aberrations differed between the 3 groups of mice: DEN-induced HCCs from control Alb-Cre mice showed the lowest amount of aberrations (Figure 37B), followed by DEN-induced HCCs derived from IKKβ(EE) mice (Figure 37B), while spontaneous IKKβ(EE) HCCs acquired the highest number of copy number variations (Figure 37A). Taken together, the data confirmed that IKKβ(EE) mice develop aggressive HCCs with a 100% penetrance.

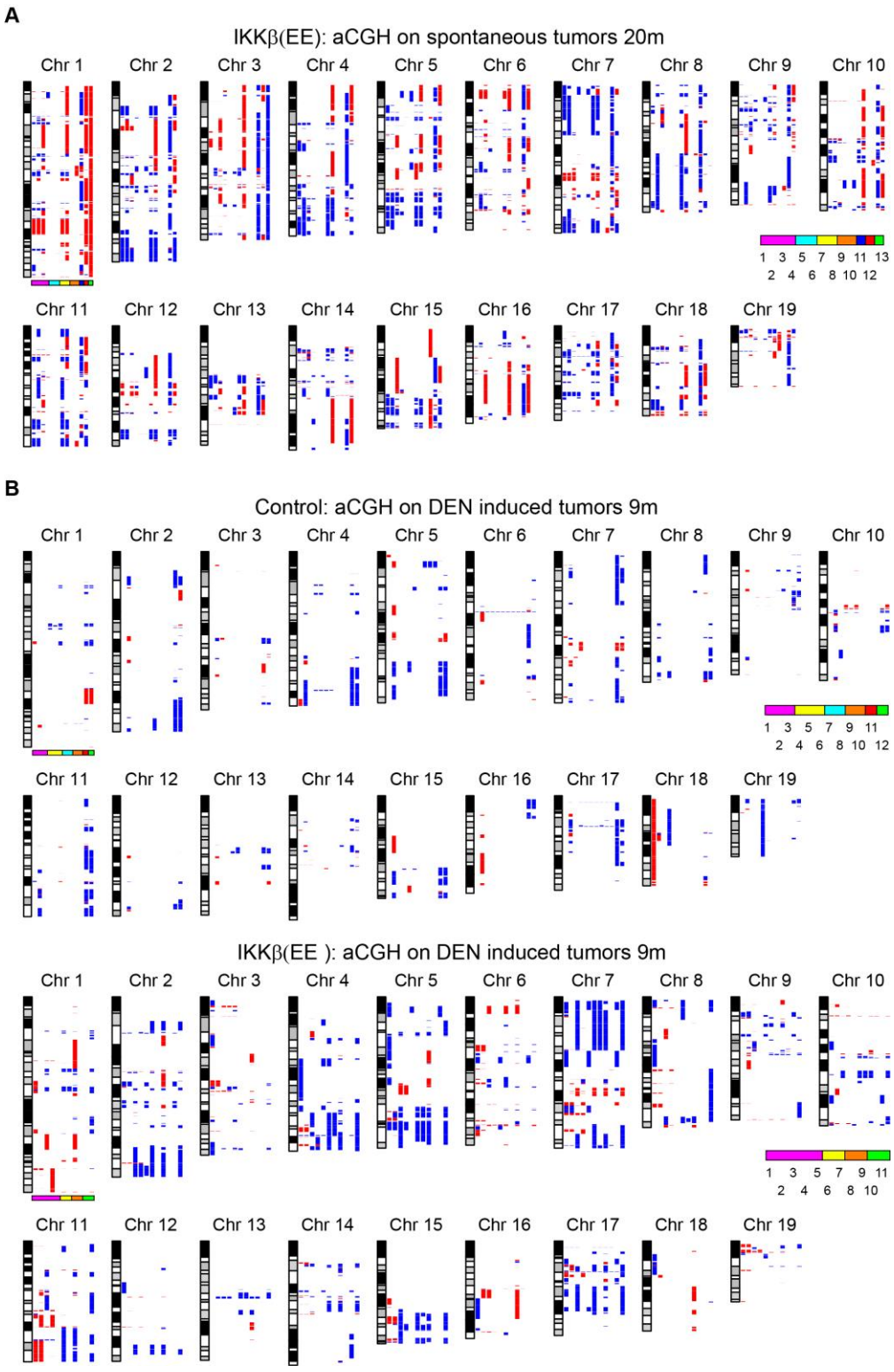

Figure 37. aCGH analysis of spontaneous IKKβ(EE) HCCs (A), DEN-induced HCCs from control mice and IKKβ(EE) mice. Bioinformatic analysis was done by PD Dr. Kristian Unger.

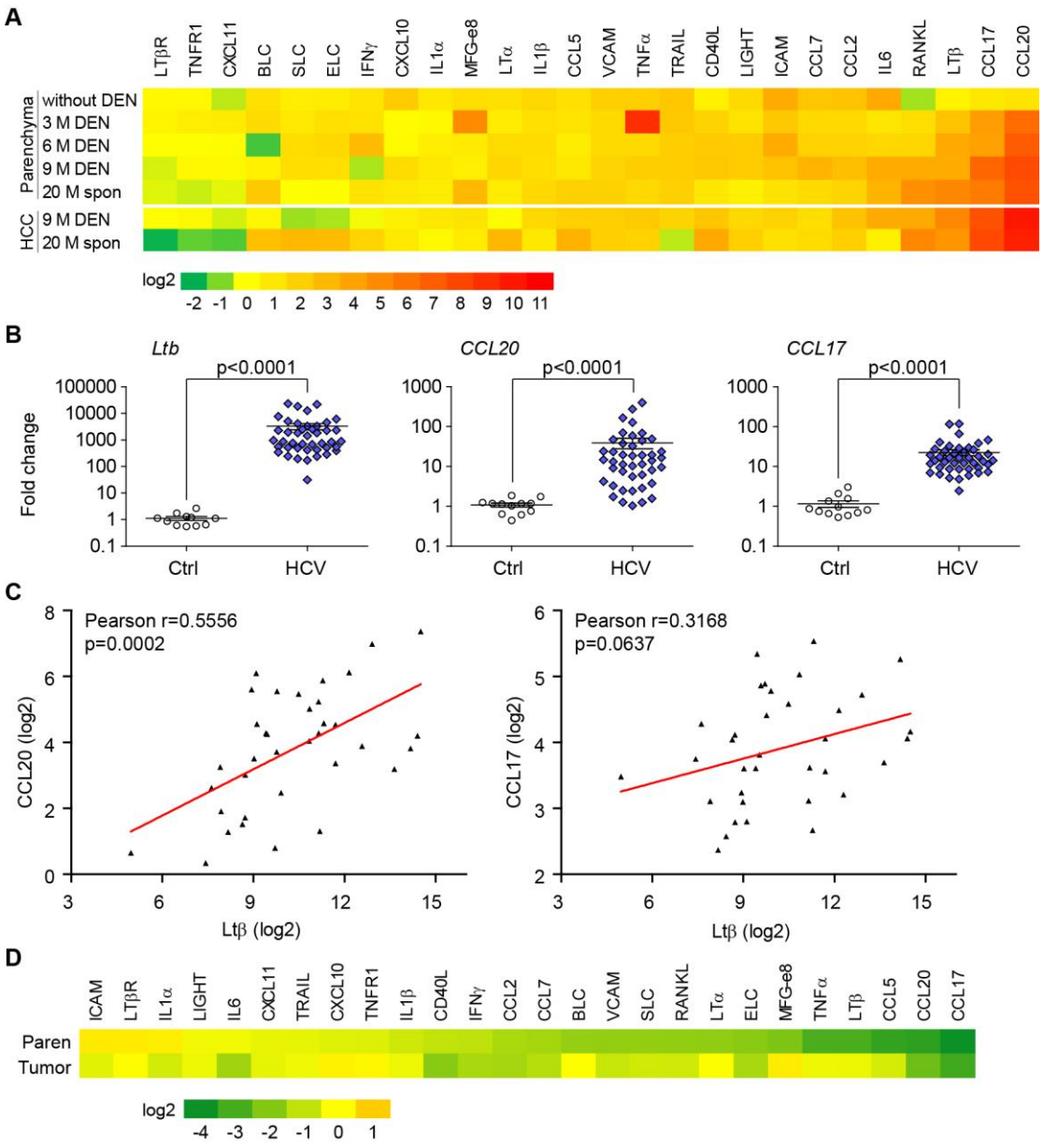

Figure 38. Activation of LT pathway in IKKβ(EE) mice and HCV infected patients.

(A) mRNA qPCR analysis of liver parenchyma and HCCs from IKKβ(EE) or DEN-treated IKKβ(EE) mice at the indicated ages, as well as in liver parenchyma of 3 months old IKKβ(EE) mice without DEN treatment. Each data point reflects the median expression, normalized to the mean expression of the same gene in control livers derived from the equivalent Alb-Cre mice (n≥5, besides n=1 for a single HCC that developed spontaneously in 20-months old Alb-Cre mice and n=4 for 3 months old Alb-Cre mice).

(B) Scatter plot representations of mRNA qPCR analyses of liver tissue from HCV-infected patients (n=43) relative to healthy controls (n=12, ***p<0.0001). Scatter plots depict mRNA amounts of the LT pathway chemokines LTβ, CCL17 and CCL20.
(C) Spearman correlation plots of mRNA expression levels of *ltβ* vs. *ccl17* and *ltβ* vs. *ccl20*, respectively in livers from HCV infected patients.
(D) Heat map representation of mRNA qPCR analysis of liver parenchyma and HCCs from 33-weeks-old IKKβ(EE) mice treated with LTβR-Ig for 10 consecutive weeks. Each data point reflects the median expression, normalized to the mean expression of the same gene in equivalent MOPC21 (control murine-IgG1)-injected IKKβ(EE) mice (n≥7, Log2 scale).

3.3.3 Growth promoting cytokines in IKKβ(EE) livers promote HCC development

Previous work by Shlomi Finkin identified inflammatory structures prior to the appearance of HCCs in IKKβ(EE) livers (data not shown). I hypothesized that cytokines possibly present at high concentrations in these inflammatory structures could mediate the tumor promoting effects. To identify pro-tumorigenic signals, we measured expression of multiple cytokines in liver parenchyma, livers and HCCs from IKKβ(EE) mice. Among others, lymphotoxin (LT) family members, in particular LTβ and LIGHT, and their downstream effectors, CCL17 and CCL20, were prominently overexpressed in IKKβ(EE) livers (Figure 38A). LTβ is also expressed in livers of patients with chronic HCV infection (Figure 38B). Moreover, I noted a significant correlation between CCL17 and CCL20 expression and that of LTβ in human samples (Figure 38C). This suggests that LTβR activation by LTα/β and/or LIGHT could play a key role in pro-tumorigenic processes.

To test this hypothesis, blockade of LT cytokines in IKKβ(EE) mice using a soluble LTβR fused to a murine immunoglobulin Fc portion (LTβR-Ig) was performed by Shlomi Finkin. Measurements of expression of multiple cytokines in liver parenchyma showed significant reduction in many of the pro-inflammatory and of the LT-mediated cytokines (Figure 38D). LTβR inhibition dramatically reduced HCC burden in IKKβ(EE) mice (data from Shlomi), indicating that LT signaling may be a promising drug target for HCC.

4. DISCUSSION

4.1 Role of pro-inflammatory signaling in adult stem cell homeostasis

Adult stem cells are tightly controlled in and embedded by their niches, which are highly dynamic and interactive with the involvement of many stromal cell types and soluble factors. Here, we present a series of genetic and pharmacologic experiments to investigate the role of TNFα/JNK signaling axis in inducing cholangiolar lineage commitment (Figure 39). First, cholangiolar differentiation was inhibited in HSP60$^{\Delta Hep}$ mice with JNK inhibition or pharmacological Kupffer cell depletion, the latter of which can be reversed by additional TNFα treatment. Second, TNFα stimulation promoted cholangiolar lineage commitment of bipotential hepatoblasts and HepRG cell line, whereas JNK inhibition impaired this process. Third, knockout of TNFR1 shifted the lineage commitment of LPCs from cholangiocyte differentiation into hepatocyte differentiation. Last, by using the established mouse ICC cell line and human CCC cell lines, we demonstrate that murine and human ICC cells intrinsically possessed higher TNFR1 expression and JNK activation, and were thereby sensitive to JNK inhibition.

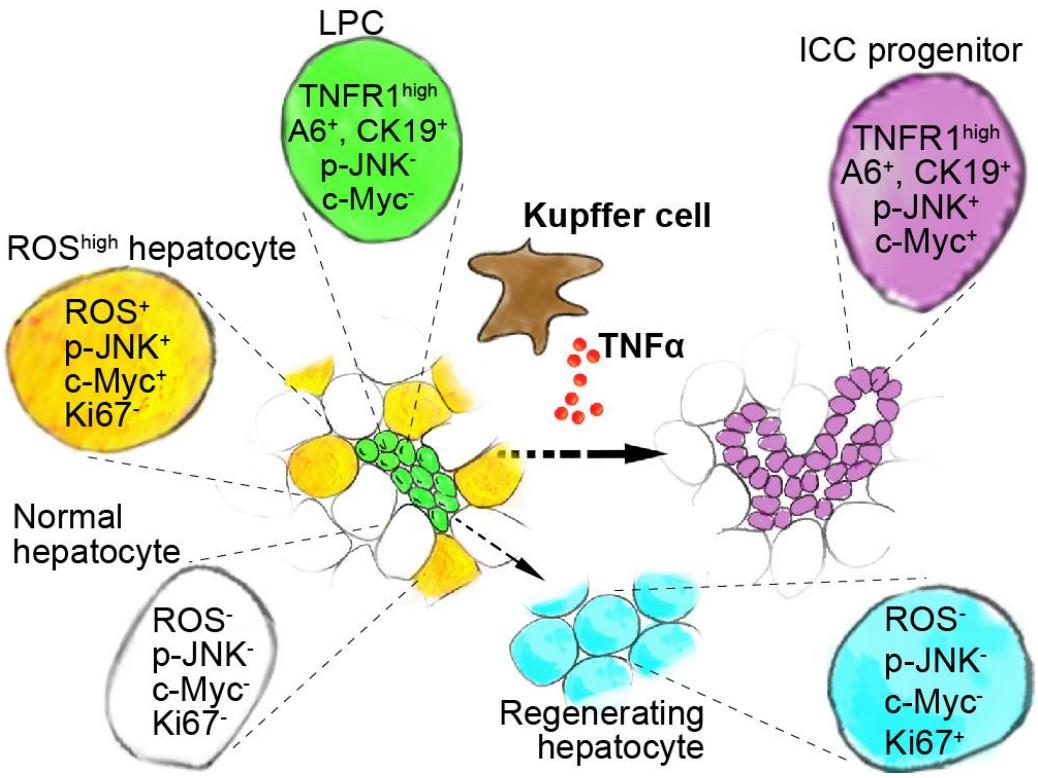

Figure 39. A model for non-autonomous ICC initiation by oxidative stress in hepatocytes.

It may help to gain more insight into TNFα's role in liver homeostasis by comparing our mechanism with the role of TNFα in other physiological or pathological conditions, such as liver development and liver regeneration. A representative study of TNFα in liver development was done by Akihide Kamiya and Frank J. Gonzalez [35]: TNFα mRNA was detected from midfetal livers and continued to be expressed in 14-day-old mouse livers, but not in 21-day-old livers and the adult livers, whereas TNFR1 is expressed in both fetal and adult livers. Using cultured fetal hepatocytes, TNFα was characterized as a suppressive factor of hepatic maturation through inhibiting the expression of HNF4a and several mature liver-specific genes. However, TNFα promotes cell division by inducing the expression of cyclin A2. In contrast, hepatic maturation factor oncostatin M (OSM), an IL-6 family cytokine expressed in the late-fetal liver, induces hepatic maturation but at the same time reduces the relative proliferation of fetal hepatocytes. The authors interpreted the temporal and spatial co-exist of these factors as a balance of liver's hematopoiesis function and hepatic function around the perinatal stage. Another possible reason for this complexity we would like to add is that TNFα may prevent premature differentiation of fetal hepatocytes before the liver reaches its normal mass. TNFα and OSM balance the growth and the function of fetal liver by subtle temporal regulation that TNFα expresses mainly during the perinatal and postnatal stages while OSM expresses in the late-fetal liver. Their work demonstrated the role of TNFα in the progress of fetal liver development. Although the function of TNFα in biliary cell differentiation was investigated in their work, the suppressive role of TNFα in hepatocyte maturation is in line with our findings.

The role of TNFα signaling during liver regeneration after partial hepatectomy has been studied since 1990s. The results seem to be controversial due to: First, the dual effects of TNFα signaling in cell survival or cell death; Second, the different models researchers used; last, the different surgery procedure, for example, the extent of hepatic resection [83, 280-283]. A currently accepted paradigm is that TNFα is one of the immediate-early cytokines upregulated during the first step of liver regeneration and act as a primer to sensitize hepatocytes to the proliferative effects of growth factors like IL-6 [284-286]. Administration of anti-TNF antibodies or genetically knockout TNFR1 harms DNA replication, resulting into delayed liver regeneration and significant mortality [287]. It is worthy to note that activation of JNK and c-Jun has been demonstrated shortly after partial hepatectomy [288] and c-Jun is essential in hepatogenesis during embryonic development and in vitro differentiation [83, 84, 289]. The work with fetal liver

development and partial hepatectomy demonstrates that TNFα/TNFR1-JNK axis enhances hepatocytes plasticity by keeping them in the less differentiated and more proliferative state. Recently, TNFα was shown to contribute to trans-differentiation of rat hepatocytes into cholangiocytes [273]. Our data further extended these results by showing that TNFα exerts an important role in lineage specification of LPCs under the context of mitochondrial defects induced liver damage. Collectively, these results indicate that TNFα/TNFR1 signaling regulates liver homeostasis in both physiological and pathological situations by inducing fate decision. The effect of TNFα in keeping cells away from hepatic lineage seems to be similar in both fetal and terminally differentiated hepatocytes, as well as in LPCs, suggesting a developmental conservatism of these cells. In addition, it remains to determine how the cross-talk of TNFα signaling with the other signaling pathways (for example, IL-6 signaling, TGFβ signaling, Notch signaling, et al) coordinates liver cell plasticity in different models.

Our observations together with the data provided by Nishikawa suggest that TNFα/TNFR1-JNK signaling can induce a biliary differentiation program in hepatocytes or hepatic progenitor cells, implicating this signaling pathway in the pathogenesis of human ICC. Indeed, we pathological examination of human HCC and ICC samples showed that TNFα and p-JNK were found in ICC cells, whereas they were mostly absent from HCC samples. In line with our findings, Hefetz-Sela and colleagues did pathological examination of human HCC samples and demonstrated that malignant hepatocytes are mostly negative for p-JNK [276]. To date, ICC currently lacks effective chemotherapeutic options due to the lack of identification of critical ICC relevant factors. Our results with human HCC and ICC samples reveal distinct molecular traits of these two different pathological entities. This finding was further substantiated by the fact that cancer cells isolated from human ICC are more sensitive to JNK inhibition compared to cells from HCC. JNK inhibition also led to the regression of established xenotransplant tumors derived from ICC cell lines in vivo. In our study, very low levels of p-JNK^{+}CK19^{+} cells are also present in “unaffected” liver tissues from ICC patients. Due to the small number of cases, detailed statistical analyses could not be performed to evaluate the correlation between these cells and ICC relapse. Further investigation of the link between TNFα positivity and clinic-pathological features of ICC patients may provide important clues for disease surveillance. In addition, targeting TNFα or JNK might provide a new therapeutic approach for the treatment of aggressive ICC.

Our data highlight the role of mitochondrial dysfunction and oxidative stress in liver pathogenesis. Mitochondrial dysfunction and oxidative stress have been reported to play widespread roles in aging, cancer and other human pathologies [290-293]. The evidence of oxidative stress is also one of the common features of acute and chronic liver diseases, contributing to disease progression [26, 41, 291]. Mitochondrial dysfunction and oxidative stress exert their functions via diverse mechanisms, including DNA damage accumulation, maintaining mitogenic signals, promoting angiogenesis, metabolism reprogramming, and modulation of immune response [294-298]. Most recently, new data from a genetic screen in Drosophila have indicated that mitochondrial defect and ROS production can activate oncogenic signaling in the neighboring cells by forming a carcinogenic environment [268]. In this study, we demonstrated that mitochondrial defect in hepatocytes triggers ROS accumulation and recruits TNFα-producing Kupffer cells, which constitute a favorable niche for cholangiolar lineage specification by activating TNFα/JNK signaling axis in LPCs. Attenuating the accumulation of ROS abolishes cholangiolar overgrowth in the mice. To our knowledge, this is the first indication that ROS produced in hepatocytes play a role in the pathogenesis of ICC in a cell-non-autonomous way, which also suggests that the liver microenvironment could be pharmacologically manipulated to improve liver function in advanced liver disease like acute hepatitis. A better insight into the intrinsic and/or extrinsic role of oxidative stress in liver cancer progress will give implications for the prevention and therapy.

In conclusion, we show that TNFα, a cytokine that has become the paradigm for induction of inflammatory responses, is also key in the establishment of the cholangiolar lineage in mitochondrial defect induced liver damage. In addition to the known signaling inputs required to establish cholangiolar fate, inflammatory signals should now be added to this list. As a reciprocal supportive interplay between cancer cells and their niche may be critical to promote cancer initiation and progression, blocking ROS accumulation, targeting TNFα signaling and/or JNK activation are likely to be attractive therapeutic approaches for the prevention and treatment of human ICC. Our finding not only provides another example to a mechanism in which pro-inflammatory microenvironment may function as niche to coordinate adult stem cell differentiation, but also suggests TNFα and JNK as an attractive ICC therapeutic target.

4.2 Specific role of HDAC2 in liver homeostasis

The role of individual HDAC in liver homeostasis and the underlying molecular mechanisms are being extensively investigated these days. Loss of HDAC2 alone has shown to be compensated by HDAC1 in many tissues, including epidermis and T cells [299, 300]. Zimmermann and colleagues even showed that mice bearing mutant HDAC2 are compatible to survival, even though the mutant mice show reduced body size and decreased intestinal tumor rates [301]. Notably, Xia and colleagues have most recently shown that inactivation of either HDAC1 or HDAC2 severely reduced liver regeneration after hepatectomy [302], indicating that the functions of HDAC1 and 2 are not completely redundancy in livers. Our finding that HDAC2 deficiency in hepatocytes leads to tumor development at 1-year-old of age is surprising. However, further studies are urgently necessary for the proper interpretation of these results.

First, the low incidence of tumor formation in HDAC2$^{\Delta Hep}$ mice needs to be confirmed by larger cohort of mice. Since we didn't see even a single case of tumor development in livers of WT mice, the cancer phenotype of HDAC2$^{\Delta Hep}$ mice is not likely due to housing conditions like occasional virus infection or food contamination. The low tumor incidence could be resulted from compensation of HDAC1. However, even in hepatocytic HDAC1/2 double knock-out mice, the livers didn't show any abnormalities expect in pathological conditions such as hepatectomy mentioned above. Nevertheless, our results didn't conflict with this report because the authors didn't age their knock-out mice. Increasing the cohort of aged mice will not only help to confirm the phenotype but also provide clues for mechanism study.

Second, the differences between aged mice without HCC and mice with HCC need to be clarified. The reason for the low tumor incidence might be that HDAC2 deficiency itself is not sufficient to induce cancer development. Loss of HDAC2 could facilitate tumorigenesis triggered by other stimulus. Comparing the aged livers with or without tumors is important for understanding the specific role HDAC2 in liver homeostasis and liver cancer progression.

Finally, our histological subtyping of liver tumors in HDAC2$^{\Delta Hep}$ mice already pointed to a specific group of HCC - steatohepatitic HCC. The ballooning cancer cells as well as the surrounding ballooning hepatocytes indicate that the lipogenesis of hepatocytes was dysregulated. Whether HDAC2 deficiency leads to increased lipogenesis or HDAC2 deficiency facilitates tumor initiation triggered by increased lipogenesis needs further

investigations. The preference of steatohepatitic HCC in HDAC2$^{\Delta Hep}$ mice also suggests that monitoring metabolism changes, in our case lipogenesis of hepatocytes, is important to predict the drug reactivity for clinical trials of HDAC inhibitors, and supply of HDAC inhibitors to patients with hepatosteatosis or nonalcoholic steatohepatitis should be very cautious.

4.3 Inflammatory micro-niche for tumorigenesis

The study of HCC development in IKKβ(EE) mice shows that constitutive activation of the IKKβ-NF-κB pathway can result in spontaneous hepatocarcinogenesis and accelerate carcinogen induced HCC. This is driven at least partly via expression of cytokines that are presented to transforming hepatocytes within defined inflammatory micro-niche. Remarkably, similar micro-niche is commonly found in human livers in which the NF-κB pathway is constitutively activated due to infection with hepatitis viruses (e.g. HBV, HCV). Blockade of LTβR signaling sufficed to reverse some of the pro-tumorigenic effect of constitutive IKKβ activation in the liver. Of note, this marked tumor inhibition took place without any effect of the LTβR inhibitor on activation of the canonical NF-κB pathway in hepatocytes. Although the link between inflammation and cancer is well established and the role of NF-κB in orchestrating this link has been extensively studied, such intimate relationship between the inflammatory microenvironment and evolving cancer cells has not been described in solid malignancies.

It is noteworthy that the IKKβ(EE) driven mouse HCCs were histologically more aggressive than the HCCs that developed in control mice as assessed by histologic type. Also, two molecular markers of bad prognosis HCC were prevalent in IKKβ(EE) driven tumors: expression pattern of the 16 gene signature and higher numbers of genomic aberrations.

Of note, our study suggests that apart from the well-known cell-autonomous anti-apoptotic function of hepatocyte NF-κB, the non-cell autonomous effect of NF-κB signaling (promoting formation of inflammatory micro-niches) may be a critical pro-oncogenic mechanism. Our findings highlight the role of a specific inflammatory topology in a solid malignancy - formation of spatially-defined inflammatory micro-niches in tumor promotion in the liver. This is supported by both the compelling histological sequence and the functional studies in which we blocked signaling by specific cytokines that are

expressed in the micro-niche. Histological analyses revealed a continuous spectrum of lesions in livers with IKKβ activation: the smallest and earliest lesions composed solely of inflammatory cells, followed with appearance of atypical hepatocytes in these lesions, displaying markers of HCC progenitors. These atypical hepatocytes coalesced to form small clusters of cells, then sheets of malignant hepatocytes within the micro-niche eventually growing out of the boundaries of the inflammatory micro-niche to form bulky tumors. This entire spectrum was repeatedly observed in aged mice solely affected by chronic activation of IKKβ in hepatocytes, where multiple lesions representing different progression phases were concurrently seen in every mouse that was examined. DEN treatment dramatically accelerates inflammatory foci appearance suggests the possibility that tissue damage could be of relevance, either by sporadic enhancement of hepatocyte NF-κB activation, or by triggering another cooperating pro-inflammatory pathway. Interestingly, the early premalignant cells did not express LTβ on their own, but larger tumors that cannot be contained in the supportive micro-niche showed LTβ expression in malignant epithelial cells. Moreover, we consistently observed expression of LTβ in the periphery of inflammatory foci, often marking malignant hepatocytes that were migrating out. This raises the possibility that in order to exit the micro-niche, the expanding cancer cells must find an alternative source of supportive cytokines. We speculate that the acquisition of independence of a supportive niche could be a hallmark prerequisite of solid tumors, which first develop in a defined niche: either an inflammatory micro-niche as in the current case, or any other relevant micro-niche which can occur either physiologically or pathologically in a given tissue and provide the earliest tumor cells with a supportive environment. Specifically, it will be of interest to determine what other factors besides NF-κB, contribute to autocrine LTβ expression within these cells.

The presence of inflammatory follicles in human hepatitis is well known and is even considered a histologic hallmark of HCV infection. However, the role of these follicles in HCC development was never studied. Here we characterized the cellular and cytokine composition of such follicles and found them to be remarkably similar to the micro-niches we detected in mice with constitutive activation of IKKβ. We therefore propose that as in mice, in HCV infected livers, chronic activation of IKK and NF-κB signaling by viral proteins supports the formation of discrete inflammatory follicles that are rich in pro-tumorigenic cytokines, of which LTβR ligands are probably only one example. In support of this hypothesis, we find high levels of LTβ and its downstream effectors in inflammatory aggregates in human livers infected with HCV. The connection between

chronic inflammation and cancer is now well established. Our new findings suggest that defined microscopic foci of chronic inflammation can form discrete niches nesting the seeds of cancer, which germinate upon acquiring sufficient hallmark capabilities that allow them to spread out of their nursing niche to form full blown malignant tumors.

REFERENCES

1. Alison, M.R. and W.R. Lin, *Hepatocyte turnover and regeneration: virtually a virtuoso performance.* Hepatology, 2011. **53**(4): p. 1393-6.
2. Miyajima, A., M. Tanaka, and T. Itoh, *Stem/progenitor cells in liver development, homeostasis, regeneration, and reprogramming.* Cell Stem Cell, 2014. **14**(5): p. 561-74.
3. Malato, Y., et al., *Fate tracing of mature hepatocytes in mouse liver homeostasis and regeneration.* J Clin Invest, 2011. **121**(12): p. 4850-60.
4. Higgins, G.M.A., R. M, *Restoration of the liver of the white rat following partial surgical removal.* Arch. Pathol., 1931. **12**: p. 186~202.
5. Younossi, Z.M., et al., *Changes in the prevalence of the most common causes of chronic liver diseases in the United States from 1988 to 2008.* Clin Gastroenterol Hepatol, 2011. **9**(6): p. 524-530 e1; quiz e60.
6. Dogra, S. and R. Jindal, *Cutaneous manifestations of common liver diseases.* J Clin Exp Hepatol, 2011. **1**(3): p. 177-84.
7. Ferrell, L., *Liver pathology: cirrhosis, hepatitis, and primary liver tumors. Update and diagnostic problems.* Mod Pathol, 2000. **13**(6): p. 679-704.
8. Ekataksin, W. and K. Kaneda, *Liver microvascular architecture: an insight into the pathophysiology of portal hypertension.* Semin Liver Dis, 1999. **19**(4): p. 359-82.
9. Pfeiffer, E., et al., *Featured Article: Isolation, characterization, and cultivation of human hepatocytes and non-parenchymal liver cells.* Exp Biol Med (Maywood), 2015. **240**(5): p. 645-56.
10. Blouin, A., R.P. Bolender, and E.R. Weibel, *Distribution of organelles and membranes between hepatocytes and nonhepatocytes in the rat liver parenchyma. A stereological study.* J Cell Biol, 1977. **72**(2): p. 441-55.
11. Malik, R., C. Selden, and H. Hodgson, *The role of non-parenchymal cells in liver growth.* Semin Cell Dev Biol, 2002. **13**(6): p. 425-31.
12. Kmiec, Z., *Cooperation of liver cells in health and disease.* Adv Anat Embryol Cell Biol, 2001. **161**: p. III-XIII, 1-151.
13. Hosseini-Yeganeh, M. and A.J. McLachlan, *Physiologically based pharmacokinetic model for terbinafine in rats and humans.* Antimicrob Agents Chemother, 2002. **46**(7): p. 2219-28.
14. Konig, M., S. Bulik, and H.G. Holzhutter, *Quantifying the contribution of the liver to glucose homeostasis: a detailed kinetic model of human hepatic glucose metabolism.* PLoS Comput Biol, 2012. **8**(6): p. e1002577.
15. Lin, D.W., S. Johnson, and C.A. Hunt, *Modeling liver physiology: combining fractals, imaging and animation.* Conf Proc IEEE Eng Med Biol Soc, 2004. **5**: p. 3120-3.
16. Thalhammer, T., et al., *Separation of hepatocytes of different acinar zones by flow cytometry.* Cytometry, 1989. **10**(6): p. 772-8.
17. Bhunchet, E. and K. Fujieda, *Capillarization and venularization of hepatic sinusoids in porcine serum-induced rat liver fibrosis: a mechanism to maintain liver blood flow.* Hepatology, 1993. **18**(6): p. 1450-8.

18. Pasarin, M., et al., *Sinusoidal endothelial dysfunction precedes inflammation and fibrosis in a model of NAFLD.* PLoS One, 2012. **7**(4): p. e32785.
19. Kawata, K., et al., *The immunophysiology and apoptosis of biliary epithelial cells: primary biliary cirrhosis and primary sclerosing cholangitis.* Clin Rev Allergy Immunol, 2012. **43**(3): p. 230-41.
20. Kanno, N., et al., *Functional heterogeneity of the intrahepatic biliary epithelium.* Hepatology, 2000. **31**(3): p. 555-61.
21. Glaser, S., et al., *Gastrin inhibits cholangiocyte growth in bile duct-ligated rats by interaction with cholecystokinin-B/Gastrin receptors via D-myo-inositol 1,4,5-triphosphate-, Ca(2+)-, and protein kinase C alpha-dependent mechanisms.* Hepatology, 2000. **32**(1): p. 17-25.
22. Alpini, G., et al., *Bile acid feeding increased proliferative activity and apical bile acid transporter expression in both small and large rat cholangiocytes.* Hepatology, 2001. **34**(5): p. 868-76.
23. Lai, G.H., et al., *erbB-2/neu transformed rat cholangiocytes recapitulate key cellular and molecular features of human bile duct cancer.* Gastroenterology, 2005. **129**(6): p. 2047-57.
24. Liaskou, E., D.V. Wilson, and Y.H. Oo, *Innate immune cells in liver inflammation.* Mediators Inflamm, 2012. **2012**: p. 949157.
25. Boltjes, A., et al., *The role of Kupffer cells in hepatitis B and hepatitis C virus infections.* J Hepatol, 2014. **61**(3): p. 660-71.
26. Maeda, S., et al., *IKKbeta couples hepatocyte death to cytokine-driven compensatory proliferation that promotes chemical hepatocarcinogenesis.* Cell, 2005. **121**(7): p. 977-90.
27. Roberts, R.A., et al., *Role of the Kupffer cell in mediating hepatic toxicity and carcinogenesis.* Toxicol Sci, 2007. **96**(1): p. 2-15.
28. Sedger, L.M. and M.F. McDermott, *TNF and TNF-receptors: From mediators of cell death and inflammation to therapeutic giants - past, present and future.* Cytokine Growth Factor Rev, 2014. **25**(4): p. 453-72.
29. Espin-Palazon, R., et al., *Proinflammatory signaling regulates hematopoietic stem cell emergence.* Cell, 2014. **159**(5): p. 1070-85.
30. Iimuro, Y. and J. Fujimoto, *TLRs, NF-kappaB, JNK, and Liver Regeneration.* Gastroenterol Res Pract, 2010. **2010**.
31. Luo, D., et al., *Differential functions of tumor necrosis factor receptor 1 and 2 signaling in ischemia-mediated arteriogenesis and angiogenesis.* Am J Pathol, 2006. **169**(5): p. 1886-98.
32. Janes, K.A., et al., *The response of human epithelial cells to TNF involves an inducible autocrine cascade.* Cell, 2006. **124**(6): p. 1225-39.
33. Makki, K., P. Froguel, and I. Wolowczuk, *Adipose tissue in obesity-related inflammation and insulin resistance: cells, cytokines, and chemokines.* ISRN Inflamm, 2013. **2013**: p. 139239.
34. Liu, B., et al., *Maternal hematopoietic TNF, via milk chemokines, programs hippocampal development and memory.* Nat Neurosci, 2014. **17**(1): p. 97-105.
35. Kamiya, A. and F.J. Gonzalez, *TNF-alpha regulates mouse fetal hepatic maturation induced by oncostatin M and extracellular matrices.* Hepatology, 2004. **40**(3): p. 527-36.

36. Tsutsui, H. and S. Nishiguchi, *Importance of Kupffer cells in the development of acute liver injuries in mice.* Int J Mol Sci, 2014. **15**(5): p. 7711-30.
37. Yang, J., et al., *Kupffer cell-derived Fas ligand plays a role in liver injury and hepatocyte death.* J Gastrointest Surg, 2004. **8**(2): p. 166-74.
38. Wu, J., et al., *The proinflammatory myeloid cell receptor TREM-1 controls Kupffer cell activation and development of hepatocellular carcinoma.* Cancer Res, 2012. **72**(16): p. 3977-86.
39. Lanaya, H., et al., *EGFR has a tumour-promoting role in liver macrophages during hepatocellular carcinoma formation.* Nat Cell Biol, 2014. **16**(10): p. 972-81, 1-7.
40. Nakagawa, H., et al., *ER stress cooperates with hypernutrition to trigger TNF-dependent spontaneous HCC development.* Cancer Cell, 2014. **26**(3): p. 331-43.
41. Kamata, H., et al., *Reactive oxygen species promote TNFalpha-induced death and sustained JNK activation by inhibiting MAP kinase phosphatases.* Cell, 2005. **120**(5): p. 649-61.
42. Nikolaou, K., et al., *Inactivation of the deubiquitinase CYLD in hepatocytes causes apoptosis, inflammation, fibrosis, and cancer.* Cancer Cell, 2012. **21**(6): p. 738-50.
43. Lowes, K.N., et al., *Oval cell numbers in human chronic liver diseases are directly related to disease severity.* Am J Pathol, 1999. **154**(2): p. 537-41.
44. Lu, L., et al., *Hippo signaling is a potent in vivo growth and tumor suppressor pathway in the mammalian liver.* Proc Natl Acad Sci U S A, 2010. **107**(4): p. 1437-42.
45. Strick-Marchand, H., et al., *Lymphocytes support oval cell-dependent liver regeneration.* J Immunol, 2008. **181**(4): p. 2764-71.
46. Ferlay, J., et al., *Estimates of worldwide burden of cancer in 2008: GLOBOCAN 2008.* Int J Cancer, 2010. **127**(12): p. 2893-917.
47. Lee, W.S., et al., *Comparison of combined hepatocellular and cholangiocarcinoma with hepatocellular carcinoma and intrahepatic cholangiocarcinoma.* Surg Today, 2006. **36**(10): p. 892-7.
48. Sapisochin, G., et al., *Mixed hepatocellular cholangiocarcinoma and intrahepatic cholangiocarcinoma in patients undergoing transplantation for hepatocellular carcinoma.* Liver Transpl, 2011. **17**(8): p. 934-42.
49. Jiao, Y., et al., *Exome sequencing identifies frequent inactivating mutations in BAP1, ARID1A and PBRM1 in intrahepatic cholangiocarcinomas.* Nat Genet, 2013. **45**(12): p. 1470-3.
50. Fujimoto, A., et al., *Whole-genome mutational landscape of liver cancers displaying biliary phenotype reveals hepatitis impact and molecular diversity.* Nat Commun, 2015. **6**: p. 6120.
51. Shaib, Y.H., et al., *Rising incidence of intrahepatic cholangiocarcinoma in the United States: a true increase?* J Hepatol, 2004. **40**(3): p. 472-7.
52. Zhang, Y., et al., *International trends in primary liver cancer incidence from 1973 to 2007.* BMC Cancer, 2015. **15**: p. 94.
53. Calle, E.E., et al., *Overweight, obesity, and mortality from cancer in a prospectively studied cohort of U.S. adults.* N Engl J Med, 2003. **348**(17): p. 1625-38.
54. El-Serag, H.B., *Hepatocellular carcinoma.* N Engl J Med, 2011. **365**(12): p. 1118-27.

55. Perz, J.F., et al., *The contributions of hepatitis B virus and hepatitis C virus infections to cirrhosis and primary liver cancer worldwide.* J Hepatol, 2006. **45**(4): p. 529-38.
56. Pikarsky, E., et al., *NF-kappaB functions as a tumour promoter in inflammation-associated cancer.* Nature, 2004. **431**(7007): p. 461-6.
57. Coussens, L.M. and Z. Werb, *Inflammation and cancer.* Nature, 2002. **420**(6917): p. 860-7.
58. Yu, G.Y., et al., *Hepatic expression of HCV RNA-dependent RNA polymerase triggers innate immune signaling and cytokine production.* Mol Cell, 2012. **48**(2): p. 313-21.
59. Gatto, M. and D. Alvaro, *New insights on cholangiocarcinoma.* World J Gastrointest Oncol, 2010. **2**(3): p. 136-45.
60. Maroni, L., et al., *The significance of genetics for cholangiocarcinoma development.* Ann Transl Med, 2013. **1**(3): p. 28.
61. Ustundag, Y. and Y. Bayraktar, *Cholangiocarcinoma: a compact review of the literature.* World J Gastroenterol, 2008. **14**(42): p. 6458-66.
62. Tarlow, B.D., et al., *Bipotential adult liver progenitors are derived from chronically injured mature hepatocytes.* Cell Stem Cell, 2014. **15**(5): p. 605-18.
63. Zhang, F., et al., *Combined hepatocellular cholangiocarcinoma originating from hepatic progenitor cells: immunohistochemical and double-fluorescence immunostaining evidence.* Histopathology, 2008. **52**(2): p. 224-32.
64. Guest, R.V., et al., *Cell lineage tracing reveals a biliary origin of intrahepatic cholangiocarcinoma.* Cancer Res, 2014. **74**(4): p. 1005-10.
65. Komuta, M., et al., *Clinicopathological study on cholangiolocellular carcinoma suggesting hepatic progenitor cell origin.* Hepatology, 2008. **47**(5): p. 1544-56.
66. Govaere, O., et al., *Keratin 19: a key role player in the invasion of human hepatocellular carcinomas.* Gut, 2014. **63**(4): p. 674-85.
67. Ariizumi, S.I. and M. Yamamoto, *Intrahepatic cholangiocarcinoma and cholangiolocellular carcinoma in cirrhosis and chronic viral hepatitis.* Surg Today, 2014.
68. Qureshi, K., R. Jesudoss, and A.M. Al-Osaimi, *The treatment of cholangiocarcinoma: a hepatologist's perspective.* Curr Gastroenterol Rep, 2014. **16**(10): p. 412.
69. Tyson, G.L. and H.B. El-Serag, *Risk factors for cholangiocarcinoma.* Hepatology, 2011. **54**(1): p. 173-84.
70. Kang, L.I., W.M. Mars, and G.K. Michalopoulos, *Signals and cells involved in regulating liver regeneration.* Cells, 2012. **1**(4): p. 1261-92.
71. Dusabineza, A.C., et al., *Participation of liver progenitor cells in liver regeneration: lack of evidence in the AAF/PH rat model.* Lab Invest, 2012. **92**(1): p. 72-81.
72. Fujii, T., et al., *Mouse model of carbon tetrachloride induced liver fibrosis: Histopathological changes and expression of CD133 and epidermal growth factor.* BMC Gastroenterol, 2010. **10**: p. 79.
73. Meng, Z., et al., *FXR regulates liver repair after CCl4-induced toxic injury.* Mol Endocrinol, 2010. **24**(5): p. 886-97.
74. Sukhotnik, I., et al., *Intestinal involvement during 3,5-diethoxycarbonyl-1,4-dihydrocollidine-induced chronic liver injury in a mouse model.* J Pediatr Surg, 2011. **46**(8): p. 1495-502.

75. Wang, C., et al., *Hepatitis B virus X (HBx) induces tumorigenicity of hepatic progenitor cells in 3,5-diethoxycarbonyl-1,4-dihydrocollidine-treated HBx transgenic mice.* Hepatology, 2012. **55**(1): p. 108-20.
76. Taub, R., *Liver regeneration: from myth to mechanism.* Nat Rev Mol Cell Biol, 2004. **5**(10): p. 836-47.
77. Cressman, D.E., R.H. Diamond, and R. Taub, *Rapid activation of the Stat3 transcription complex in liver regeneration.* Hepatology, 1995. **21**(5): p. 1443-9.
78. Wang, Y., et al., *STAT3 activation in response to IL-6 is prolonged by the binding of IL-6 receptor to EGF receptor.* Proc Natl Acad Sci U S A, 2013. **110**(42): p. 16975-80.
79. Kim, S.M., et al., *Activation of IL-6R/JAK1/STAT3 signaling induces de novo resistance to irreversible EGFR inhibitors in non-small cell lung cancer with T790M resistance mutation.* Mol Cancer Ther, 2012. **11**(10): p. 2254-64.
80. Balabko, L., et al., *Increased expression of the Th17-IL-6R/pSTAT3/BATF/RorgammaT-axis in the tumoural region of adenocarcinoma as compared to squamous cell carcinoma of the lung.* Sci Rep, 2014. **4**: p. 7396.
81. Amemiya, H., H. Kono, and H. Fujii, *Liver regeneration is impaired in macrophage colony stimulating factor deficient mice after partial hepatectomy: the role of M-CSF-induced macrophages.* J Surg Res, 2011. **165**(1): p. 59-67.
82. Cressman, D.E., et al., *Liver failure and defective hepatocyte regeneration in interleukin-6-deficient mice.* Science, 1996. **274**(5291): p. 1379-83.
83. Yamada, Y., et al., *Initiation of liver growth by tumor necrosis factor: deficient liver regeneration in mice lacking type I tumor necrosis factor receptor.* Proc Natl Acad Sci U S A, 1997. **94**(4): p. 1441-6.
84. Yamada, Y., et al., *Analysis of liver regeneration in mice lacking type 1 or type 2 tumor necrosis factor receptor: requirement for type 1 but not type 2 receptor.* Hepatology, 1998. **28**(4): p. 959-70.
85. Diehl, A.M., et al., *Tumor necrosis factor-alpha induces c-jun during the regenerative response to liver injury.* Am J Physiol, 1994. **267**(4 Pt 1): p. G552-61.
86. Pediaditakis, P., et al., *The processing and utilization of hepatocyte growth factor/scatter factor following partial hepatectomy in the rat.* Hepatology, 2001. **34**(4 Pt 1): p. 688-93.
87. Huh, C.G., et al., *Hepatocyte growth factor/c-met signaling pathway is required for efficient liver regeneration and repair.* Proc Natl Acad Sci U S A, 2004. **101**(13): p. 4477-82.
88. Lee, M.W., et al., *Activated type 2 innate lymphoid cells regulate beige fat biogenesis.* Cell, 2015. **160**(1-2): p. 74-87.
89. Scheeren, F.A., et al., *A cell-intrinsic role for TLR2-MYD88 in intestinal and breast epithelia and oncogenesis.* Nat Cell Biol, 2014. **16**(12): p. 1238-48.
90. Haybaeck, J., et al., *A lymphotoxin-driven pathway to hepatocellular carcinoma.* Cancer Cell, 2009. **16**(4): p. 295-308.
91. Rezza, A., R. Sennett, and M. Rendl, *Adult stem cell niches: cellular and molecular components.* Curr Top Dev Biol, 2014. **107**: p. 333-72.
92. Hackenbrock, C.R., et al., *Oxidative phosphorylation and ultrastructural transformation in mitochondria in the intact ascites tumor cell.* J Cell Biol, 1971. **51**(1): p. 123-37.

93. Takagi, S., M.S. Islam, and K. Iwabuchi, *Dynamic behavior of double-membrane-bounded organelles in plant cells.* Int Rev Cell Mol Biol, 2011. **286**: p. 181-222.
94. Wu, S., et al., *Mitochondrial oxidative stress causes mitochondrial fragmentation via differential modulation of mitochondrial fission-fusion proteins.* FEBS J, 2011. **278**(6): p. 941-54.
95. Youle, R.J. and A.M. van der Bliek, *Mitochondrial fission, fusion, and stress.* Science, 2012. **337**(6098): p. 1062-5.
96. Lai, J.C. and K.L. Behar, *Glycolysis-citric acid cycle interrelation: a new approach and some insights in cellular and subcellular compartmentation.* Dev Neurosci, 1993. **15**(3-5): p. 181-93.
97. Green, D.E. and H. Vande Zande, *On the enzymic mechanism of oxidative phosphorylation.* Proc Natl Acad Sci U S A, 1982. **79**(4): p. 1064-8.
98. Penefsky, H.S., *Molecular mechanism of ATP synthesis in oxidative phosphorylation.* Biochem Soc Trans, 1987. **15**(1): p. 97-9.
99. Smeitink, J.A., et al., *Mitochondrial medicine: a metabolic perspective on the pathology of oxidative phosphorylation disorders.* Cell Metab, 2006. **3**(1): p. 9-13.
100. Chinnery, P.F. and D.M. Turnbull, *Mitochondrial DNA mutations in the pathogenesis of human disease.* Mol Med Today, 2000. **6**(11): p. 425-32.
101. Greaves, L.C. and R.W. Taylor, *Mitochondrial DNA mutations in human disease.* IUBMB Life, 2006. **58**(3): p. 143-51.
102. Stojanovski, D., et al., *Import of nuclear-encoded proteins into mitochondria.* Exp Physiol, 2003. **88**(1): p. 57-64.
103. Boengler, K., G. Heusch, and R. Schulz, *Nuclear-encoded mitochondrial proteins and their role in cardioprotection.* Biochim Biophys Acta, 2011. **1813**(7): p. 1286-94.
104. Voos, W. and K. Rottgers, *Molecular chaperones as essential mediators of mitochondrial biogenesis.* Biochim Biophys Acta, 2002. **1592**(1): p. 51-62.
105. Jonckheere, A.I., J.A. Smeitink, and R.J. Rodenburg, *Mitochondrial ATP synthase: architecture, function and pathology.* J Inherit Metab Dis, 2012. **35**(2): p. 211-25.
106. Wallace, D.C., et al., *Mitochondrial DNA mutation associated with Leber's hereditary optic neuropathy.* Science, 1988. **242**(4884): p. 1427-30.
107. Toro, J.R., et al., *Mutations in the fumarate hydratase gene cause hereditary leiomyomatosis and renal cell cancer in families in North America.* Am J Hum Genet, 2003. **73**(1): p. 95-106.
108. Smit, D.L., et al., *Hereditary leiomyomatosis and renal cell cancer in families referred for fumarate hydratase germline mutation analysis.* Clin Genet, 2011. **79**(1): p. 49-59.
109. Gidalevitz, T., V. Prahlad, and R.I. Morimoto, *The stress of protein misfolding: from single cells to multicellular organisms.* Cold Spring Harb Perspect Biol, 2011. **3**(6).
110. Lloyd, R.E. and J.E. McGeehan, *Structural analysis of mitochondrial mutations reveals a role for bigenomic protein interactions in human disease.* PLoS One, 2013. **8**(7): p. e69003.
111. Pellegrino, M.W., A.M. Nargund, and C.M. Haynes, *Signaling the mitochondrial unfolded protein response.* Biochim Biophys Acta, 2013. **1833**(2): p. 410-6.

112. Haynes, C.M. and D. Ron, *The mitochondrial UPR - protecting organelle protein homeostasis.* J Cell Sci, 2010. **123**(Pt 22): p. 3849-55.
113. Martin, J., *Molecular chaperones and mitochondrial protein folding.* J Bioenerg Biomembr, 1997. **29**(1): p. 35-43.
114. Chakraborty, K., et al., *Chaperonin-catalyzed rescue of kinetically trapped states in protein folding.* Cell, 2010. **142**(1): p. 112-22.
115. Kang, P.J., et al., *Requirement for hsp70 in the mitochondrial matrix for translocation and folding of precursor proteins.* Nature, 1990. **348**(6297): p. 137-43.
116. Palmeira, C.M., et al., *Hyperglycemia decreases mitochondrial function: the regulatory role of mitochondrial biogenesis.* Toxicol Appl Pharmacol, 2007. **225**(2): p. 214-20.
117. Sena, L.A. and N.S. Chandel, *Physiological roles of mitochondrial reactive oxygen species.* Mol Cell, 2012. **48**(2): p. 158-67.
118. Bonnard, C., et al., *Mitochondrial dysfunction results from oxidative stress in the skeletal muscle of diet-induced insulin-resistant mice.* J Clin Invest, 2008. **118**(2): p. 789-800.
119. Jovaisaite, V. and J. Auwerx, *The mitochondrial unfolded protein response-synchronizing genomes.* Curr Opin Cell Biol, 2015. **33**: p. 74-81.
120. Mottis, A., V. Jovaisaite, and J. Auwerx, *The mitochondrial unfolded protein response in mammalian physiology.* Mamm Genome, 2014. **25**(9-10): p. 424-33.
121. Cano, M., et al., *Oxidative stress induces mitochondrial dysfunction and a protective unfolded protein response in RPE cells.* Free Radic Biol Med, 2014. **69**: p. 1-14.
122. Cortopassi, G., et al., *Mitochondrial disease activates transcripts of the unfolded protein response and cell cycle and inhibits vesicular secretion and oligodendrocyte-specific transcripts.* Mitochondrion, 2006. **6**(4): p. 161-75.
123. Horibe, T. and N.J. Hoogenraad, *The chop gene contains an element for the positive regulation of the mitochondrial unfolded protein response.* PLoS One, 2007. **2**(9): p. e835.
124. Zhao, Q., et al., *A mitochondrial specific stress response in mammalian cells.* EMBO J, 2002. **21**(17): p. 4411-9.
125. Rainbolt, T.K., et al., *Stress-regulated translational attenuation adapts mitochondrial protein import through Tim17A degradation.* Cell Metab, 2013. **18**(6): p. 908-19.
126. Takemoto, K., et al., *Mitochondrial TRAP1 regulates the unfolded protein response in the endoplasmic reticulum.* Neurochem Int, 2011. **58**(8): p. 880-7.
127. Yoshida, H., *ER stress response, peroxisome proliferation, mitochondrial unfolded protein response and Golgi stress response.* IUBMB Life, 2009. **61**(9): p. 871-9.
128. Malhotra, J.D. and R.J. Kaufman, *The endoplasmic reticulum and the unfolded protein response.* Semin Cell Dev Biol, 2007. **18**(6): p. 716-31.
129. Rainbolt, T.K., J.M. Saunders, and R.L. Wiseman, *Stress-responsive regulation of mitochondria through the ER unfolded protein response.* Trends Endocrinol Metab, 2014. **25**(10): p. 528-37.
130. Back, S.H., et al., *ER stress signaling by regulated splicing: IRE1/HAC1/XBP1.* Methods, 2005. **35**(4): p. 395-416.

131. Shuda, M., et al., *Activation of the ATF6, XBP1 and grp78 genes in human hepatocellular carcinoma: a possible involvement of the ER stress pathway in hepatocarcinogenesis.* J Hepatol, 2003. **38**(5): p. 605-14.
132. Saleem, M., et al., *Review-Epigenetic therapy for cancer.* Pak J Pharm Sci, 2015. **28**(3): p. 1023-32.
133. Sui, X., et al., *Epigenetic modifications as regulatory elements of autophagy in cancer.* Cancer Lett, 2015. **360**(2): p. 106-13.
134. Nowsheen, S., et al., *Epigenetic inactivation of DNA repair in breast cancer.* Cancer Lett, 2014. **342**(2): p. 213-22.
135. Vincent, A. and I. Van Seuningen, *On the epigenetic origin of cancer stem cells.* Biochim Biophys Acta, 2012. **1826**(1): p. 83-8.
136. Duenas-Gonzalez, A., et al., *Valproic acid as epigenetic cancer drug: preclinical, clinical and transcriptional effects on solid tumors.* Cancer Treat Rev, 2008. **34**(3): p. 206-22.
137. Ganesan, A., et al., *Epigenetic therapy: histone acetylation, DNA methylation and anti-cancer drug discovery.* Curr Cancer Drug Targets, 2009. **9**(8): p. 963-81.
138. Wei, S.H., R. Brown, and T.H. Huang, *Aberrant DNA methylation in ovarian cancer: is there an epigenetic predisposition to drug response?* Ann N Y Acad Sci, 2003. **983**: p. 243-50.
139. Bird, A., *Perceptions of epigenetics.* Nature, 2007. **447**(7143): p. 396-8.
140. Jaenisch, R. and A. Bird, *Epigenetic regulation of gene expression: how the genome integrates intrinsic and environmental signals.* Nat Genet, 2003. **33 Suppl**: p. 245-54.
141. Saxonov, S., P. Berg, and D.L. Brutlag, *A genome-wide analysis of CpG dinucleotides in the human genome distinguishes two distinct classes of promoters.* Proc Natl Acad Sci U S A, 2006. **103**(5): p. 1412-7.
142. Fujita, N., et al., *Methylation-mediated transcriptional silencing in euchromatin by methyl-CpG binding protein MBD1 isoforms.* Mol Cell Biol, 1999. **19**(9): p. 6415-26.
143. McGaughey, D.M., et al., *Genomics of CpG methylation in developing and developed zebrafish.* G3 (Bethesda), 2014. **4**(5): p. 861-9.
144. Ollikainen, M., et al., *Genome-wide blood DNA methylation alterations at regulatory elements and heterochromatic regions in monozygotic twins discordant for obesity and liver fat.* Clin Epigenetics, 2015. **7**(1): p. 39.
145. Peng, J.C. and G.H. Karpen, *Heterochromatic genome stability requires regulators of histone H3 K9 methylation.* PLoS Genet, 2009. **5**(3): p. e1000435.
146. Wood, H., *Alzheimer disease: AD-susceptible brain regions exhibit altered DNA methylation.* Nat Rev Neurol, 2014. **10**(10): p. 548.
147. Xiao, F.H., et al., *A genome-wide scan reveals important roles of DNA methylation in human longevity by regulating age-related disease genes.* PLoS One, 2015. **10**(3): p. e0120388.
148. Johnson, A.A., et al., *The role of DNA methylation in aging, rejuvenation, and age-related disease.* Rejuvenation Res, 2012. **15**(5): p. 483-94.
149. Lin, Z., et al., *Identification of disease-associated DNA methylation in intestinal tissues from patients with inflammatory bowel disease.* Clin Genet, 2011. **80**(1): p. 59-67.
150. Ehrlich, M., *DNA hypomethylation in cancer cells.* Epigenomics, 2009. **1**(2): p. 239-59.

151. Cheah, M.S., C.D. Wallace, and R.M. Hoffman, *Hypomethylation of DNA in human cancer cells: a site-specific change in the c-myc oncogene.* J Natl Cancer Inst, 1984. **73**(5): p. 1057-65.
152. Friso, S., et al., *Global DNA hypomethylation in peripheral blood mononuclear cells as a biomarker of cancer risk.* Cancer Epidemiol Biomarkers Prev, 2013. **22**(3): p. 348-55.
153. Esteller, M., *CpG island hypermethylation and tumor suppressor genes: a booming present, a brighter future.* Oncogene, 2002. **21**(35): p. 5427-40.
154. Bestor, T.H., *The DNA methyltransferases of mammals.* Hum Mol Genet, 2000. **9**(16): p. 2395-402.
155. Lan, J., et al., *DNA methyltransferases and methyl-binding proteins of mammals.* Acta Biochim Biophys Sin (Shanghai), 2010. **42**(4): p. 243-52.
156. Unterberger, A., et al., *DNA methyltransferase 1 knockdown activates a replication stress checkpoint.* Mol Cell Biol, 2006. **26**(20): p. 7575-86.
157. Okano, M., et al., *DNA methyltransferases Dnmt3a and Dnmt3b are essential for de novo methylation and mammalian development.* Cell, 1999. **99**(3): p. 247-57.
158. Li, E., T.H. Bestor, and R. Jaenisch, *Targeted mutation of the DNA methyltransferase gene results in embryonic lethality.* Cell, 1992. **69**(6): p. 915-26.
159. Szerlong, H.J. and J.C. Hansen, *Nucleosome distribution and linker DNA: connecting nuclear function to dynamic chromatin structure.* Biochem Cell Biol, 2011. **89**(1): p. 24-34.
160. Prendergast, J.G., et al., *A genome-wide screen in human embryonic stem cells reveals novel sites of allele-specific histone modification associated with known disease loci.* Epigenetics Chromatin, 2012. **5**(1): p. 6.
161. Sadri-Vakili, G. and J.H. Cha, *Mechanisms of disease: Histone modifications in Huntington's disease.* Nat Clin Pract Neurol, 2006. **2**(6): p. 330-8.
162. Haring, M., et al., *Chromatin immunoprecipitation: optimization, quantitative analysis and data normalization.* Plant Methods, 2007. **3**: p. 11.
163. Zhou, V.W., A. Goren, and B.E. Bernstein, *Charting histone modifications and the functional organization of mammalian genomes.* Nat Rev Genet, 2011. **12**(1): p. 7-18.
164. Demeret, C., Y. Vassetzky, and M. Mechali, *Chromatin remodelling and DNA replication: from nucleosomes to loop domains.* Oncogene, 2001. **20**(24): p. 3086-93.
165. Struhl, K., *Histone acetylation and transcriptional regulatory mechanisms.* Genes Dev, 1998. **12**(5): p. 599-606.
166. Haberland, M., R.L. Montgomery, and E.N. Olson, *The many roles of histone deacetylases in development and physiology: implications for disease and therapy.* Nat Rev Genet, 2009. **10**(1): p. 32-42.
167. Choi, S. and P. Reddy, *HDAC inhibition and graft versus host disease.* Mol Med, 2011. **17**(5-6): p. 404-16.
168. Ouaissi, M., et al., *Further characterization of HDAC and SIRT gene expression patterns in pancreatic cancer and their relation to disease outcome.* PLoS One, 2014. **9**(9): p. e108520.
169. Eigl, B.J., et al., *A phase II study of the HDAC inhibitor SB939 in patients with castration resistant prostate cancer: NCIC clinical trials group study IND195.* Invest New Drugs, 2015.

170. Govindaraj, C., et al., *Reducing TNF receptor 2+ regulatory T cells via the combined action of azacitidine and the HDAC inhibitor, panobinostat for clinical benefit in acute myeloid leukemia patients.* Clin Cancer Res, 2014. **20**(3): p. 724-35.
171. Razak, A.R., et al., *Phase I clinical, pharmacokinetic and pharmacodynamic study of SB939, an oral histone deacetylase (HDAC) inhibitor, in patients with advanced solid tumours.* Br J Cancer, 2011. **104**(5): p. 756-62.
172. Shankar, S. and R.K. Srivastava, *Histone deacetylase inhibitors: mechanisms and clinical significance in cancer: HDAC inhibitor-induced apoptosis.* Adv Exp Med Biol, 2008. **615**: p. 261-98.
173. New, M., H. Olzscha, and N.B. La Thangue, *HDAC inhibitor-based therapies: can we interpret the code?* Mol Oncol, 2012. **6**(6): p. 637-56.
174. Hanessian, S., et al., *Exploring alternative Zn-binding groups in the design of HDAC inhibitors: squaric acid, N-hydroxyurea, and oxazoline analogues of SAHA.* Bioorg Med Chem Lett, 2006. **16**(18): p. 4784-7.
175. Huang, J., et al., *Identification of an epigenetic signature of early mouse liver regeneration that is disrupted by Zn-HDAC inhibition.* Epigenetics, 2014. **9**(11): p. 1521-31.
176. Neugebauer, R.C., W. Sippl, and M. Jung, *Inhibitors of NAD+ dependent histone deacetylases (sirtuins).* Curr Pharm Des, 2008. **14**(6): p. 562-73.
177. Voelter-Mahlknecht, S., A.D. Ho, and U. Mahlknecht, *Chromosomal organization and localization of the novel class IV human histone deacetylase 11 gene.* Int J Mol Med, 2005. **16**(4): p. 589-98.
178. Khochbin, S. and H.Y. Kao, *Histone deacetylase complexes: functional entities or molecular reservoirs.* FEBS Lett, 2001. **494**(3): p. 141-4.
179. Tsai, S.C. and E. Seto, *Regulation of histone deacetylase 2 by protein kinase CK2.* J Biol Chem, 2002. **277**(35): p. 31826-33.
180. Heideman, M.R., et al., *Sin3a-associated Hdac1 and Hdac2 are essential for hematopoietic stem cell homeostasis and contribute differentially to hematopoiesis.* Haematologica, 2014. **99**(8): p. 1292-303.
181. Laugesen, A. and K. Helin, *Chromatin repressive complexes in stem cells, development, and cancer.* Cell Stem Cell, 2014. **14**(6): p. 735-51.
182. Fogg, P.C., et al., *Class IIa histone deacetylases are conserved regulators of circadian function.* J Biol Chem, 2014. **289**(49): p. 34341-8.
183. Kuniyasu, H., Y. Chihara, and H. Kondo, *A role of histone H4 hypoacetylation in vascular endothelial growth factor expression in colon mucosa adjacent to implanted cancer in athymic mice cecum.* Pathobiology, 2002. **70**(6): p. 348-52.
184. Kwong, J., et al., *Candidate tumor-suppressor gene DLEC1 is frequently downregulated by promoter hypermethylation and histone hypoacetylation in human epithelial ovarian cancer.* Neoplasia, 2006. **8**(4): p. 268-78.
185. Ma, J., et al., *Promoter hypermethylation and histone hypoacetylation contribute to pancreatic-duodenal homeobox 1 silencing in gastric cancer.* Carcinogenesis, 2010. **31**(9): p. 1552-60.

186. Fraga, M.F., et al., *Loss of acetylation at Lys16 and trimethylation at Lys20 of histone H4 is a common hallmark of human cancer.* Nat Genet, 2005. **37**(4): p. 391-400.
187. Yasui, W., et al., *Histone acetylation and gastrointestinal carcinogenesis.* Ann N Y Acad Sci, 2003. **983**: p. 220-31.
188. Seligson, D.B., et al., *Global histone modification patterns predict risk of prostate cancer recurrence.* Nature, 2005. **435**(7046): p. 1262-6.
189. Bianco, C., et al., *Regulation of human Cripto-1 expression by nuclear receptors and DNA promoter methylation in human embryonal and breast cancer cells.* J Cell Physiol, 2013. **228**(6): p. 1174-88.
190. Wilson, A.J., et al., *Histone deacetylase 3 (HDAC3) and other class I HDACs regulate colon cell maturation and p21 expression and are deregulated in human colon cancer.* J Biol Chem, 2006. **281**(19): p. 13548-58.
191. Krusche, C.A., et al., *Histone deacetylase-1 and -3 protein expression in human breast cancer: a tissue microarray analysis.* Breast Cancer Res Treat, 2005. **90**(1): p. 15-23.
192. Huang, B.H., et al., *Inhibition of histone deacetylase 2 increases apoptosis and p21Cip1/WAF1 expression, independent of histone deacetylase 1.* Cell Death Differ, 2005. **12**(4): p. 395-404.
193. Song, J., et al., *Increased expression of histone deacetylase 2 is found in human gastric cancer.* APMIS, 2005. **113**(4): p. 264-8.
194. Zhu, P., et al., *Induction of HDAC2 expression upon loss of APC in colorectal tumorigenesis.* Cancer Cell, 2004. **5**(5): p. 455-63.
195. Noh, J.H., et al., *HDAC2 provides a critical support to malignant progression of hepatocellular carcinoma through feedback control of mTORC1 and AKT.* Cancer Res, 2014. **74**(6): p. 1728-38.
196. J.H. Noh, J.W.E., S.Y. Ryu, K.W. Jeong, J.K. Kim, S.H. Lee, W.S. Park, N.J. Yoo, J.Y. Lee, S.W. Nam, *Increased expression of histone deacetylase 2 is found in human hepatocellular carconoma.* Mol. Cell. Toxicol., 2006. **2**(3): p. 166-169.
197. Zhang, Z., et al., *HDAC6 expression is correlated with better survival in breast cancer.* Clin Cancer Res, 2004. **10**(20): p. 6962-8.
198. Oehme, I., et al., *Histone deacetylase 8 in neuroblastoma tumorigenesis.* Clin Cancer Res, 2009. **15**(1): p. 91-9.
199. Gui, C.Y., et al., *Histone deacetylase (HDAC) inhibitor activation of p21WAF1 involves changes in promoter-associated proteins, including HDAC1.* Proc Natl Acad Sci U S A, 2004. **101**(5): p. 1241-6.
200. Alsheyab, F.M., M.T. Ziadeh, and K.E. Bani-Hani, *Expression of p21 and p27 in gallbladder cancer.* Saudi Med J, 2007. **28**(5): p. 683-7.
201. Hill, R., et al., *Hypersensitivity to chromium-induced DNA damage correlates with constitutive deregulation of upstream p53 kinases in p21-/- HCT116 colon cancer cells.* DNA Repair (Amst), 2008. **7**(2): p. 239-52.
202. Ogino, S., et al., *Down-regulation of p21 (CDKN1A/CIP1) is inversely associated with microsatellite instability and CpG island methylator phenotype (CIMP) in colorectal cancer.* J Pathol, 2006. **210**(2): p. 147-54.

203. Peinado, H., et al., *Snail mediates E-cadherin repression by the recruitment of the Sin3A/histone deacetylase 1 (HDAC1)/HDAC2 complex.* Mol Cell Biol, 2004. **24**(1): p. 306-19.
204. Glozak, M.A., et al., *Acetylation and deacetylation of non-histone proteins.* Gene, 2005. **363**: p. 15-23.
205. Brochier, C., et al., *Specific acetylation of p53 by HDAC inhibition prevents DNA damage-induced apoptosis in neurons.* J Neurosci, 2013. **33**(20): p. 8621-32.
206. Zhao, Y., et al., *Acetylation of p53 at lysine 373/382 by the histone deacetylase inhibitor depsipeptide induces expression of p21(Waf1/Cip1).* Mol Cell Biol, 2006. **26**(7): p. 2782-90.
207. Xue, Y., et al., *NURD, a novel complex with both ATP-dependent chromatin-remodeling and histone deacetylase activities.* Mol Cell, 1998. **2**(6): p. 851-61.
208. Baltus, G.A., et al., *A positive regulatory role for the mSin3A-HDAC complex in pluripotency through Nanog and Sox2.* J Biol Chem, 2009. **284**(11): p. 6998-7006.
209. Bilodeau, S., et al., *Role of Brg1 and HDAC2 in GR trans-repression of the pituitary POMC gene and misexpression in Cushing disease.* Genes Dev, 2006. **20**(20): p. 2871-86.
210. Muller, B.M., et al., *Differential expression of histone deacetylases HDAC1, 2 and 3 in human breast cancer--overexpression of HDAC2 and HDAC3 is associated with clinicopathological indicators of disease progression.* BMC Cancer, 2013. **13**: p. 215.
211. Chang, H.H., et al., *Histone deacetylase 2 expression predicts poorer prognosis in oral cancer patients.* Oral Oncol, 2009. **45**(7): p. 610-4.
212. Weichert, W., et al., *Histone deacetylases 1, 2 and 3 are highly expressed in prostate cancer and HDAC2 expression is associated with shorter PSA relapse time after radical prostatectomy.* Br J Cancer, 2008. **98**(3): p. 604-10.
213. Lodrini, M., et al., *MYCN and HDAC2 cooperate to repress miR-183 signaling in neuroblastoma.* Nucleic Acids Res, 2013. **41**(12): p. 6018-33.
214. Seo, J., et al., *Expression of Histone Deacetylases HDAC1, HDAC2, HDAC3, and HDAC6 in Invasive Ductal Carcinomas of the Breast.* J Breast Cancer, 2014. **17**(4): p. 323-31.
215. Fritsche, P., et al., *HDAC2 mediates therapeutic resistance of pancreatic cancer cells via the BH3-only protein NOXA.* Gut, 2009. **58**(10): p. 1399-409.
216. Quint, K., et al., *Clinical significance of histone deacetylases 1, 2, 3, and 7: HDAC2 is an independent predictor of survival in HCC.* Virchows Arch, 2011. **459**(2): p. 129-39.
217. Miura, K., et al., *Hepatitis C virus-induced oxidative stress suppresses hepcidin expression through increased histone deacetylase activity.* Hepatology, 2008. **48**(5): p. 1420-9.
218. Yoo, Y.G., et al., *Hepatitis B virus X protein induces the expression of MTA1 and HDAC1, which enhances hypoxia signaling in hepatocellular carcinoma cells.* Oncogene, 2008. **27**(24): p. 3405-13.
219. Hollebecque, A., et al., *Systemic treatment of advanced hepatocellular carcinoma: from disillusions to new horizons.* Eur J Cancer, 2015. **51**(3): p. 327-39.
220. Wei, Z., C. Doria, and Y. Liu, *Targeted therapies in the treatment of advanced hepatocellular carcinoma.* Clin Med Insights Oncol, 2013. **7**: p. 87-102.
221. Caamano, J. and C.A. Hunter, *NF-kappaB family of transcription factors: central regulators of innate and adaptive immune functions.* Clin Microbiol Rev, 2002. **15**(3): p. 414-29.

222. Oeckinghaus, A. and S. Ghosh, *The NF-kappaB family of transcription factors and its regulation.* Cold Spring Harb Perspect Biol, 2009. **1**(4): p. a000034.
223. Tam, W.F., et al., *Cytoplasmic sequestration of rel proteins by IkappaBalpha requires CRM1-dependent nuclear export.* Mol Cell Biol, 2000. **20**(6): p. 2269-84.
224. Karin, M. and Y. Ben-Neriah, *Phosphorylation meets ubiquitination: the control of NF-[kappa]B activity.* Annu Rev Immunol, 2000. **18**: p. 621-63.
225. Fuseler, J.W., et al., *Analysis and quantitation of NF-kappaB nuclear translocation in tumor necrosis factor alpha (TNF-alpha) activated vascular endothelial cells.* Microsc Microanal, 2006. **12**(3): p. 269-76.
226. Zandi, E., et al., *The IkappaB kinase complex (IKK) contains two kinase subunits, IKKalpha and IKKbeta, necessary for IkappaB phosphorylation and NF-kappaB activation.* Cell, 1997. **91**(2): p. 243-52.
227. Kim, H.J., et al., *IkappaB kinase gamma/nuclear factor-kappaB-essential modulator (IKKgamma/NEMO) facilitates RhoA GTPase activation, which, in turn, activates Rho-associated KINASE (ROCK) to phosphorylate IKKbeta in response to transforming growth factor (TGF)-beta1.* J Biol Chem, 2014. **289**(3): p. 1429-40.
228. Israel, A., *The IKK complex, a central regulator of NF-kappaB activation.* Cold Spring Harb Perspect Biol, 2010. **2**(3): p. a000158.
229. Dejardin, E., *The alternative NF-kappaB pathway from biochemistry to biology: pitfalls and promises for future drug development.* Biochem Pharmacol, 2006. **72**(9): p. 1161-79.
230. Gommerman, J.L. and L. Summers deLuca, *LTbetaR and CD40: working together in dendritic cells to optimize immune responses.* Immunol Rev, 2011. **244**(1): p. 85-98.
231. Vu, F., et al., *ICOS, CD40, and lymphotoxin beta receptors signal sequentially and interdependently to initiate a germinal center reaction.* J Immunol, 2008. **180**(4): p. 2284-93.
232. Coope, H.J., et al., *CD40 regulates the processing of NF-kappaB2 p100 to p52.* EMBO J, 2002. **21**(20): p. 5375-85.
233. Dobrzanski, P., R.P. Ryseck, and R. Bravo, *Specific inhibition of RelB/p52 transcriptional activity by the C-terminal domain of p100.* Oncogene, 1995. **10**(5): p. 1003-7.
234. Kang, M.R., et al., *NF-kappaB signalling proteins p50/p105, p52/p100, RelA, and IKKepsilon are over-expressed in oesophageal squamous cell carcinomas.* Pathology, 2009. **41**(7): p. 622-5.
235. Balkwill, F.R. and A. Mantovani, *Cancer-related inflammation: common themes and therapeutic opportunities.* Semin Cancer Biol, 2012. **22**(1): p. 33-40.
236. Ben-Neriah, Y. and M. Karin, *Inflammation meets cancer, with NF-kappaB as the matchmaker.* Nat Immunol, 2011. **12**(8): p. 715-23.
237. Wang, F., et al., *Nuclear-factor-kappaB (NF-kappaB) and radical oxygen species play contrary roles in transforming growth factor-beta1 (TGF-beta1)-induced apoptosis in hepatocellular carcinoma (HCC) cells.* Biochem Biophys Res Commun, 2008. **377**(4): p. 1107-12.
238. Wang, H., et al., *CD68(+)HLA-DR(+) M1-like macrophages promote motility of HCC cells via NF-kappaB/FAK pathway.* Cancer Lett, 2014. **345**(1): p. 91-9.

239. Wang, Y.H., et al., *Vascular endothelial cells facilitated HCC invasion and metastasis through the Akt and NF-kappaB pathways induced by paracrine cytokines.* J Exp Clin Cancer Res, 2013. **32**(1): p. 51.
240. Yang, S.T., et al., *SUMOylated CPAP is required for IKK-mediated NF-kappaB activation and enhances HBx-induced NF-kappaB signaling in HCC.* J Hepatol, 2013. **58**(6): p. 1157-64.
241. Nemeth, J., et al., *S100A8 and S100A9 are novel nuclear factor kappa B target genes during malignant progression of murine and human liver carcinogenesis.* Hepatology, 2009. **50**(4): p. 1251-62.
242. Hassan, M., et al., *Apoptosis and molecular targeting therapy in cancer.* Biomed Res Int, 2014. **2014**: p. 150845.
243. Urbanik, T., et al., *Down-regulation of CYLD as a trigger for NF-kappaB activation and a mechanism of apoptotic resistance in hepatocellular carcinoma cells.* Int J Oncol, 2011. **38**(1): p. 121-31.
244. Nakagawa, H. and S. Maeda, *Inflammation- and stress-related signaling pathways in hepatocarcinogenesis.* World J Gastroenterol, 2012. **18**(31): p. 4071-81.
245. O'Neil, J., et al., *FBW7 mutations in leukemic cells mediate NOTCH pathway activation and resistance to gamma-secretase inhibitors.* J Exp Med, 2007. **204**(8): p. 1813-24.
246. DiDonato, J.A., F. Mercurio, and M. Karin, *NF-kappaB and the link between inflammation and cancer.* Immunol Rev, 2012. **246**(1): p. 379-400.
247. Barashi, N., et al., *Inflammation-induced hepatocellular carcinoma is dependent on CCR5 in mice.* Hepatology, 2013. **58**(3): p. 1021-30.
248. Karin, M., *NF-kappaB as a critical link between inflammation and cancer.* Cold Spring Harb Perspect Biol, 2009. **1**(5): p. a000141.
249. Luedde, T. and R.F. Schwabe, *NF-kappaB in the liver--linking injury, fibrosis and hepatocellular carcinoma.* Nat Rev Gastroenterol Hepatol, 2011. **8**(2): p. 108-18.
250. He, G., et al., *Hepatocyte IKKbeta/NF-kappaB inhibits tumor promotion and progression by preventing oxidative stress-driven STAT3 activation.* Cancer Cell, 2010. **17**(3): p. 286-97.
251. Luedde, T., et al., *Deletion of NEMO/IKKgamma in liver parenchymal cells causes steatohepatitis and hepatocellular carcinoma.* Cancer Cell, 2007. **11**(2): p. 119-32.
252. Yau, T.O., et al., *Hepatocyte-specific activation of NF-kappaB does not aggravate chemical hepatocarcinogenesis in transgenic mice.* J Pathol, 2009. **217**(3): p. 353-61.
253. Nitou, M., et al., *Purification of fetal mouse hepatoblasts by magnetic beads coated with monoclonal anti-e-cadherin antibodies and their in vitro culture.* Exp Cell Res, 2002. **279**(2): p. 330-43.
254. Zender, L., et al., *Generation and analysis of genetically defined liver carcinomas derived from bipotential liver progenitors.* Cold Spring Harb Symp Quant Biol, 2005. **70**: p. 251-61.
255. Postic, C., et al., *Dual roles for glucokinase in glucose homeostasis as determined by liver and pancreatic beta cell-specific gene knock-outs using Cre recombinase.* J Biol Chem, 1999. **274**(1): p. 305-15.
256. Livet, J., et al., *Transgenic strategies for combinatorial expression of fluorescent proteins in the nervous system.* Nature, 2007. **450**(7166): p. 56-62.

257. Li, D., et al., *Hepatic loss of survivin impairs postnatal liver development and promotes expansion of hepatic progenitor cells in mice.* Hepatology, 2013. **58**(6): p. 2109-21.
258. Wang, E.Y., et al., *Depletion of beta-catenin from mature hepatocytes of mice promotes expansion of hepatic progenitor cells and tumor development.* Proc Natl Acad Sci U S A, 2011. **108**(45): p. 18384-9.
259. Yamaji, S., et al., *Hepatocyte-specific deletion of DDB1 induces liver regeneration and tumorigenesis.* Proc Natl Acad Sci U S A, 2010. **107**(51): p. 22237-42.
260. Rougemont, A.L., et al., *Extensive biliary intraepithelial neoplasia (BilIN) and multifocal early intrahepatic cholangiocarcinoma in non-biliary cirrhosis.* Virchows Arch, 2010. **456**(6): p. 711-7.
261. Sato, Y., et al., *Histological Characterization of Biliary Intraepithelial Neoplasia with respect to Pancreatic Intraepithelial Neoplasia.* Int J Hepatol, 2014. **2014**: p. 678260.
262. Sato, Y., et al., *Histological characteristics of biliary intraepithelial neoplasia-3 and intraepithelial spread of cholangiocarcinoma.* Virchows Arch, 2013. **462**(4): p. 421-7.
263. Bross, P., R. Magnoni, and A.S. Bie, *Molecular chaperone disorders: defective Hsp60 in neurodegeneration.* Curr Top Med Chem, 2012. **12**(22): p. 2491-503.
264. Rath, E. and D. Haller, *Mitochondria at the interface between danger signaling and metabolism: role of unfolded protein responses in chronic inflammation.* Inflamm Bowel Dis, 2012. **18**(7): p. 1364-77.
265. Wei, Y.H., et al., *Oxidative stress in human aging and mitochondrial disease-consequences of defective mitochondrial respiration and impaired antioxidant enzyme system.* Chin J Physiol, 2001. **44**(1): p. 1-11.
266. Chen, H.M., Y.H. Lee, and Y.J. Wang, *ROS-Triggered Signaling Pathways Involved in the Cytotoxicity and Tumor Promotion Effects of Pentachlorophenol and Tetrachlorohydroquinone.* Chem Res Toxicol, 2015.
267. Benhar, M., et al., *Enhanced ROS production in oncogenically transformed cells potentiates c-Jun N-terminal kinase and p38 mitogen-activated protein kinase activation and sensitization to genotoxic stress.* Mol Cell Biol, 2001. **21**(20): p. 6913-26.
268. Ohsawa, S., et al., *Mitochondrial defect drives non-autonomous tumour progression through Hippo signalling in Drosophila.* Nature, 2012. **490**(7421): p. 547-51.
269. Santoni-Rugiu, E., et al., *Progenitor cells in liver regeneration: molecular responses controlling their activation and expansion.* APMIS, 2005. **113**(11-12): p. 876-902.
270. Dubois-Pot-Schneider, H., et al., *Inflammatory cytokines promote the retrodifferentiation of tumor-derived hepatocyte-like cells to progenitor cells.* Hepatology, 2014. **60**(6): p. 2077-90.
271. Zeisberger, S.M., et al., *Clodronate-liposome-mediated depletion of tumour-associated macrophages: a new and highly effective antiangiogenic therapy approach.* Br J Cancer, 2006. **95**(3): p. 272-81.
272. Inokuchi, S., et al., *Disruption of TAK1 in hepatocytes causes hepatic injury, inflammation, fibrosis, and carcinogenesis.* Proc Natl Acad Sci U S A, 2010. **107**(2): p. 844-9.

273. Nishikawa, Y., et al., *Tumor necrosis factor-alpha promotes bile ductular transdifferentiation of mature rat hepatocytes in vitro.* J Cell Biochem, 2013. **114**(4): p. 831-43.
274. Nitou, M., *Purification of Fetal Mouse Hepatoblasts by Magnetic Beads Coated with Monoclonal Anti-E-Cadherin Antibodies and Their In Vitro Culture.* Experimental Cell Research, 2002. **279**(2): p. 330-343.
275. Mathew, S.J., et al., *Looking beyond death: a morphogenetic role for the TNF signalling pathway.* J Cell Sci, 2009. **122**(Pt 12): p. 1939-46.
276. Hefetz-Sela, S., et al., *Acquisition of an immunosuppressive protumorigenic macrophage phenotype depending on c-Jun phosphorylation.* Proc Natl Acad Sci U S A, 2014. **111**(49): p. 17582-7.
277. Jain, D., et al., *Steatohepatitic hepatocellular carcinoma, a morphologic indicator of associated metabolic risk factors: a study from India.* Arch Pathol Lab Med, 2013. **137**(7): p. 961-6.
278. Sasaki, Y., et al., *Canonical NF-kappaB activity, dispensable for B cell development, replaces BAFF-receptor signals and promotes B cell proliferation upon activation.* Immunity, 2006. **24**(6): p. 729-39.
279. Cairo, S., et al., *Hepatic stem-like phenotype and interplay of Wnt/beta-catenin and Myc signaling in aggressive childhood liver cancer.* Cancer Cell, 2008. **14**(6): p. 471-84.
280. Webber, E.M., et al., *Tumor necrosis factor primes hepatocytes for DNA replication in the rat.* Hepatology, 1998. **28**(5): p. 1226-34.
281. Yamada, Y. and N. Fausto, *Deficient liver regeneration after carbon tetrachloride injury in mice lacking type 1 but not type 2 tumor necrosis factor receptor.* Am J Pathol, 1998. **152**(6): p. 1577-89.
282. Fujita, J., et al., *Effect of TNF gene depletion on liver regeneration after partial hepatectomy in mice.* Surgery, 2001. **129**(1): p. 48-54.
283. Scotte, M., et al., *Cytokine gene expression in liver following minor or major hepatectomy in rat.* Cytokine, 1997. **9**(11): p. 859-67.
284. Fausto, N., *Liver regeneration.* J Hepatol, 2000. **32**(1 Suppl): p. 19-31.
285. Tilg, H. and A.M. Diehl, *Cytokines in alcoholic and nonalcoholic steatohepatitis.* N Engl J Med, 2000. **343**(20): p. 1467-76.
286. Satoh, M., et al., *TNF-driven inflammation during mouse liver regeneration after partial hepatectomy and its role in growth regulation of liver.* Mol Biother, 1991. **3**(3): p. 136-47.
287. Akerman, P., et al., *Antibodies to tumor necrosis factor-alpha inhibit liver regeneration after partial hepatectomy.* Am J Physiol, 1992. **263**(4 Pt 1): p. G579-85.
288. Westwick, J.K., et al., *Activation of Jun kinase is an early event in hepatic regeneration.* J Clin Invest, 1995. **95**(2): p. 803-10.
289. Hilberg, F., et al., *c-jun is essential for normal mouse development and hepatogenesis.* Nature, 1993. **365**(6442): p. 179-81.
290. Lin, M.T. and M.F. Beal, *Mitochondrial dysfunction and oxidative stress in neurodegenerative diseases.* Nature, 2006. **443**(7113): p. 787-95.

291. Thanan, R., et al., *Oxidative stress and its significant roles in neurodegenerative diseases and cancer.* Int J Mol Sci, 2015. **16**(1): p. 193-217.
292. Cui, H., Y. Kong, and H. Zhang, *Oxidative stress, mitochondrial dysfunction, and aging.* J Signal Transduct, 2012. **2012**: p. 646354.
293. Liu, L., et al., *Glial lipid droplets and ROS induced by mitochondrial defects promote neurodegeneration.* Cell, 2015. **160**(1-2): p. 177-90.
294. Schieber, M. and N.S. Chandel, *ROS function in redox signaling and oxidative stress.* Curr Biol, 2014. **24**(10): p. R453-62.
295. Silva, A., et al., *Intracellular reactive oxygen species are essential for PI3K/Akt/mTOR-dependent IL-7-mediated viability of T-cell acute lymphoblastic leukemia cells.* Leukemia, 2011. **25**(6): p. 960-7.
296. Kerr, B.A. and T.V. Byzova, *The dark side of the oxidative force in angiogenesis.* Nat Med, 2012. **18**(8): p. 1184-5.
297. Finley, L.W., et al., *SIRT3 opposes reprogramming of cancer cell metabolism through HIF1alpha destabilization.* Cancer Cell, 2011. **19**(3): p. 416-28.
298. Lu, T. and D.I. Gabrilovich, *Molecular pathways: tumor-infiltrating myeloid cells and reactive oxygen species in regulation of tumor microenvironment.* Clin Cancer Res, 2012. **18**(18): p. 4877-82.
299. Winter, M., et al., *Divergent roles of HDAC1 and HDAC2 in the regulation of epidermal development and tumorigenesis.* EMBO J, 2013. **32**(24): p. 3176-91.
300. Dovey, O.M., et al., *Histone deacetylase 1 and 2 are essential for normal T-cell development and genomic stability in mice.* Blood, 2013. **121**(8): p. 1335-44.
301. Zimmermann, S., et al., *Reduced body size and decreased intestinal tumor rates in HDAC2-mutant mice.* Cancer Res, 2007. **67**(19): p. 9047-54.
302. Xia, J., et al., *Loss of histone deacetylases 1 and 2 in hepatocytes impairs murine liver regeneration through Ki67 depletion.* Hepatology, 2013. **58**(6): p. 2089-98.

LIST OF PUBLICATIONS

1. “Hepatic mitochondrial dysfunction causes cholangiolar hyperproliferation and neoplasia via Kupffer cell-mediated TNF.”

Detian Yuan, Emanuel Berger, Nicole Simonavicius, Lei Liu, Daniel Hartmann, Nina Gross, Julia Weber, Florian Reisinger, Marc Ringelhan, Ruediger Meyer, Maria Reich, Valentina Leone, Dirk Wohlleber, Simone Jörs, Fabian Geisler, Marco Prinz, Percy Knolle, Verena Keitel, Kristian Unger, Thomas Ried, Norbert Hüser, Roland Rad, Achim Weber, Dirk Haller, Mathias Heikenwälder

(Manuscript preparation)

2. “Mitochondrial dysfunction in the epithelium activates paracrine WNT-signaling and causes hyperproliferation of the intestinal stem cell compartment.”

Emanuel Berger, **Detian Yuan**, Waldschmitt N, Rath E, Allgäuer M, Staszewski O, Kober O, Lobner E, Schöttl T, Prinz M, Weber A, Gerhard M, Klingenspor M, Janssen KP, Mathias Heikenwälder, Dirk Haller.

(Manuscript preparation)

3. “Ectopic lymphoid structures as microniches for tumor progenitor cells.”

Shlomi Finkin, **Detian Yuan**, Ilan Stein, Koji Taniguchi, Achim Weber, Kristian Unger, Jeffrey L. Browning, Nicolas Goossens, Yujin Hoshida, Michael Berger, Orit Pappo, Klaus Rajewsky, Michael Karin, Mathias Heikenwalder, Yinon Ben-Neriah and Eli Pikarsky. Nature Immunology. 2015 Dec;16(12):1235-44. doi: 10.1038/ni.3290.

4. “CRISPR/Cas9 somatic multiplex-mutagenesis for high-throughput functional cancer genomics in mice.”

Julia Weber, Rupert Öllinger, Mathias Friedrich, Ursula Ehmer, Maxim Barenboim, Katja Steiger, Irina Heide, Sebastian Mueller, Roman Maresch, Thomas Engleitner, Nina Gross, Ulf Geumann, Beiyuan Fu, Angela Segler, **Detian Yuan**, Sebastian Lange, Alexander Strong, Jorge de la Rosa, Irene Esposito, Pentao Liu, Juan Cadiñanos, George S. Vassiliou, Roland M. Schmid, Günter Schneider, Kristian Unger, Fengtang Yang, Rickmer Braren, Mathias Heikenwälder, Ignacio Varela, Dieter Saur, Allan Bradley,

and Roland Rad. Proc Natl Acad Sci U S A. 2015 Nov 10;112(45):13982-7. doi: 10.1073/pnas.1512392112.

5. “Hepatocellular carcinoma originates from hepatocytes and not from progenitor cells.”

Xueru Mu, Regina Espanol-Suner, Christine Sempoux, Frederic P. Lemaigre, Arlind Adili, **Detian Yuan**, Achim Weber, Kristian Unger, Mathias Heikenwälder, Isabelle A. Leclercq, Robert Schwabe, Silvia Affo, Ingmar Mederacke, Rita Manco. J Clin Invest. 2015 Oct 1;125(10):3891-903. doi: 10.1172/JCI77995.

6. “Modeling human liver cancer heterogeneity: virally induced transgenic models and mouse genetic models of chronic liver inflammation.” *Review*

Marc Ringelhan, Florian Reisinger, **Detian Yuan**, Achim Weber, Mathias Heikenwälder. Curr Protoc Pharmacol 2014 1;67:14.31.1-14.31.17.

7. “Lymphotoxin, NF-κB, and cancer: the dark side of cytokines.” *Review*

Judith Bauer, Sukumar Namineni, Florian Reisinger, Jessica Zöller, **Detian Yuan**, Mathias Heikenwälder. Dig Dis 2012 24;30(5):453-68.

CURRICULUM VITAE

Personal details	
First names / Surname	Detian Yuan
Address	South Cangshan Road 17, 276700, Linshu, Shandong, China
Nationality	Chinese
Date of birth	02.03.1986
Gender	Male
Educational qualifications	
Dates	August, 2011 ~ present
Occupation or position held	PhD student
Name and type of organization	Institute of Virology, Technische Universität München / HelmholtzZentrum München
Main activities and responsibilities	• Investigating the casual link between mitochondrial defects and cancer initiation • Functional analysis of HDAC2 in liver homeostasis • Characterization of histological and molecular changes during HCC development driven by inflammatory micro-niche
Publications	Refer to “List of publications”
Dates	August, 2007 ~ January, 2011
Title of qualification awarded	Master of Cell biology
Name and type of organization providing education and training	Institute of Biochemistry and Cell Biology, Chinese Academy of Sciences, Shanghai, China
Main activities and responsibilities	• Role of E-cadherin-mediated cell-cell contact in the generation of induced pluripotent stem cells • Screening of chemicals that facilitate iPS cell generation.
Publication	E-Cadherin-Mediated Cell–Cell Contact Is Critical for Induced Pluripotent Stem Cell Generation. STEM CELLS, (2010) 28, 1315–1325.

Dates	September, 2003 ~ June, 2007
Title of qualification awarded	Bachelor in Biology
Name and type of organisation providing education and training	School of Life Science, Shandong University, Jinan, China • Intrathymic injection of heterogenic antigen impacts on T-cell development and induces lymphocytic infiltration in the thymus

ACKNOWLEDGEMENTS

I would like to express my gratitude to all those who helped me during the writing of this thesis. I would never be able to finish my dissertation without support from my family, guidance of my thesis committee members and help from my colleagues and friends.

My deepest gratitude first goes to my beloved parents and my brothers, for their great love, confidence and patience in me all through these years, although I never tried to convey my projects and experiments into the words they could understand. I wish we will have chances to celebrate my successes together in the future.

Grateful acknowledgement is made to Prof. Mathias Heikenwälder, my supervisor, for his constant encouragement and guidance. He has walked me through all the stages of the writing of this thesis. Without his consistent and illuminating instruction, this thesis could not have reached its present form. I would also like to thank my other thesis committee members, Prof. Dirk Haller and Prof. Martin Göttlicher, who have been always providing insightful and constructive feedbacks.

High tribute shall be paid to Mrs. Ruth Hillermann, Mrs. Olga Lesina, Mr. Robert Baier and Mrs. Annett Käsewieter, for their profound knowledge and tremendous technical support. I have benefited a great deal from their performance characteristics such as accuracy, precision and strong sense of responsibility.

I would like to express my heartfelt gratitude to Prof. Eli Pikarsky, Dr. Ilan Stein and Dr. Shlomi Finkin, for the nice collaborations and their instructive advice on my thesis. I am also greatly indebted to Prof. Achim Weber, Dr. Norbert Hüser and Dr. Kristian Unger, who have instructed and helped me a lot in the past years.

Special thanks should go to Dr. Nicole Simonavicius, Dr. Emmanuel Berger, Dr. Anna Lorentzen, Dr. Florian Reisinger, Dr. Lei Liu and Miao Lu, who have put considerable time and effort into my PhD research. The scientific and non-scientific interactions with them were enjoyable and unforgettable.

I also owe my sincere gratitude to Arlind, Sukumar, Marc, Jessi, Judith, Gabi and my Chinese friends Shanze and Xiaoming who gave me their help and time in listening to me and helping me work out my problems during the difficult courses of the thesis. I felt

so lucky that I had them in accompany and they have definitely become much more than colleagues to my life.

My PhD career in Germany started from a selection by Helmholtz Zentrum München. I would like to express my thanks to Dr. Monika Beer, Mrs. Gaby Hellmann and all the other members within this network for their support.

To those all I offer my sincerest gratitude.